OUTCROP-BASED GAMMA-RAY CHARACTERIZATION OF THE WOODFORD SHALE OF SOUTH-CENTRAL OKLAHOMA

By

ALISCHA M. KRYSTYNIAK

Bachelor Science in Geology

Lake Superior State University

Sault Sainte Marie, Michigan

2003

Submitted to the Faculty of the
Graduate College of the
Oklahoma State University
in partial fulfillment of
the requirements for
the Degree of
MASTER OF SCIENCE
December, 2005

OUTCROP-BASED GAMMA-RAY

CHARACTERIZATION OF THE WOODFORD SHALE

OF SOUTH-CENTRAL OKLAHOMA

Thesis Approved:

Stanley T. Paxton

Darwin Boardman

Jim Puckette

William Coffey

Dr. Gordon Emslie

Dean of the Graduate College

Acknowledgements

I would like to express deep gratitude to my thesis advisor, Dr. Stan Paxton. Without his dedication to this project, his motivational talks and the countless hours spent with me in the scorching heat of Oklahoma, bush-whacking through poison ivy and dodging chiggers, this project may not have been completed. I would also like to thank the rest of my committee; Dr. Bill Coffey, Dr. Darwin Boardman, and Dr. Jim Puckette for their ideas, support and encouragement throughout my graduate career.

I want to thank Devon Energy Corporation for allowing me access to all of their resources for this project. I would like to extend special thanks to David Deering for helping with figures and adjustments to my thesis. I would also like to thank Brad Biddy, Pam Peters, Jenny Munday and Rick Coleman for their assistance. I would like to thank Dr. Elizabeth Catlos for allowing me to use her digital camera to photograph thin-sections. I would like to give the Oklahoma Geological Society my gratitude for the Kate Scholarship that helped with the funding of this project. Special thanks are also given to Julie Turrentine, Willie Parker, and Ali Jaffri for assisting me with fieldwork.

I would like to thank my family for their endless support of my academic pursuits. Steven Bates, Rebecca Klein and Melissa Stefos are acknowledged for boosting my morale, especially for the times when I wanted to give up and move to Alaska. Most importantly, I would like to thank my best friend, Gregory Gromadzki, for the technical assistance that he provided me as well as the constant moral and emotional support. I couldn't have done this thesis without you.

TABLE OF CONTENTS

LIST OF FIGURES

Figure **Page**

LIST OF PLATES

Plate **Page**

Chapter I

Introduction

Problem Statement

The rise in oil prices as well as the depletion of natural resources has led many companies to consider unconventional gas-shale plays. One such possibility that may prove to be economically viable is the Woodford Shale. The Woodford is considered to be the most prolific source rock for oil and gas in Oklahoma (Johnson et al., 1990). The Woodford is present throughout most parts of the Oklahoma Basin and ranges from 200-900 ft thick in the southern Oklahoma aulacogen to 50-100 ft thick in most of the shelf areas (Amsden, 1975; Johnson and others, 1988). The Woodford is considered to be a "hot shale" on well logs with API readings of 150 and higher. This organic rich black shale contains Types II and III kerogen. Type II is oil prone and is composed of mixed terrestrial and marine source material. Type III organic matter is gas prone and contains a woody terrestrial source material (Raymond, 2002).

A detailed study of the Woodford would result in a better conceptual understanding of hydrocarbon source rocks and their role as possible unconventional gas-shale plays. For instance, to evaluate this possibility, the relationship between the lithofacies both in outcrop and subsurface can be established relative to gamma-ray profile on the well log. Analyzing the results of the gamma-ray readings relative to lithofacies character (bedding style, internal thickness, and lithology) along with Total Organic Carbon (TOC) and mineralogy from x-ray diffraction (XRD) could potentially reveal much needed information regarding the economic viability of the Woodford Shale.

Study Area

The Woodford Shale is found extensively in the subsurface throughout the state of Oklahoma. Outcrop exposures are found in both the south-central portion of the state as well as some exposures in the northeast. This study focused on five Woodford outcrops that are located in south-central Oklahoma (Fig. 1). Outcrops that were analyzed are located in Murray, Carter, and Pontotoc counties (Plate. 1). This area offered the best outcrops for the purpose of this study in terms of size, location, and accessibility.

Objective & Approach

The rising cost of energy resources has caused many petroleum companies to explore unconventional gas-shale plays. In the basins for which estimates have been made, shale-gas resources are substantial, with in-place volumes of 497-783 tcf (Curtis, 2002). The Woodford Shale of south-central Oklahoma is a possible gas-shale resource. The objective of this study is to establish and document the geochemical and geological characters of this organic-rich black shale relative to lithology and in correspondence with spectral gamma-ray response (potassium, uranium, and thorium). This approach has the potential to improve our ability to predict properties of black shales and to project the characteristics of these black shales into the subsurface by way of outcrop-based gamma-ray logs.

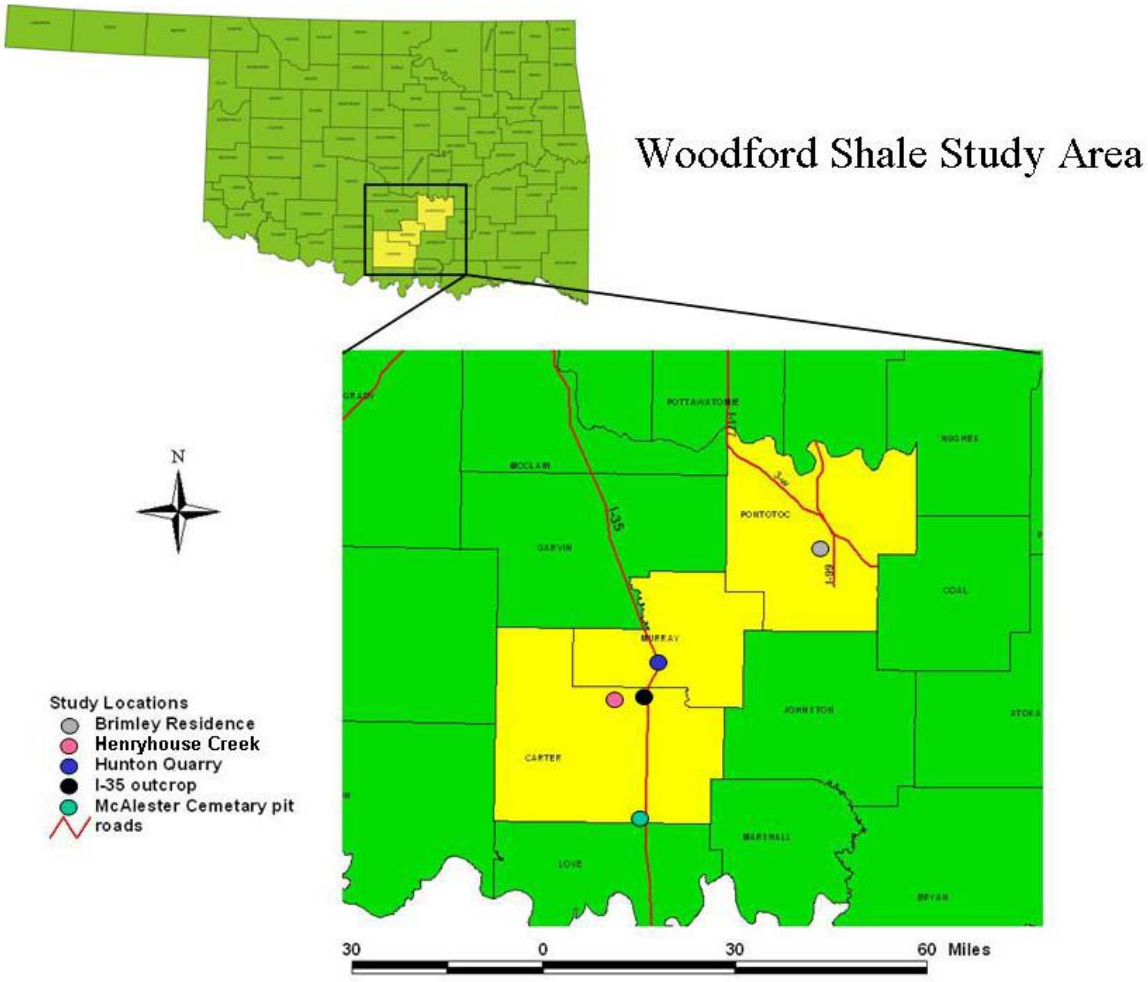

Figure 1. Map of the five Woodford Shale outcrop locations.

Approach:

1. Perform fieldwork to collect gamma-ray data and construct vertical gamma-ray profiles from five outcrops in Carter, Murray and Pontotoc counties. The gamma-ray measurements (K, U, and Th) are used to classify the lithofacies, identify depositional environments (Gromadzki, 2004), and possibly assist in locating gas-bearing zones

2. Collect samples from outcrops for thin sections, TOC and XRD.

(A). Perform thin-section analysis of samples to document details of texture and composition of different lithofacies found within the outcrop sections. Thin section analysis helps to determine the types of minerals making up the shale, some of which are detrital and others diagenetic.

(B). Evaluate the TOC and XRD data. TOC provides the amount of organic material found within a sample. XRD analysis of the samples is used to determine the mineralogy and relative proportions of minerals, including clays and clay types.

3. Construct a detailed lithofacies description of outcrops. Compare and contrast the lithofacies description in relation to the gamma-ray data, and attempt to quantitatively establish the correspondence between gamma-ray and lithofacies.

4. Determine the strength of statistical association between gamma-ray response and lithofacies using SAS (Statistical Analysis System). Assuming these associations yield significant relationships, recommend methods by which the gamma-ray profile in the outcrop can be used to define lithofacies in the subsurface.

5. Test the assumption that outcrop based gamma-ray profiles can be correlated into the subsurface by comparison with well log data.

Stratigraphy

The Woodford Shale is exposed in a series of folds and faults of the Arbuckle Mountains, the result of late Pennsylvanian deformation (Fig. 2), (Over, 1990). This organic-rich black shale is late Devonian (Frasnian, Fammenian) and basal Mississippian (Tournasian) in age and consists of gray-black siliceous and fissile shale and phosphatic shale. The Woodford also contains rare chert, some bedded limestone, bedded dolomite, and phosphate nodules. The term Woodford is derived from the town of Woodford in Carter County. This name was first used by Taff (1903, 1904) in studies of strata exposed in Indian Territory and Oklahoma at the turn of the century (Over, 1990).

The Woodford Shale was deposited when the southern margin of North America was located in the tropics (Woodrow et al., 1973). The Late Devonian was characterized by widespread deposition of black shales in the eastern and central United States (U.S. Department of Energy, Morgantown Energy Technology Center, 1981). The Woodford Shale records a transition from primarily carbonate deposition in the early Paleozoic to predominately clastic deposition in the late Paleozoic (Ham and Wilson, 1967, p. 393-396). Time-stratigraphic equivalents of the Woodford Shale include the New Albany, Chattanooga, Ohio, Millboro, Burket, Geneseo, and Antrim Shales and the Arkansas Novaculite (Conant and Swanson, 1961). The Woodford Shale and its equivalents form the base of the Kaskaskia sequence in the Midcontinent (Sloss, 1963). A period of regional exposure and erosion prior to the deposition of these rocks resulted in the incision of major stream channels in pre-Kaskaskian strata, and was followed by a marine transgression that

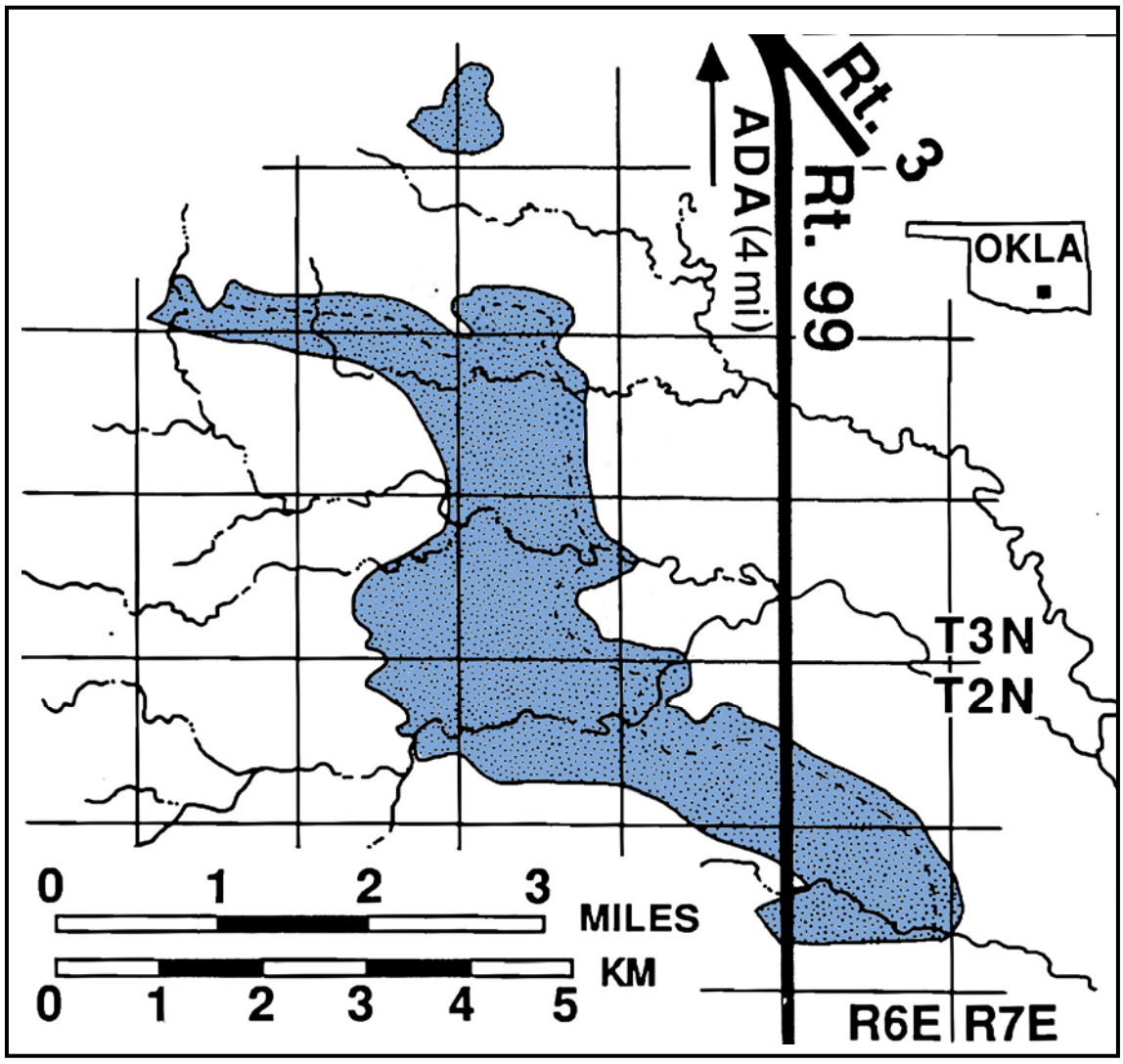

Figure 2. Woodford Shale exposure in the Arbuckle Mountains (modified after Over, 1990).

advanced onto the craton from the south (Bunker et al., 1988). A minor regression at the end of the Woodford deposition marks the upper boundary of the Kaskaskia (Sloss 1988).

The base of the Woodford is composed of the Misener sandstone in north-central and eastern Oklahoma. This sandstone is known as the Sylamore in northwestern Arkansas. When the Misener is present, it is often only 3.3 ft (1m) or less in thickness (Lee, 1956; Hilpman, 1967, Amsden and Klapper, 1972; Newell, 1989). It apparently developed where Ordovician –age Simpson Group sandstones subcropped beneath the pre-Kaskaskian erosional surface, becoming a source of sand-sized clastic detritus in the early stages of the Kaskaskian transgression (Lambert, 1993). There is no well-developed basal sandstone in the Woodford shale exposures in the Arbuckle Mountain region, although locally a few inches of conglomerate is present (Amsden and Klapper 1972). The Woodford unconformably overlies either Silurian to Early Devonian Hunton Group carbonates or older sediments (Sullivan, 1985).

The Hunton Group (Fig. 3) are mainly shallow-marine carbonates that are clean-washed skeletal limestones in the lower part (Chimneyhill Subgroup), argillaceous and silty carbonates in the middle (Henryhouse and Haragan-Bois d'Arc formations) and clean-washed limestones at the top (Frisco Formation), (Jolly, 1988). Above the Woodford lies the upper Mississippian Sycamore Formation. The Sycamore is a fine-grained, silty limestone with interbedded thin dark shales (Jolly, 1988).

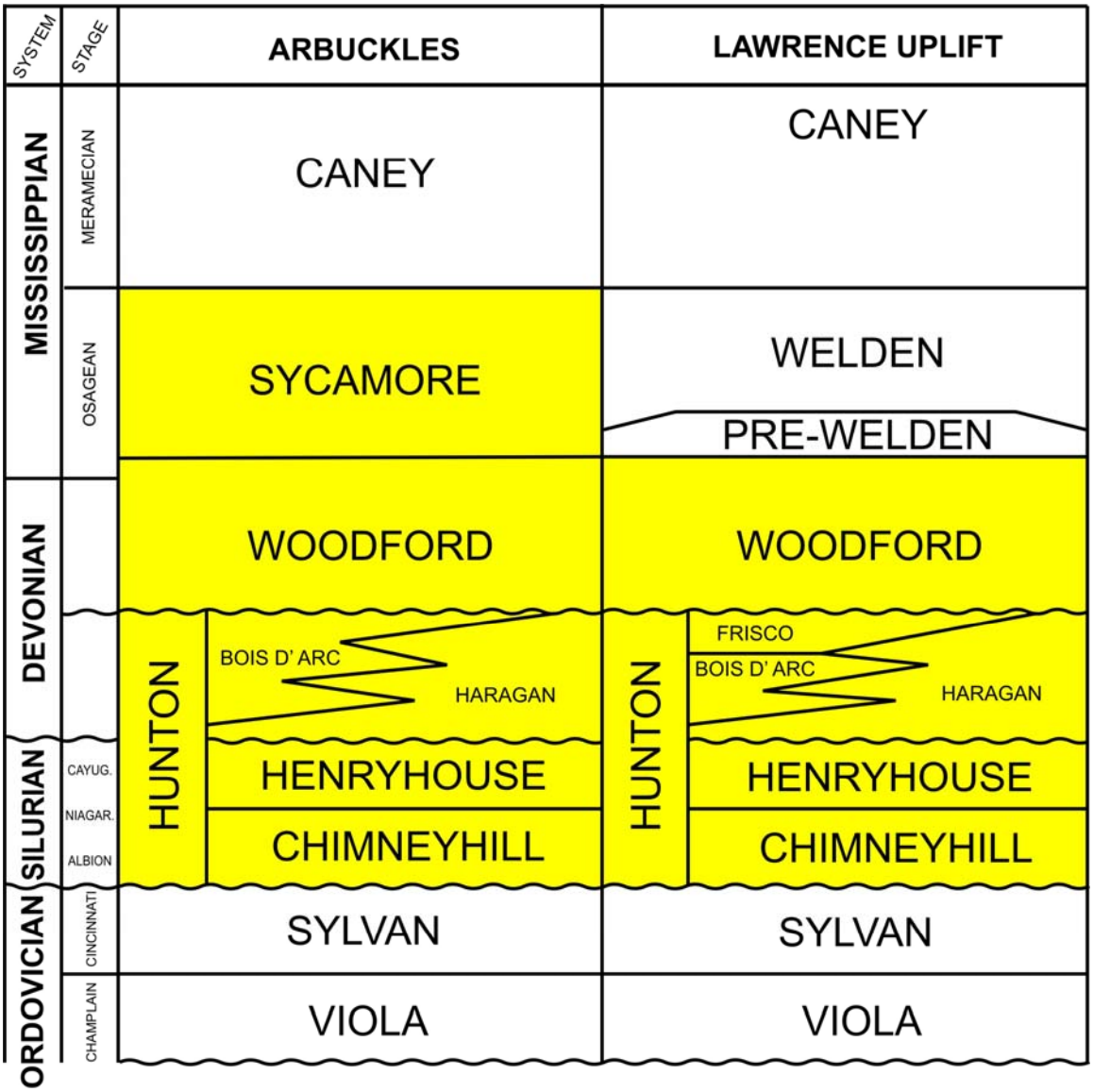

Figure 3. Stratigraphic relationship of the Woodford Shale with overlying Sycamore and underlying Hunton Group

Structural History

According to Cardott and Lambert (1982), the Anadarko basin of the southern Oklahoma aulacogen is a northwest-trending, axially asymmetric, sedimentary structural basin of Paleozoic age in western Oklahoma and the Texas panhandle. The aulacogen is bordered on the south by the Amarillo-Wichita uplift and the Marietta basin (Cardott and Lambert, 1982). The aulacogen is bordered on the southeast by the Ardmore basin and the Arbuckle uplift and on the east by the Nemaha ridge, and on the north and west by the northern shelf areas (Cardott and Lambert 1982). Crustal extension occurred in the southern Oklahoma aulacogen during the Cambrian (Burke and Dewey, 1973). This event produced normal faults and emplaced igneous rocks in the deepest part of the present Anadarko basin and Amarillo-Wichita uplift (Cardott and Lambert, 1982). Subsidence of the aulacogen occurred in many phases from the Late Cambrian through early Mississippian (Hoffman et al., 1974). During the early Pennsylvanian intense crustal shortening occurred in this region (Cardott and Lambert, 1982). This shortening is potentially associated with late Paleozoic continental collision involving the Ouachita orogenic belt (Cardott and Lambert, 1982). This event raised vertical blocks in the Amarillo-Wichita uplift along reactivated zones of weakness produced during the initial graben stage (Ham et al., 1964). Intense folds and faults were produced in the frontal Wichita fault zone and the adjacent deep Anadarko basin with less intense activity toward the north (Amsden, 1975). The Desmoinesian through the Permian represented a time when the rate of subsidence slowed, owing to “thermal contraction as the lithosphere returned to thermal equilibrium” (Garner and Turcotte, 1984, p. 5).

According to Over (1990), the Woodford is exposed in a series of folds and fault blocks of the Arbuckle Mountains in an eight county area of south-central Oklahoma. The current outcrop exposures in this region are found in Criner Hills, an outlier of Paleozoic strata at the southern limit of the Arbuckles, the southern, northern, and eastern Arbuckles that comprise the main Arbuckle Mountain region, and the Lawrence uplift, a fault-bound block of gently dipping predominantly Lower Paleozoic strata exposed in the northernmost extension of the Arbuckles (Over, 1990).

Deposition

The Woodford Shale represents a transition from thick, Early Paleozoic carbonates to Paleozoic clastics (Cardott and Lambert, 1985). The shales of the Woodford Formation were deposited from the northeast and east, during late Devonian to early Mississippian shelf sedimentation (Denison, 1982; Cardott and Lambert, 1985). The Deposition occurred slowly, with low oxygen content at the sediment-water interface (Sullivan, 1985). According to Over (1990), a stratified water column and anoxic bottom waters developed after initial Woodford sedimentation as the water deepened. The depth of the water during the Woodford deposition is estimated to have been between 50 to 400 meters (Over, 1990). This depth is based upon modern studies of depth to the oxygen minimum zone, and phosphatic sedimentation in upwelling areas.

Chapter 2

Literature Review

The Woodford Shale of south-central Oklahoma is an extensively studied hydrocarbon source rock. This organic-rich black shale is of great interest to both petroleum companies and researchers. There has been much work regarding the Woodford Shale in terms of deposition, gamma-ray emitting elements, radioactivity, geochemistry and the phosphate nodules found within some intervals. There has also been much literature written about the Woodford's overlying and underlying units, the Sycamore Limestone and the Hunton Group respectively.

In a study by Over (1990), the Woodford Shale of south-central Oklahoma is described as being the result of deposition in an offshore quiet, oxygen-poor setting. This deposition occurred on the southern margin of North America. Conodonts were used to determine the Frasnian-Famennian and Devonian-Carboniferous boundaries. Over (1990), indicated that the Frasnian-Famennian (F/F) boundary occurs in the lower 20 meters of Woodford. In south-central Oklahoma, it is mentioned that the F/F boundary lies within the fine-grained, quiet water siliclastic sediments of the Woodford. According to Over (1990), the very basal Woodford unconformity is locally composed of quartzose sand, phosphate, limestone pebble conglomerate, and green-brown shale. Organic-rich black shales and cherts lie directly above the basal beds of the Woodford Shale.

Jolly (1988), investigated the correlation of individual gamma-ray emitting elements (K-wt%, U-ppm, Th-ppm) of the Woodford Shale. Eighty-four samples of Woodford were collected at one meter intervals. These samples were analyzed using laboratory methods to determine gamma-ray emittence. Results yielded ranges for K

(0.2-2.1%), uranium (up to 60 ppm) and Th (up to 9 ppm). According to Jolly (1988), potassium is transported in solution and in detritus when it occurs as a constituent of some major minerals such as orthoclase, muscovite and biotite. Thorium is transported in suspension with resistates such as minerals and clays. Uranium is transported in suspension and solution and is highly insoluble under reducing conditions, but soluble under oxidizing conditions in open ocean water.

Lambert (1993), describes the Woodford Shale as an organic rich shale that is an important source of hydrocarbons in many of the intracratonic basins of the Mid-continent. The Woodford was deposited under generally anoxic conditions during the Kaskaskian marine transgression and can be divided into several members. The middle shale member is the most radioactive and has the greatest extent and thickness in south-central Oklahoma. TOC content of the three radioactive shale members decreases towards the north, with the middle shale member being the most organic-rich. The three radioactive members of the Woodford shale represent a third-order depositional sequence that is bounded both below and above by unconformities.

Cardott and Lambert (1982), describe the thermal maturity of the Woodford Shale. Their work focused on the Anadarko Basin in western Oklahoma. This study analyzed whole-rock cuttings and core material that was selected from 10-ft intervals of the Woodford in 28 wells. The results of this analysis yielded computer-generated plots with vitrinite reflectance versus depth. This analysis produced a regression equation that can be used to predict the vitrinite reflectance of the Woodford Shale at any depth in the Anadarko Basin. This equation can also be used to determine the amount of erosion.

Olson (1982), conducted a study that involved characterizing the Woodford Shale of south-central Oklahoma in terms of uranium distribution. Samples of Woodford were collected, and analyzed for uranium. Uranium content in the Woodford Shale was found to be as high as 121 ppm. Olson (1982), found that uranium is primarily associated with the kerogen fraction of the organic material and uranium increases with increasing organic carbon content. Kerogen type was found to be quite uniform across the study area. Thermal maturity of the Woodford Shale was found to increase from immature in the central portion of Oklahoma to advanced in the Anadarko Basin. Positive (statistical) correlations were found between quartz and uranium. Negative correlations were found between illite and uranium. The negative correlation between uranium content and illite is thought to reflect the rapid burial of the organic matter, limiting the length of time available for uranium-organic interaction.

Swanson (1962), reports on a series of studies that involved the geology and geochemistry in marine black shales. Over two hundred shale formations e were checked for their radioactivity during the study period of 1944-1957. Outcrops, well core, drill cuttings and gamma-ray logs were analyzed relative to geology and geochemistry data. Swanson's (1962) studies reveal that uranium in marine black shales is thoroughly disseminated throughout the rock. The uranium in the marine black shales is from sea water. Sources for uranium in sea water are igneous, metamorphic and sedimentary rocks that have released uranium to surface and ground waters during weathering processes. Swanson (1962), also determined that there are four stages of phosphate nodule development. The Woodford Shale of south-central Oklahoma represents a stage 2, in which the uranium availability in the waters was low or had already been depleted by

direct hydrogen sulfide precipitation, leaving little or no uranium to be incorporated into the phosphate.

Siy (1988) examined the geochemical and petrographic study of phosphate nodules of the Woodford Shale of southern Oklahoma. The relationship of the phosphate nodules to the surrounding shales indicates that the nodules are early diagenetic, in situ features which formed in the upper few centimeters of organic-rich marine sediments. Conditions favoring the inorganic precipitation of marine apatite in the form of carbonate fluoro-apatite were enhanced by 1) anaerobic conditions in the lower portion of the water column, 2) the presence of a highly productive offshore algae community, and 3) the high stand of sea level brought on by a major transgressive event in the Late Devonian-Early Mississippian. Siy (1988), determined that enrichment of lathanum (La) over cesium (Ce) in the nodules and depletion of cesium in shales indicates that the depositional environment was influenced by deep oceanic bottom water.

Dennis (2004), in a study for Logan County, Oklahoma suggests that the Misener interval exhibited characteristics that would make it a potential reservoir. More than 150 wells in Oklahoma have produced petroleum from the Woodford. Dennis describes the Woodford in some localities as being porous and permeable. Subsurface matrix porosity in the Misener may be so extensive that the Woodford may be considered a widespread commercial reservoir.

Champlin (1959), conducted an investigation of the stratigraphic relationship, and depositional environments of the Sycamore and related formations. This study was an attempt to apply detailed lithologic descriptions to time rock correlations. The study determined the Sycamore to be gray to buff, dense, silty, massive bedded limestones of

the Meramecian series. Sedimentary analysis and thin section examination show that these limestones were probably deposited as fine-grained sand or silt sized carbonate material. Calcite occurs as a pore-filling cement (sparry calcite).Champlin (1959) determined that a facies change that occurs between the upper part of the Sycamore and the lower part of the Caney was controlled by a chain of low relief islands, with a north-west-southeast alignment.

Cole (1988), conducted a subsurface study of the Sycamore Limestone along the north flank of the Arbuckle Anticline. This study focused on the lithostratigraphy and depositional history of the Sycamore Formation. Cole found six facies in the Sycamore Formation that are divided based on lithological variations. These lithofacies are 1) glauconitic shale, 2) bioturbated shale, 3) organic shale, 4) fossiliferous mudstones and wackstones, 5) silty pelletal packstones, and 6) pellet rich siltstones. These lithofacies represent four depositional environments. The present day distribution of the above mentioned lithofacies is the result of tectonic activity of the Washita Valley Fault System.

Coffey (2000), conducted a study to examine the depositional system of the Sycamore Formation in the area of the Carter-Knox field. Coffey (2000) indicates that the depositional system for the Sycamore consists of a reciprocal sedimentation model where silty pelletal packstone facies were deposited in two main phases. The first stage involved a transgressive rise in sea level that allowed the moderate water depth carbonate portion of the Sycamore Formation to develop. The second stage involved a lowstand drop in sea level to allow the accumulation of fine-grained clastic material to be released into the system as derived/turbidity current deposits.

Rottmann (2000), states that the underlying Hunton Group is the principal hydrocarbon-producing carbonate reservoir in western Oklahoma. After deposition of the Hunton Group, subsequent regional uplift and erosion modified the Hunton, this created erosional features that were preserved by the Woodford Shale. According to Rottmann (2000), the shale was probably deposited by the gradual inundation by the Devonian sea. The inundation was initially confined to the post-Hunton erosional channels, filling and preserving them. A rise in sea level caused the Devonian seas to eventually spread out over the non-channnelized Hunton surface, depositing a regional Woodford Shale facies.

Chapter 3

Methodology

Gamma-ray

Outcrop gamma-ray profiles were constructed using a portable gamma-ray spectrometer from Exploranium (GR-320 enviSpec). The GR-320 (Fig. 4) is calibrated on test pads traceable to GSC (gamma-ray spectral calibration) standards to assure the accuracy of each instrument. The internal calibration constants are used to measure concentrations of potassium (K, wt %), uranium (U, ppm) and thorium (Th, ppm). The GR-320 constructs automatic natural isotope spectrum stripping, and then carries out a full peak analysis to identify any isotopes located in the stripped spectrum. The individual isotope exposure rate is then computed by using internal calibration data details available at (www.saic.com). The Gr-320 is calibrated to provide results of the area sampled within 60 seconds. This “at-surface” characteristic allows one to reliably relate the measured radioactivity contrasts to mapped bedrock, surficial geology and alterations associated with mineral deposits (Gromadzki, 2004). The detector is 4.5 inches in diameter and 15.5 inches long. The benefits of using this instrument versus laboratory measurements of radioactivity are real time readings, the minimization of costs associated with rock collection, shipping, lab preparation and chemical analysis for elements of samples collected.

Figure 4. Photograph of the portable gamma ray spectrometer that was used to collect gamma-ray measurements from the Woodford Shale (Exploranium GR-320 Manual).

The natural radioactivity of sedimentary rocks is variable and dependent upon lithology. Fluvial deposited sediments tend to have higher amounts of thorium (Th) and marine deposited sediments tend to contain higher amounts of uranium (U). The Spectral gamma ray also provides measurements of potassium (K). The occurrence of potassium can be associated with clays such as illite and smectite. Using the data provided by the gamma ray, geologists can define lithofacies and infer depositional environments.

Outcrop Selection

Five outcrop locations were selected to conduct the study on the Woodford Shale (Fig. 5). The five outcrop locations; (1) McAlester Cemetery shale pit, (2) I-35, (3) Hunton quarry, (4) Brimley residence and (5) Henryhouse Creek. The outcrops are located in Carter, Murray and Pontotoc counties. The above-mentioned outcrops offered the best exposures in terms of lithofacies, stratigraphic contacts, and accessibility.

McAlester Cemetery pit is located in the southern Criner Hills area (SW1/4, Sec. 36 T.5S., R.lE. Overbrook Quadrangle. The entire Woodford Shale is reported by Over (1990), to be exposed in the southwest sloping quarry floor and face. 87 feet (26 M) and 68 gamma-ray readings of the quarry bottom were measured perpendicular to bedding in order to construct a vertical gamma-ray profile. Attempts were made to take readings on flat surfaces of the quarry floor that were not covered by too much weathered shale.

The I-35 Woodford is exposed on the west side of the southbound lane of I-35 (NW1/4, SE1/4, Sec. 25 T.2S., R.2E, Springer Quadrangle). A 68 ft (20 m)

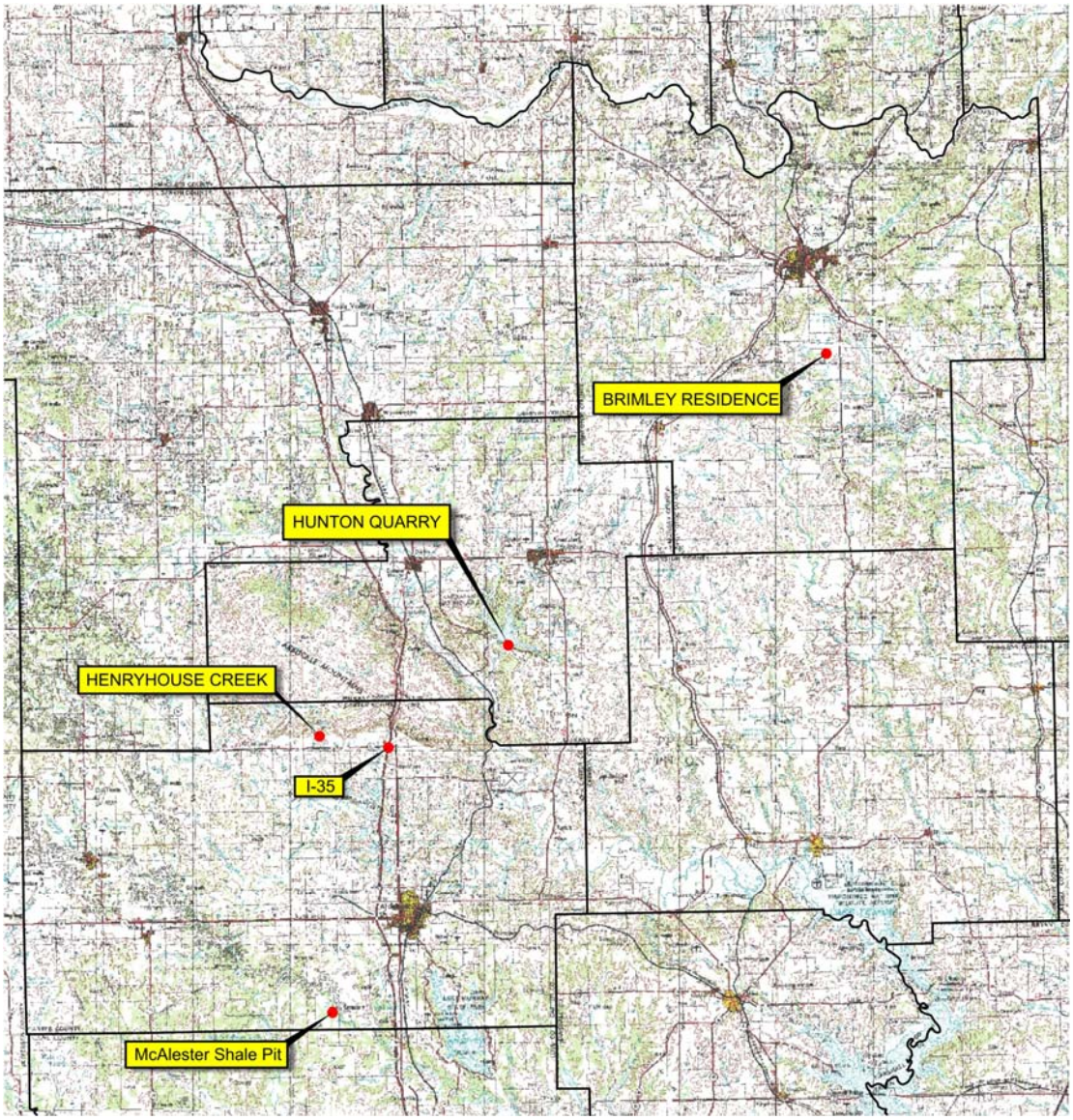

Figure 5. The location of the five Woodford Shale outcrops.

vertical profile was constructed from the base of the outcrop to the upper portion of the outcrop. Wire markers were strung perpendicular to bedding in order to measure from one bed to another. A total of 62 gamma-ray measurements were collected, and a detailed lithofacies description was constructed.

The Hunton Quarry outcrop is located in an abandoned shale quarry on the south side of Goddard Youth Camp road off of Route 10 near Sulphur, Oklahoma (NW1/4, Sec. 31, T1S., R.3E. Dougherty Quadrangle). A 55 ft (17 m) vertical profile was constructed from the base of the outcrop towards the top of the Woodford. A total of 63 gamma-ray measurements were collected perpendicular to bedding and a detailed lithofacies description was constructed.

Brimley residence outcrop exposure is located along the banks of the Jack Fork Creek near Ada, Oklahoma (NW1/4, NW1/4, Sec. 34 T.3N., R.6E. Ahloso Quadrangle). A 15 ft (4 m) vertical profile was constructed from the base of the outcrop and a total of 17 gamma-ray readings were collected perpendicular to bedding as well as a detailed lithofacies description.

The Henryhouse Creek outcrop is located along the banks of Henryhouse Creek (SW 1/4, SW 1/4, SE 1/4, SE 1/4, NE 1/4, Sec. 18 T.4S., R.2E). The Woodford Shale at this location is dipping 27^{o} almost due south in the direction of stream flow (Over, 1990). A 233 ft (71 m) vertical profile was constructed and a total of 291 gamma-ray readings were collected. Hand samples were taken of the Woodford Shale at the Henryhouse location for thin section analyses.

In an attempt to obtain an accurate reading from the gamma ray, fresh rock surfaces that provided a flat, smooth planar surface, perpendicular to bedding were

chosen when possible. This allowed the area of contact between the detector and collection site within the outcrop to be maximized. The gamma-ray detector was held steady against the outcrop for 60 seconds until the measurement was accumulated. The sampled diameter of the rock is 6.56 ft (2m) with the main contribution to the gamma-ray reading being the 1.64 ft (0.5 m) diameter around the detector (Gromadzki 2004).

In order to correlate the outcrops into the subsurface, K %, U-ppm, and Th-ppm were converted into API gamma ray units. This was accomplished with the equation available in Heron and Heron (1996). This equation provides the necessary data to convert the portable gamma-ray readings to API units:

API = 8 (+/-) 2 x (U-ppm) + 4 (+/-1) x (Th-ppm) + 16 (+-) 2 x (K wt %).

The data provided by the above equation allows for the radioactive measurements collected from outcrop to be converted into a gamma-ray profile. This gamma-ray profile can then be used to correlate into the subsurface to well logs taken from Murray County and towards the east of the studied locations.

Thin-Section Analysis

Thin sections were prepared by Mineralogy Inc., in Tulsa, Oklahoma. Thin sections were collected from two locations. Thin sections were prepared using a blue dye and were cut perpendicular to bedding. These thin sections were also pressure impregnated. Seventy-three thin sections of the Woodford Shale were visually inspected for composition, texture and grain size. Ten oversize (2'x3") thin sections were prepared for microscope analysis. Thirteen samples were prepared with special techniques because of clay sensitivity and extreme fissility. The goal of the thin sections analysis was to

obtain a more detailed view of the organic-rich matrix of the shale, the mineralogical composition of the lithofacies and the relationship between the minerals and the organics. Analysis of thin sections has the potential to determine whether the minerals are detrital or diagenetic in origin.

X – Ray Diffraction (XRD)

Thirty-eight samples from the I-35 outcrop were analyzed for XRD by Mineralogy Inc. Samples were crushed and a portion of the sample was ground in acetone in an agate mortar and then placed on a glass slide and scanned. Diagnostic peaks of minerals identified on the resulting diffractogram were rescanned on duplicate samples. The approximate weight percentages of mineral phases were determined by comparing diagnostic peak intensities with those generated by pure standard phases mixed in various known proportions. The goal of XRD is to determine the mineralogy and clays in the sample in terms of weight percent. This information can be used to help determine the composition of the shale relative to lithofacies as well as diagenetic history.

Total Organic Carbon (TOC)

Thirty-eight samples from the I-35 outcrop were analyzed for TOC by Humble Geochemical in Houston, Texas. TOC is the total organic carbon present in dry rock and is generally represented in weight percent. According to Schlumberger, TOC results represent anywhere from 70 to 90 percent of the kerogen (depending on type). Kerogen is a naturally occurring, insoluble organic matter that occurs in source rocks. Algae and woody plant material are typical organic constituents of kerogen. Kerogens are classified

based on three main types (Fig. 6). According to Schlumberger (2005), Type 1 kerogen consists of algal and amorphous material that is presumably also algal in origin. Type 1 kerogen is highly likely to generate oil. Type 2 kerogen is composed of mixed terrestrial and marine source material. Type 2 generates a waxy type of oil. Type 3 kerogen is contains a woody terrestrial source material and typically generates gas. TOC is measured by Rock Eval Pyrolysis or LECO. Humble geochemical analyzed the samples for TOC using LECO. This procedure involves the sample to be ground and weighed, the sample is then acidified with HCl (this removes all carbonates). Samples are then rinsed, dried and then analyzed in a combustion furnace. The furnace combusts the organic carbon and then the combusted organic carbon is then weighed as a percentage. Understanding the percentage of TOC and kerogen found within an outcrop could lead to the potential of predicting the hydrocarbon economic viability of the shale.

Statistical Analysis

K, U, Th and calculated API gamma-ray data were imported into SAS (Statistical Analysis System) and frequency distributions were constructed. The computer generated frequency charts from SAS provide information regarding the strength of the gamma-ray response in regards to lithofacies in the outcrops and the distribution of the key elements, K, U, and Th in the lithofacies. If these statistical associations hold significant relationships, then the gamma-ray profile in the outcrop can confidently by used to determine lithofacies in the subsurface.

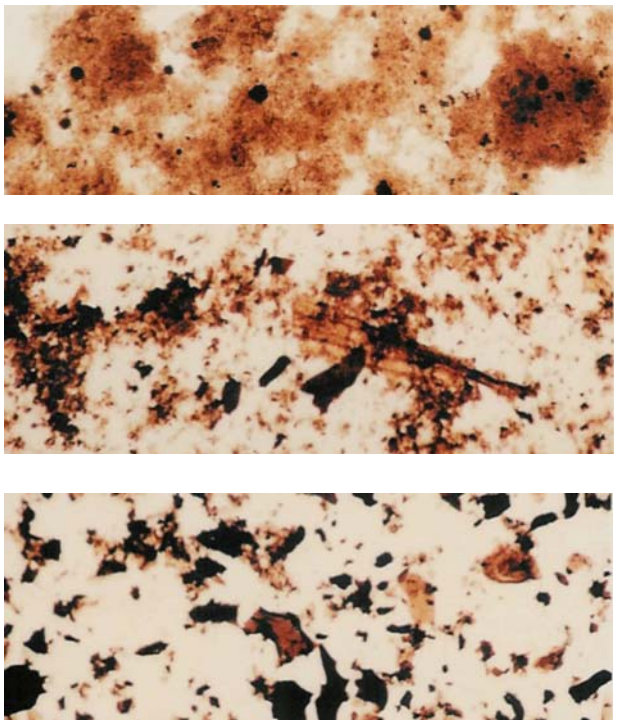

Figure 6. Thin section photographs representing the three kerogen types (Jarvie, Daniel (2004), Humble Geochemical Services).

Chapter 4

Gamma-Ray Characterization Results

Log Characteristics

The Woodford Shale of south-central Oklahoma is considered a "hot" shale that is easily identified on well logs. Radioactivity of the Woodford contrasts greatly with that of the underlying Hunton strata (Dennis, 2004). In comparison, rocks of the Hunton show gamma-ray deflection in the range of 10 to 60 API units, whereas shales of the Woodford are commonly in the range of 90 to 200+ API units (Dennis, 2004). The Woodford Shale was previously divided into three shale members from well-logs by Hester et al. (1988), (Fig. 7). According to Lambert (1996), the lower shale member has a gamma-ray deflection of more than 300 API units in the Oklahoma aulacogen. The middle shale member has a response that can be more than 320 API and the upper shale member produces a response that exceeds 213 API units in northwestern Oklahoma. Isopach maps of the shale members in northwestern Oklahoma and Kansas indicate that the middle Woodford Shale member has the greatest aerial extent and thickness (Lambert, 1996).

Gamma-Ray Characterization

A portable gamma-ray scintillometer was used to record gamma-ray radiation measurements on the surface of the Woodford Shale from the five studied outcrop locations; (1) McAlester Cemetery shale pit, (2) I-35, (3) Hunton quarry, (4) Brimley residence and (5) Henryhouse Creek. The radioactivity measurements were plotted against cumulative formation thickness in order to construct the vertical gamma-ray profile.

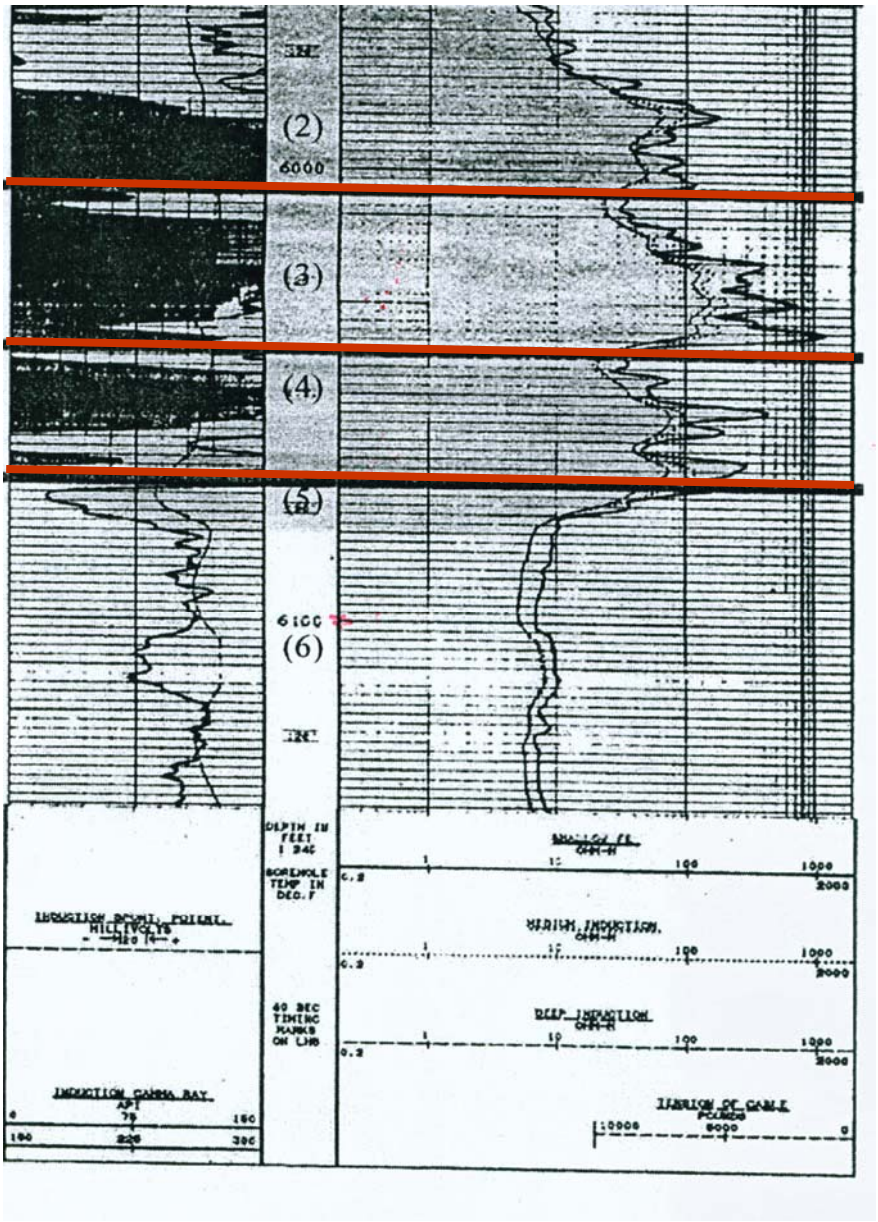

Figure 7. Well log from Logan County, Oklahoma showing the three Woodford Shale members; lower (4), middle (3) and upper (2), (as first defined by Hester 1988), (modified after Dennis, 2004).

The main objective is to determine the controls on gamma-ray response and to describe the outcrop based upon this response, so that rock properties can be deduced from sections in the subsurface.

McAlester Cemetery shale pit is located in the Criner Hills area. The Woodford Shale beds at this location are dipping 35^{o} to the northeast. The entire Woodford Shale is exposed in the southwest sloping quarry floor and face. The contact between the Hunton Group and the Woodford is represented at this location, but is not visible because of pond water coverage. McAlester outcrop transitions from fissile shale in the quarry floor, to siliceous, blocky shale, and then to a white chalk like shale moving up section that is composed of large phosphate nodules and concretions (Fig. 8). According to D.W. Kirkland and et al., (1992), the chalky white portion of the Woodford at this location is probably the result of weathering that occurred during the Quaternary. According to Kirkland et al., (1992), individual phosphate nodules in the upper Woodford contain thin, elongated nuclei that appear to be individual pieces of crustacean carapace. Some phosphate nodules contain nuclei that are interpreted to be the operculum (a plate that closed over the aperture) of ammonoids (Kirkland et al., 1992). Large, boulder size calcite concretions were noted at the McAlester location, but they were not in place. The source of these boulder-size concretions is unclear and they were not studied in detail by the author. A total of 87 feet (26 m) and 68 gamma-ray readings of the quarry bottom were measured to construct a vertical gamma-ray profile (Fig. 9). The entire gamma-ray profile is constructed from measurements taken from fissile shale. Gamma-ray results for this site yield uranium readings of 32.9 ppm (Fig.10), thorium 5.7 ppm (Fig.11) and potassium levels of 1.2% (Fig. 12)

Figure 8. (A) Soft, bleached, chalky upper Woodford Shale at McAlester Cemetery Shale Pit. (B) The abundant phosphate nodules found in the upper Woodford. (C) Yellow arrow is pointing to the large, boulder-size calcite concretions found at the McAlester Shale Pit.

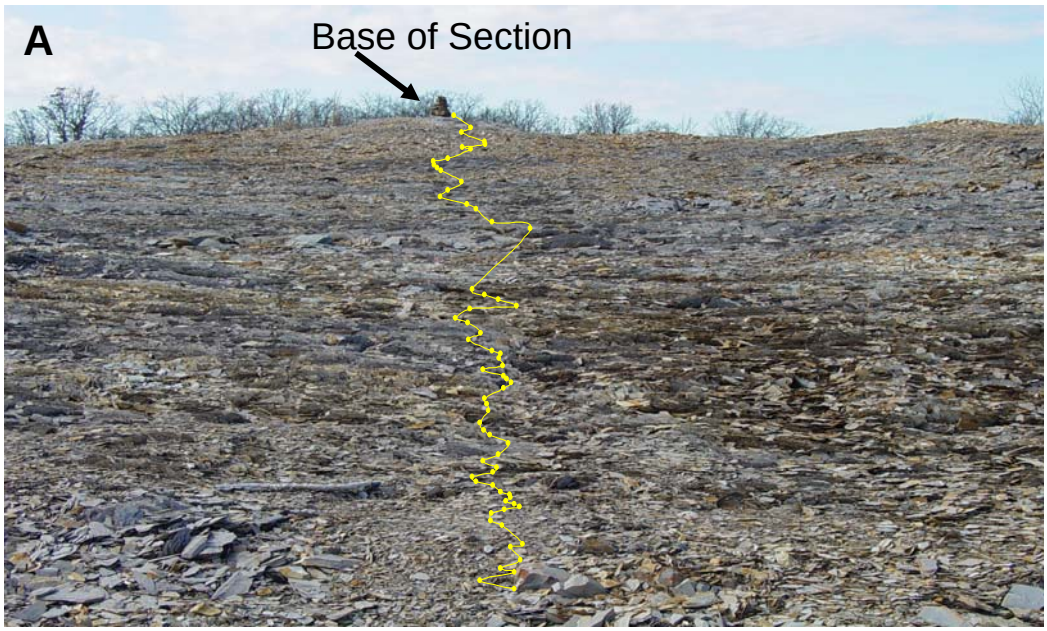

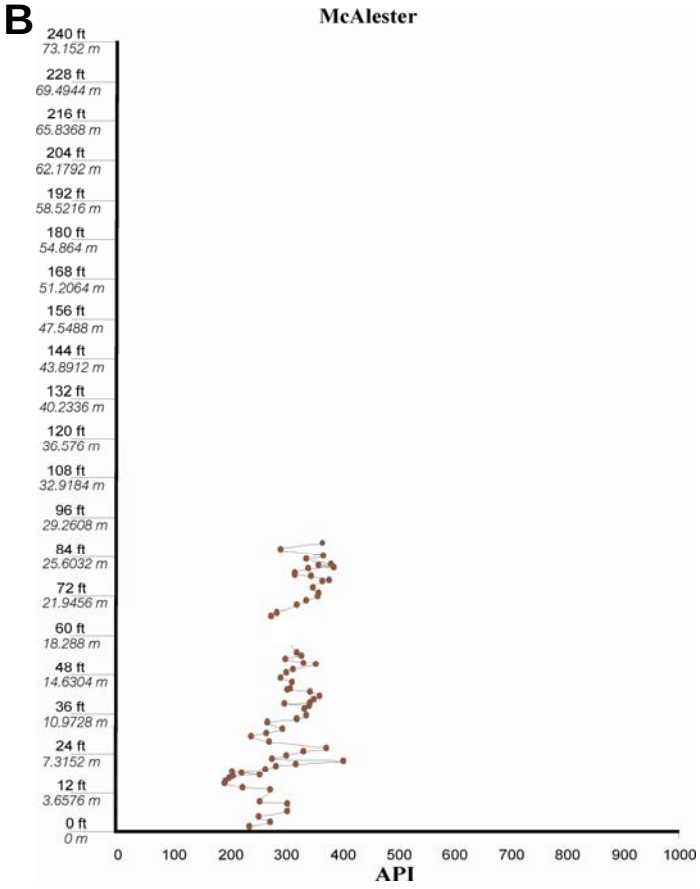

Figure 9. (A) McAlester Cemetery shale pit gamma-ray profile constructed from 87 feet (26 m) of fissile shale. (B) Gamma-ray profile constructed from data collected from McAlester Cemetery Shale Pit.

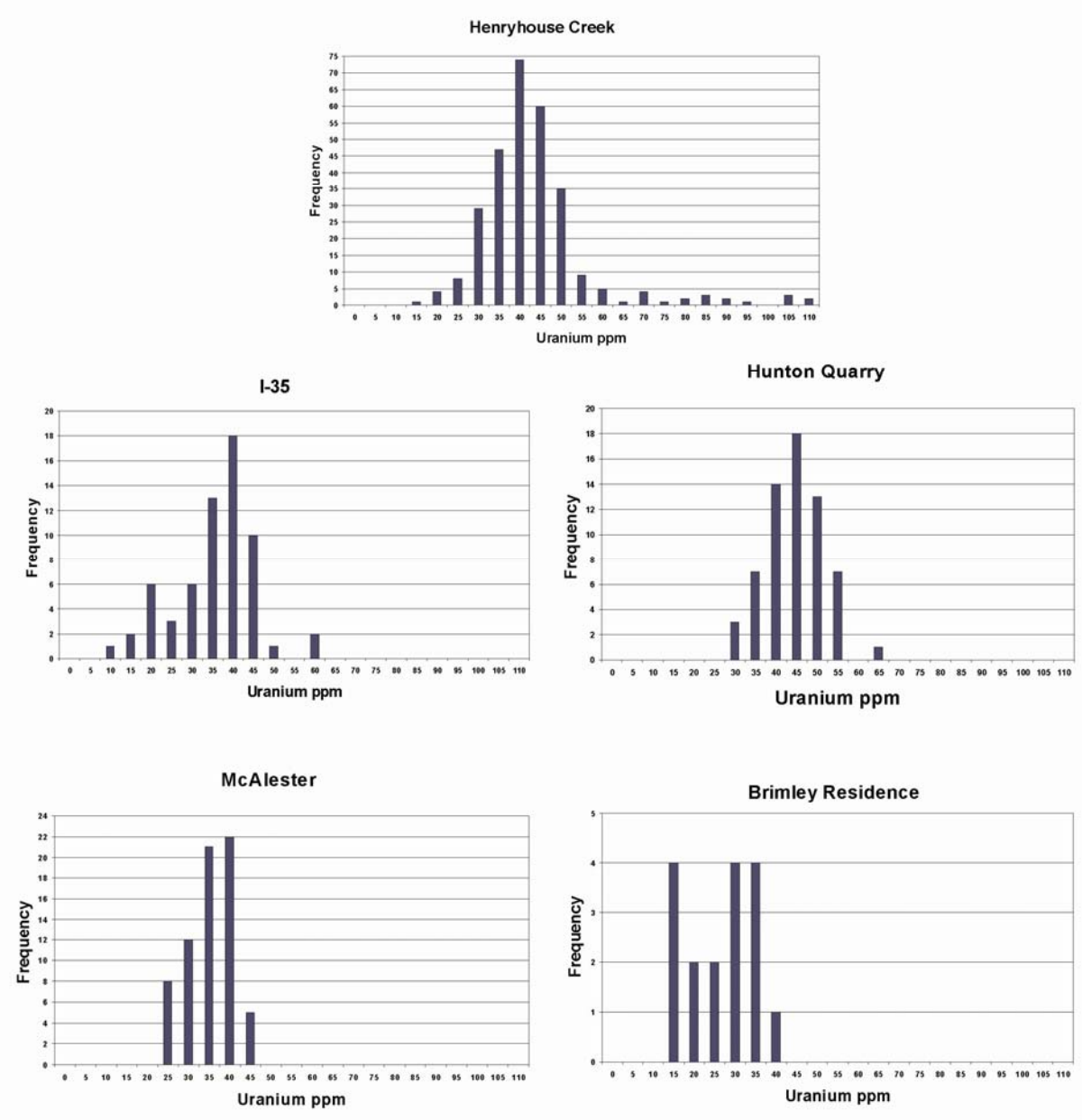

Figure 10. Gamma-ray frequency distribution for uranium measurements collected in the Woodford Shale study locations.

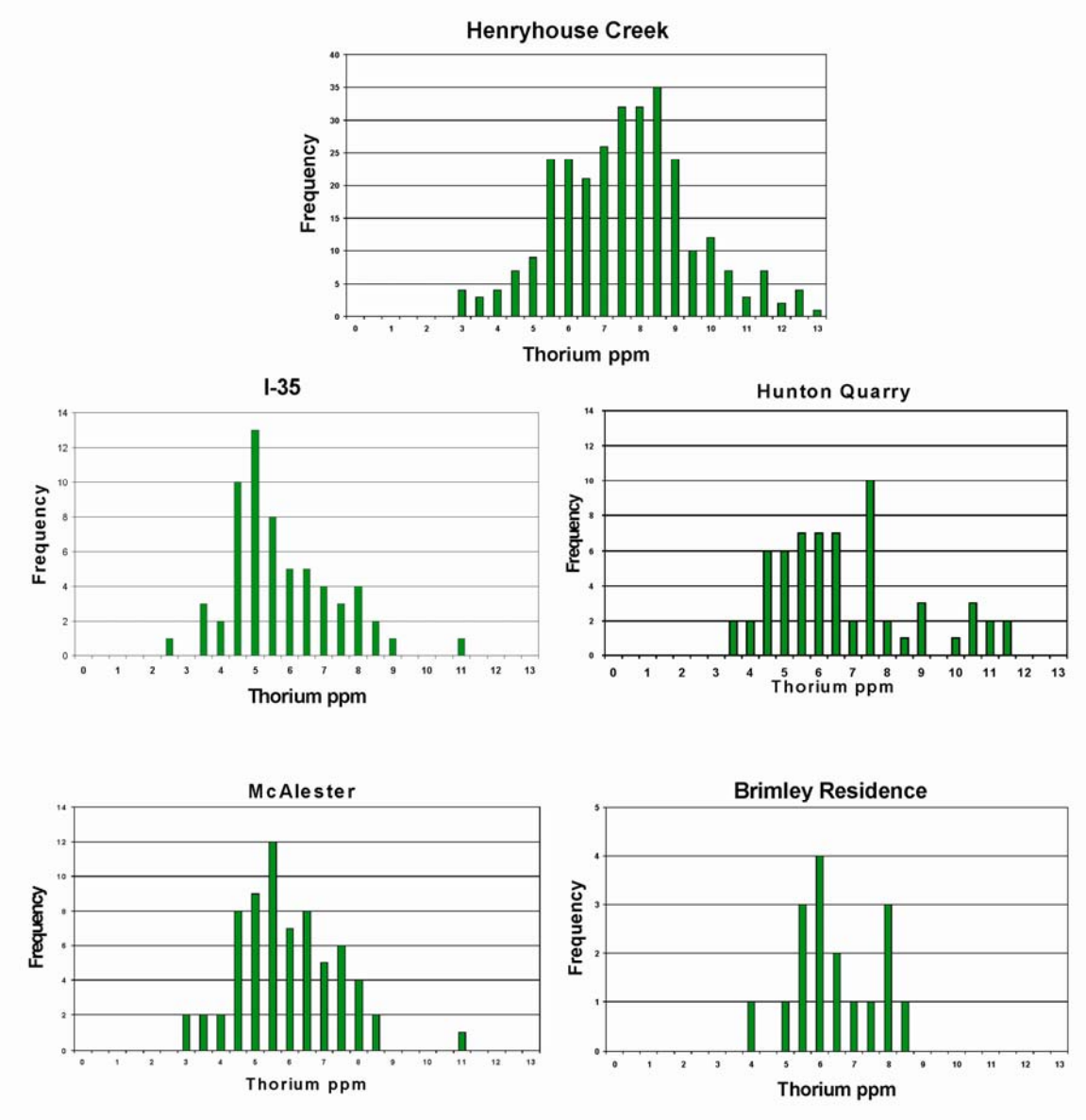

Figure 11. Gamma-Ray frequency distributions for thorium (ppm) content collected in the Woodford Shale study locations.

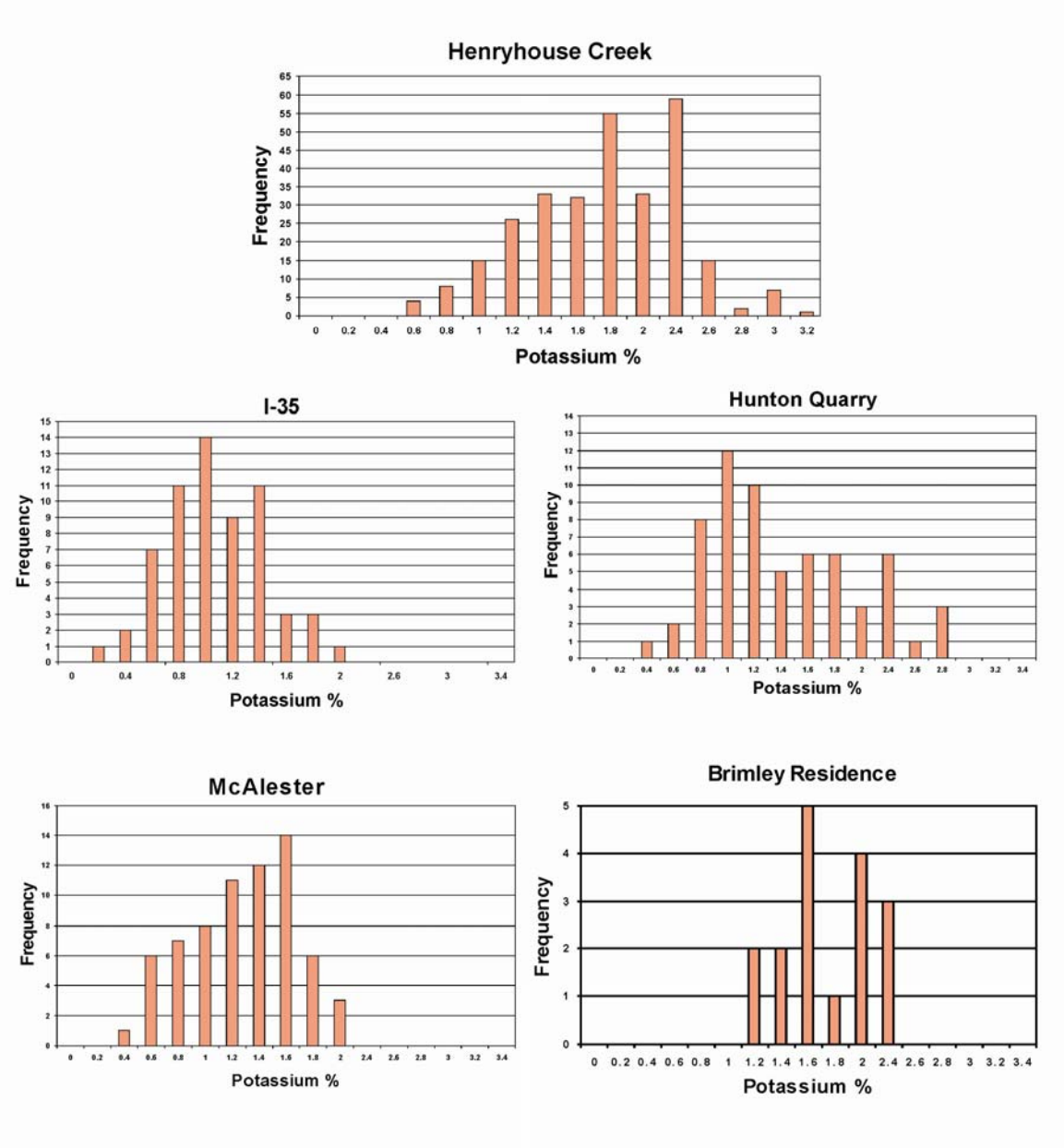

Figure 12. Gamma-ray frequency distributions for potassium % collected from the Woodford Shale study locations.

on average. The McAlester outcrop yielded uranium levels as low as 21.2 ppm and as high as 45 ppm.

The gamma-ray profile at this location (Fig. 9) is marked by transitions from increasing to decreasing API units that are documented on the profile moving up stratigraphic section. The base of the outcrop is characterized by a gamma-ray response of nearly 300 API units; this is followed by a decrease to 200 API units at 14 feet (4 m) in the section. Moving up stratigraphic section the gamma-ray profile shows an API deflection to the right that reaches over 400 units. This deflection in gamma-ray is then followed by a trend of both increasing and decreasing API units, but the API does not reach over 400 units again in this measured section. From 21 feet (6 m) to 25 feet (7 m) the gamma-ray profile is the "hottest" and is represented by over 400 API units. Weathering and an accumulation of rock debris caused missing values from 54 feet (16 m) to 65 feet (20 m).

The I-35 outcrop is located on the west side of the southbound lane of interstate 35. The upper Woodford Shale is exposed at this location with beds dipping 38^{o} to the south. The Hunton Group is located on the north side of the outcrop and the Sycamore Limestone on the south. The base of the Woodford is not exposed at this location and was probably eroded away by a small stream channel, which separates the Woodford from the Hunton Group. Because of high vegetation and precarious climbing conditions the contact point between the Sycamore Limestone and the Woodford was not established, but is presumed to be located within a highly vegetated area where a healthy Cottonwood tree is growing (Fig.13). A 68 ft (20 m) vertical profile was constructed from the base of the outcrop towards the top of the outcrop. This outcrop transitions

Figure 13. I-35 Woodford Shale outcrop. Pink arrow is pointing in the general area of the presumed Woodford and Sycamore Limestone contact. Black line is the Devonian-Carboniferous boundary according to Over (1990).

upward into fissile shale, intermittent beds of siliceous and fissile shale, phosphate nodules, and a limestone bed (Plate. 2). A total of 62 gamma-ray measurements were collected from the I-35 location (Fig. 14). Gamma-ray results yield uranium readings on average to be 33.2 ppm, thorium 5.6 ppm and potassium 1.0% (Figs 10, 11, 12). I-35 outcrop yielded uranium readings as high as 57.4 ppm and as low as 6.9 ppm. The gamma-ray profile for I-35 outcrop is representative of the upper Woodford Shale. The interval starting at the base of the I-35 section has an API unit of 400 that is followed by a decrease to 350 API units as you move up stratigraphic section. From 2 feet (0.6 m) to 15 feet (4.5 m) data is missing because of the amount of rock debris covering the outcrop. Progressing up stratigraphic section, at 16 feet (4.8 m) the gamma-ray profile has an API value of over 500. This is the "hottest" zone on the profile and is found from 16 feet (4.8 m) to about 19 feet (5.7 m). Continuing up stratigraphic section, the gamma-ray API units decrease. This decrease is represented by the light gray to darker gray shales, and the phosphate nodules that are common to the upper Woodford Shale.

The Hunton quarry outcrop is located in an abandoned shale pit on the south side of the Goddard Church Camp Road off of Route 10, heading south from Davis, Oklahoma. The Hunton Group limestone is clearly visible in this quarry, but a contact point was not established at this location. The base of the measured section is composed of siliceous shale with intermittent fissile shale. Progressing up the outcrop the Woodford Shale becomes more brittle and fissile. This is likely the result of quarrying. The Sycamore Limestone is not visible at this location. 55 feet (17 m) of vertical profile was constructed from the base of the outcrop towards the top of the outcrop. A total of 63

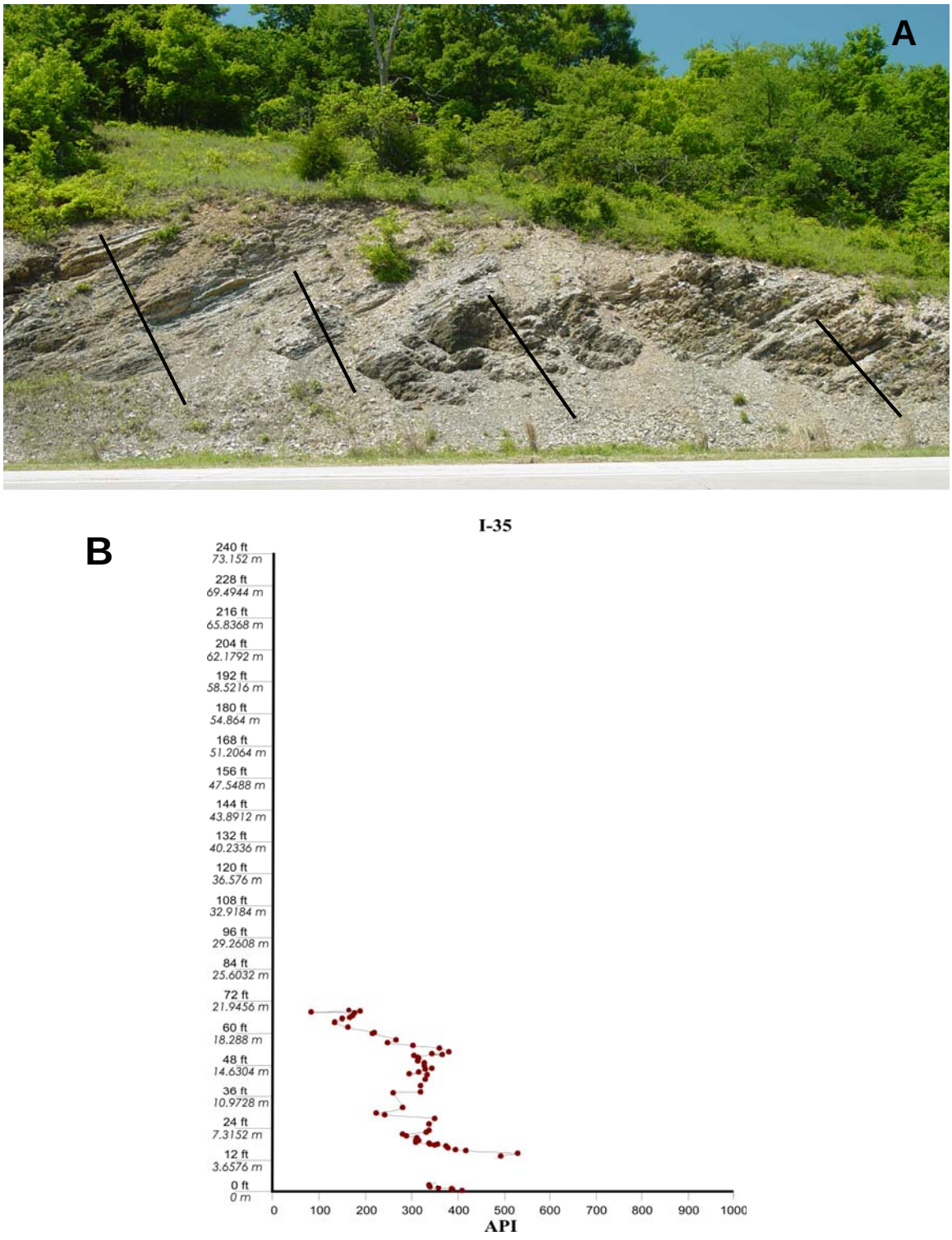

Figure 14. (A) I-35 outcrop showing general location of gamma-ray profiles. (B) Composite gamma-ray profile constructed from data collected from I-35.

gamma-ray measurements were collected from the Hunton quarry outcrop (Fig. 15). Gamma-ray results yield uranium readings on average of 42.0 ppm, thorium 6.6 ppm and potassium 1.4% (Figs. 10,11,12). The Hunton quarry yielded gamma-ray readings as high as 63.2 ppm, and as low as 28.2 ppm. The base of the Hunton Quarry gamma-ray profile is noted to be 440 API units. The API units decrease to 350 and then increase to 600 API units from 5 feet (1.5 m) to7 feet (2 m). This change in gamma-ray is followed by both increasing and decreasing API units, none of which falls below 250 or above 590 API units.

Brimley residence outcrop is located along the banks of the Jack Fork Creek near Ada, Oklahoma. The section contains gray to light gray colored shales and phosphate nodules and was determined to represent the upper Woodford Shale based on appearance alone. A 15 ft (4.5 m) vertical profile was constructed from the base of the outcrop to the top of the outcrop and a total of 17 gamma-ray readings were collected (Fig.16). Average uranium readings are around 24.2 ppm, thorium 6.3 ppm and 1.7 % potassium (Figs. 10, 11, 12). The Brimley residence yields uranium readings as high as 35.3 and as low as 11.8 ppm. Because of the thin exposure of the upper Woodford at this location, evaluations of the internal characters of the gamma-ray profile is limited.

The Henryhouse outcrop is located along the banks of Henryhouse Creek just south of the falls. The Woodford Shale at this location is dipping 27^{o} almost due south in the direction of stream flow (Over, 1990). The length of exposure along the creek is about 527 feet (160 m). The Woodford Shale in its entirety is represented at this location. The Hunton Group is visible on the northern side of the outcrop. The Sycamore Limestone is visible on the southern side of the outcrop. There is no direct contact

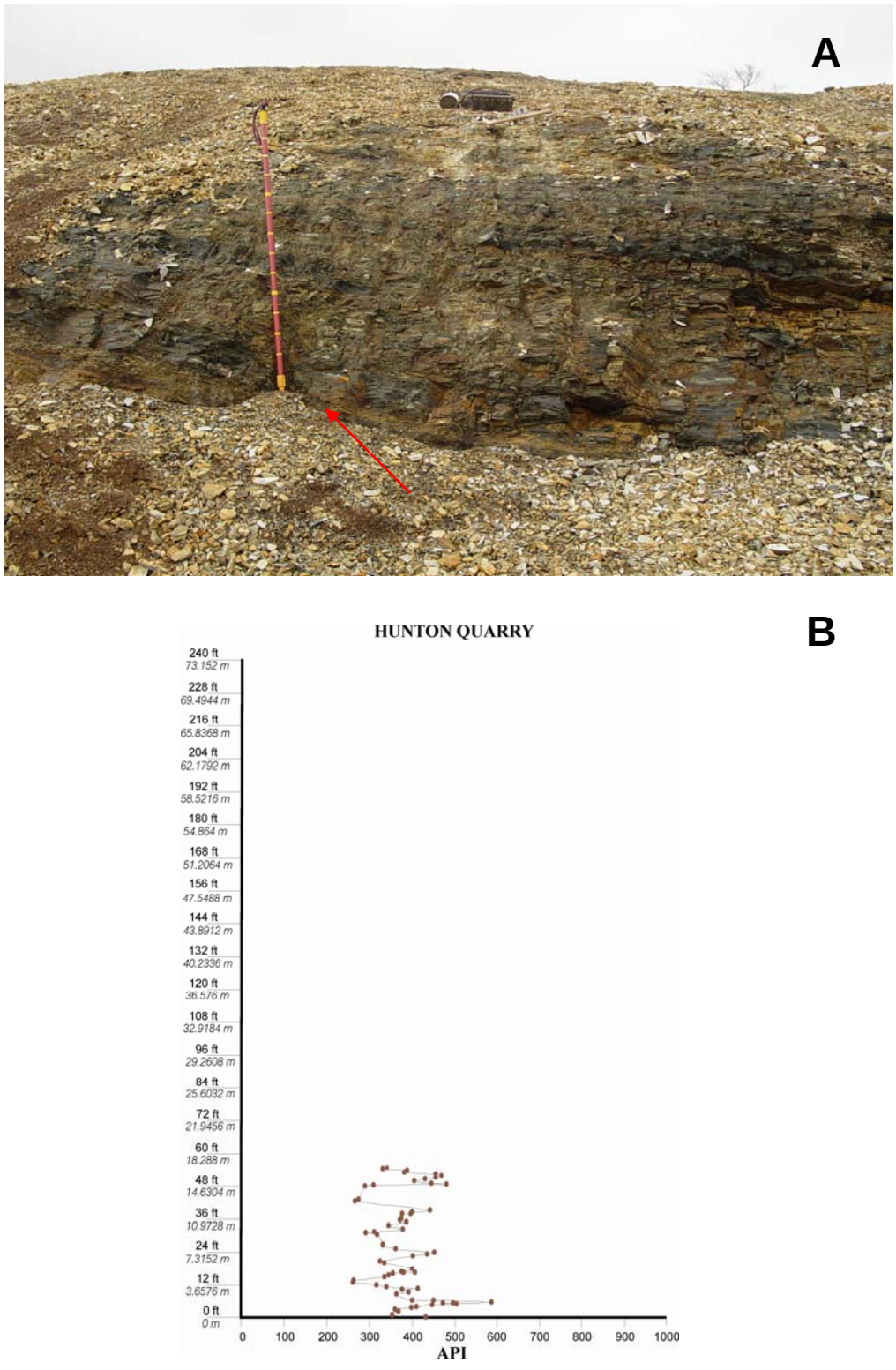

Figure 15. (A) Woodford Shale outcrop located at the Hunton quarry (staff is 1.5 m in height) Red arrow indicates the base of where the section was first measured. (B) Woodford Shale gamma-ray profile constructed from the Hunton quarry.

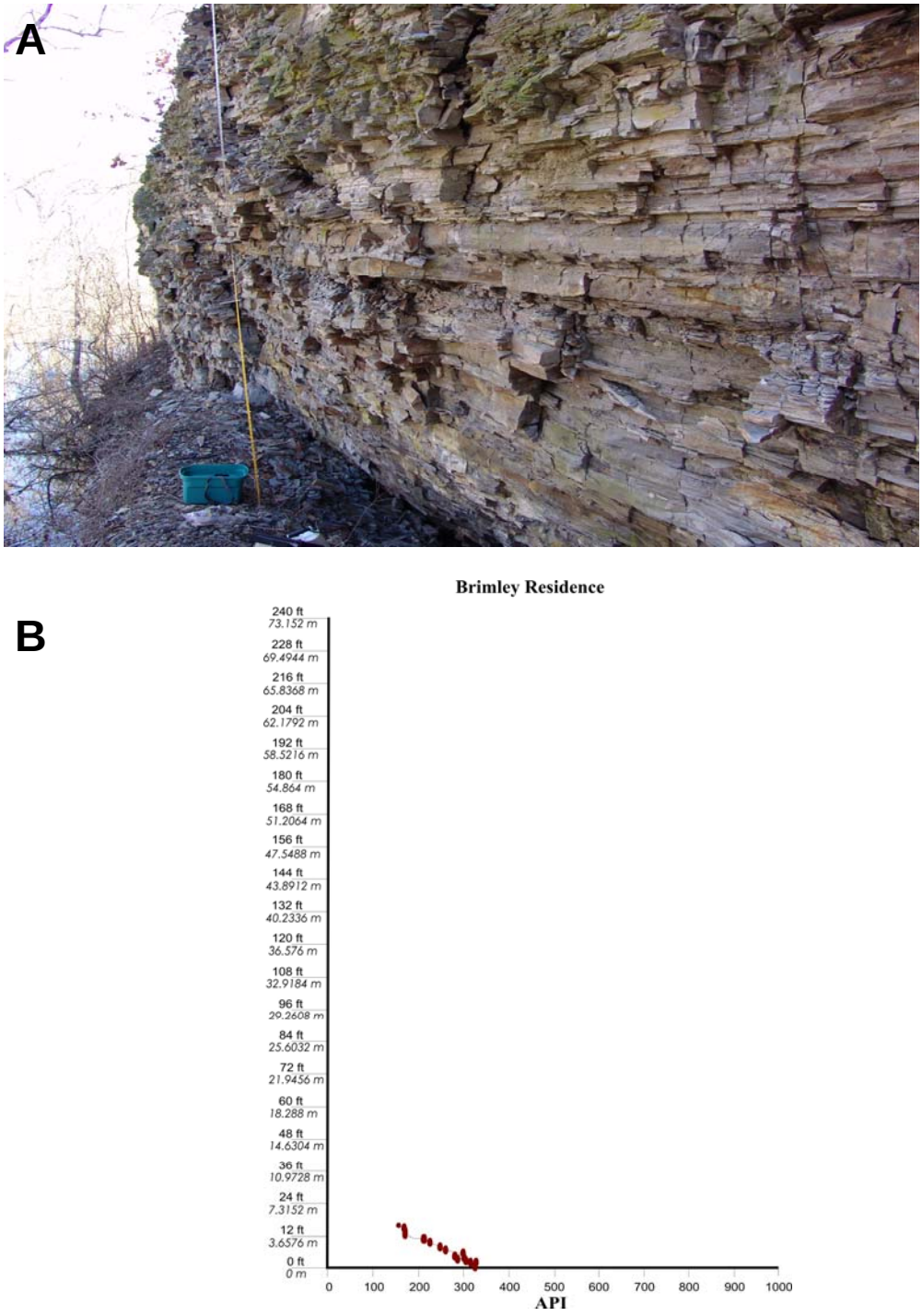

Figure 16. (A) Brimley residence Woodford Shale outcrop. (B) Woodford Shale gamma-ray profile constructed from data collected from the Brimley residence.

between the Sycamore Limestone and Woodford Shale at this location. A vertical profile of 233 feet (71 m) perpendicular to bedding was constructed from data collected at the outcrop. A total of 291 gamma-ray readings were collected from this outcrop (Fig. 17). The base is composed of organic-rich black shales, and siliceous shales with intermittent fissile shales. The middle Woodford is generally highly fissile and gray in color (weathered color). Transitioning from the middle Woodford weathering colors in the fissile shale are generally orange in color that transition into a siliceous shale that is blocky and occasionally greenish brown. The upper Woodford is composed of siliceous blocky beds, silty and phosphatic shales and phosphate nodules. Uranium was found on average to be 41.1 ppm, thorium 7.4 ppm and potassium 1.8% (Figs. 10, 11, 12). Within the Henryhouse Creek outcrop uranium is found as high as 106.3 ppm and as low as 13.3 ppm. The basal portion of the Henryhouse Creek profile is represented by a gamma-ray reading of 300 API units. Progressing up stratigraphic section, there is an increase of up to 600 API units in the gamma-ray profile between 10 feet (3 m) to 15 feet (4.5 m). Following this increase, the API units are found to vary between 250 to 450 API from 17 feet (5.1 m) to 153 feet (46.6 m). This is followed by a tremendous increase in the gamma-ray profile with API units reaching nearly 1000. This occurs from 154 feet to 173 feet (52.7 m) in the gamma-ray profile. This is then followed by a general decrease in the gamma-ray profile of API units that range from 150 to 500 API in the upper 59 feet (17.9 m) of the outcrop.

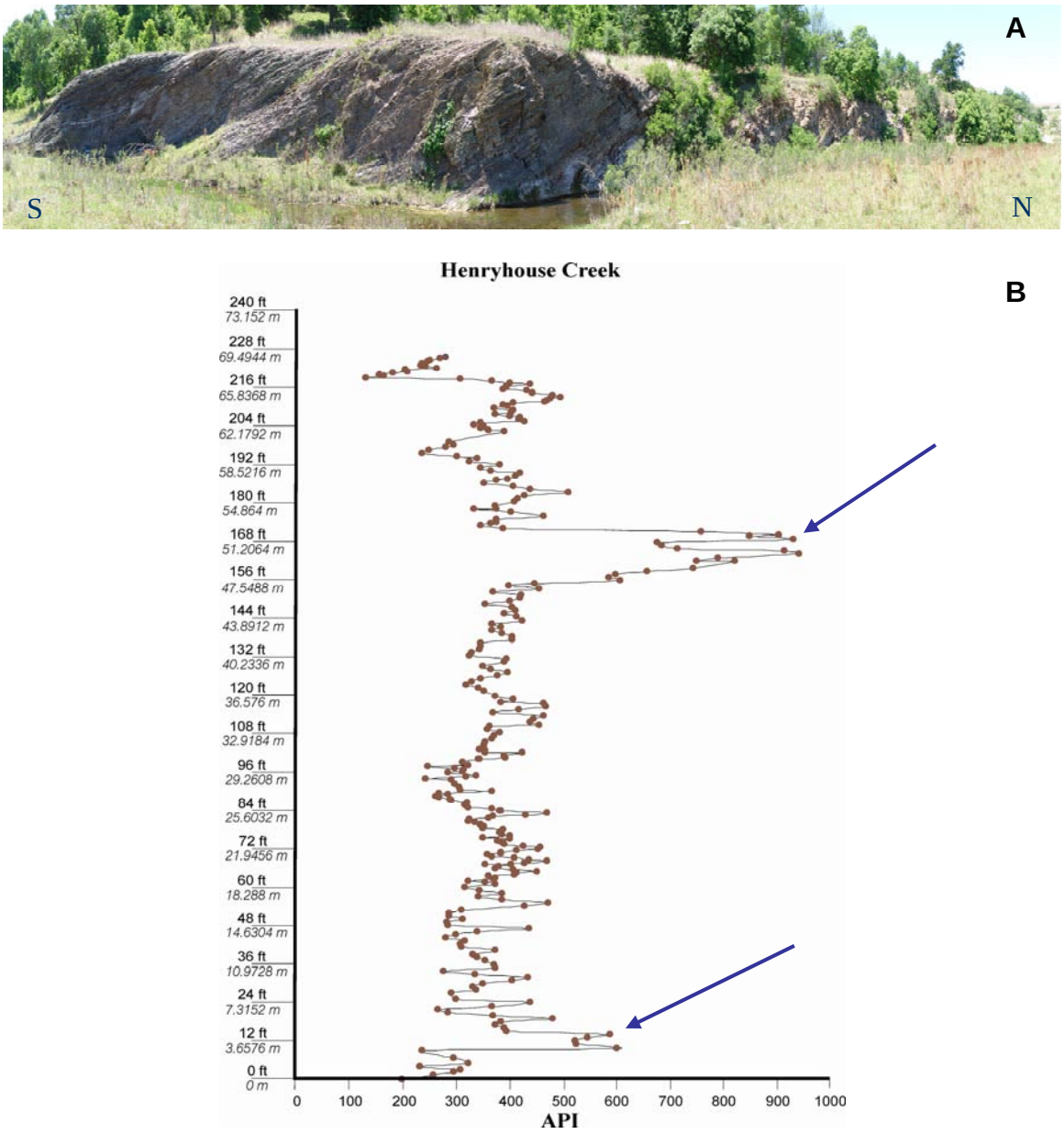

Figure 17. (A) Henryhouse Creek outcrop located near the falls area. (B) Gamma-ray profile constructed from data collected from the Henryhouse Creek section. Blue arrows indicate high gamma-ray peaks that are the direct result of the enrichment of uranium.

Discussion

Outcrop gamma-derived profiles from the five locations yield much higher API units than were previously documented by Lambert (1996). The studied outcrops yield an average API of 360 (Fig. 18) with a minimum value of 79 and a maximum value of 943 API units. The largest peaks that occur on the gamma-ray profile are interpreted to be maximum flooding surfaces (Fig. 17). These maximum flooding surfaces are enriched in uranium and suggest slow sediment accumulation period in which uranium would have ample time to diffuse downward into the chemically reducing sediment and become immobilized. Swanson (1962) calls the Woodford equivalent (Chattanooga) a uraniferous shale. To meet this classification, black shales should contain in excess 20 ppm, or 0.020 percent of uranium. The Woodford Shale outcrops in south-central Oklahoma meet this classification with average uranium content of 38.5 ppm (Fig. 19) and a maximum value of 106 ppm. Uniformity in uranium content and the high radioactivity compared with other sedimentary rocks are the reasons why the Woodford and most other black shales are used as "marker beds" in interpreting subsurface stratigraphy over large geographic areas (by gamma-ray logs from subsurface (Swanson, 1962). These observations support the conclusions that the uranium in this marine black shale was deposited nearly at the same time as the enclosing sediment and that the only logical source of the uranium in the black shales is the overlying sea water (Swanson, 1962). According to Swanson, (1962) the major sources of uranium in sea water are igneous, metamorphic, and sedimentary rocks that release their uranium to surface and ground waters as they are disintegrated by weathering processes. Most of the uranium is dissolved in the ground and surface waters and then transported to the sea in streams

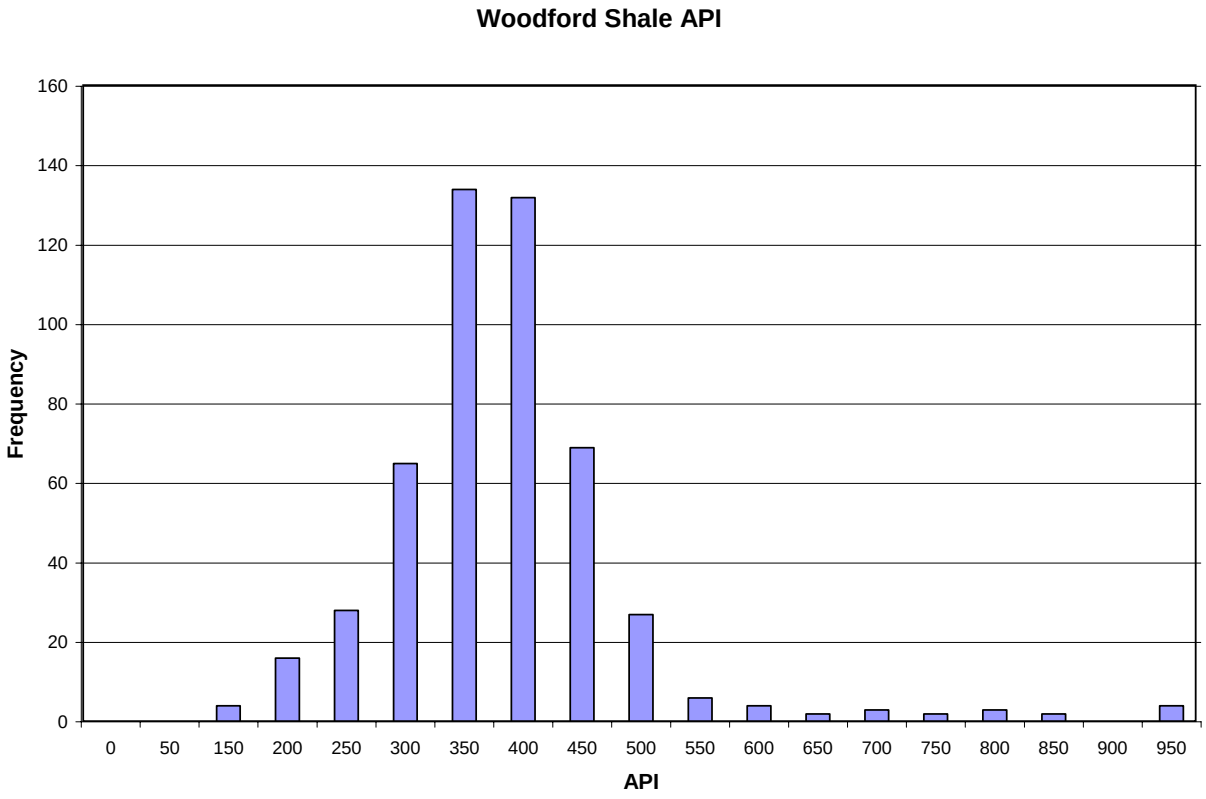

Figure 18. Frequency distributions of API units from the five Woodford Shale outcrops.

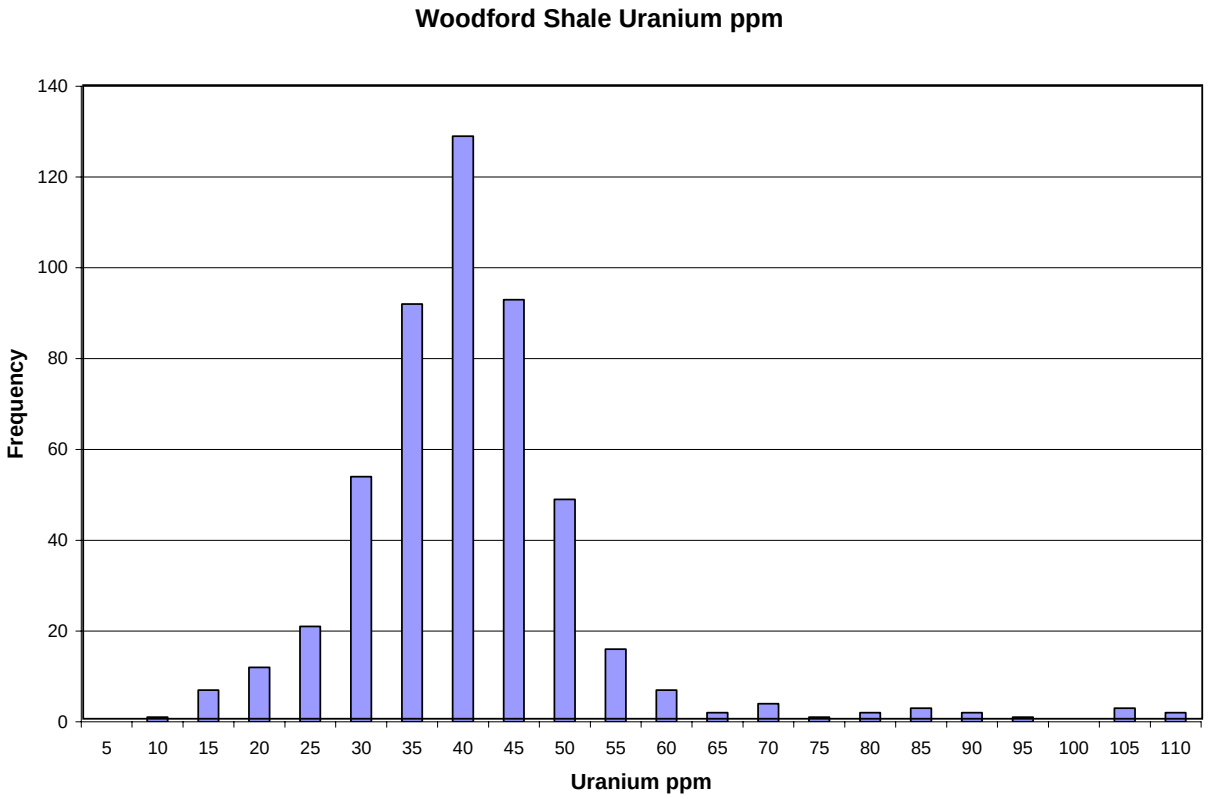

Figure 19. Uranium frequency distributions from the five studied Woodford Shale outcrops.

or rivers. More recent global mass balance calculations for uranium in the oceans support this conclusion. The dissolved uranium in the sea water may be present in several forms and is dependent mainly on the Eh of the water. Generally with a low Eh reducing environment uraninite precipitates (Jolly, 1988). In the normal slightly alkaline and oxidizing environment of sea water (pH about 8.0, Eh about +0.1), practically all the uranium is present in the hexavalent, or uranyl, form which combines with carbonate, sulfate, and other complex ions. These ions are highly soluble and widely distributed in the sea water (Swanson, 1962). Of all the sedimentary rocky types, only black shales have been found to contain large concentrations of syngenetic uranium (Olson, 1982). There are two main reasons why uranium is concentrated in black shales; (1) H_2S is produced by the decomposition of sulfur bearing organic debris. This lowers the Eh and uranium is deposited as uraninite (Swanson, 1961), (2) Uranium is extracted from sea water by humic acids. Hydrogen ions are displaced by ion exchange in slightly alkaline waters. With an Eh drop, the uranium bearing humic acids flocculate and fall to the sea floor. The uranium in black shales is disseminated in the rock (Jolly, 1988). In comparison, marine black shales that are deposited in rapidly subsiding marginal basins contain less uranium than black shales that are deposited in epicontinental seas on the more stable cratonic areas. This observation suggests sedimentation rates may influence uranium content (Swanson, 1961). If the depositional environment is humic-acid rich, such as in the case of a black shale, variations in uranium content would vary directly with sedimentation rate. In addition, Olson (1982), determined that the amount of uranium associated with the organic fraction is proportional to the length of time between introductions of the organic material to reducing marine waters through burial to a depth

where uranium can no longer effectively diffuse from the overlying water column into the pore water adjacent to the organic material. This period of time is believed to be largely controlled by the rate of sediment accumulation. Data results from elemental, visual, and pyrolysis studies indicate that organic matter type is uniform within south-central Oklahoma and therefore kerogen type cannot be a factor in controlling the uranium content of the Woodford Shale (Olson, 1982).

Gromadzki (2004), used outcrop-based gamma-ray profiles to analyze arsenic occurrence in relationship to sedimentary lithofacies and depositional environments in continental red-bed aquifers. Gromadzki's data for the mudstones and siltstones in comparison with the marine deposited shales of the Woodford yields uranium on average of 3.1 ppm, thorium 12.38 ppm and 1.5% potassium (Fig. 20). The Woodford outcrops average uranium is 38.5 ppm, thorium 6.8 ppm and 1.5% potassium. Continental red-beds and fluvial deposits in the rock record are expected to be lower in uranium content than black marine shales because uranium content is mobilized under oxidizing conditions (subarial weathering).

One might assume that a uraniferous organic-rich black shale such as the Woodford would also contain uranium-enriched nodules. Outcrop gamma-ray profiles of the upper Woodford show a decrease in the amount of uranium in the upper Woodford where the nodules are located, suggesting this is not the case. Moreover, the whole-rock geochemistry data from Siy (1988), who studied the nodules, reports no uranium. This change in the gamma-ray profile is represented in the upper portion of the Henryhouse Creek and I-35 outcrops (Figs. 21, 22) and at the Brimley residence.

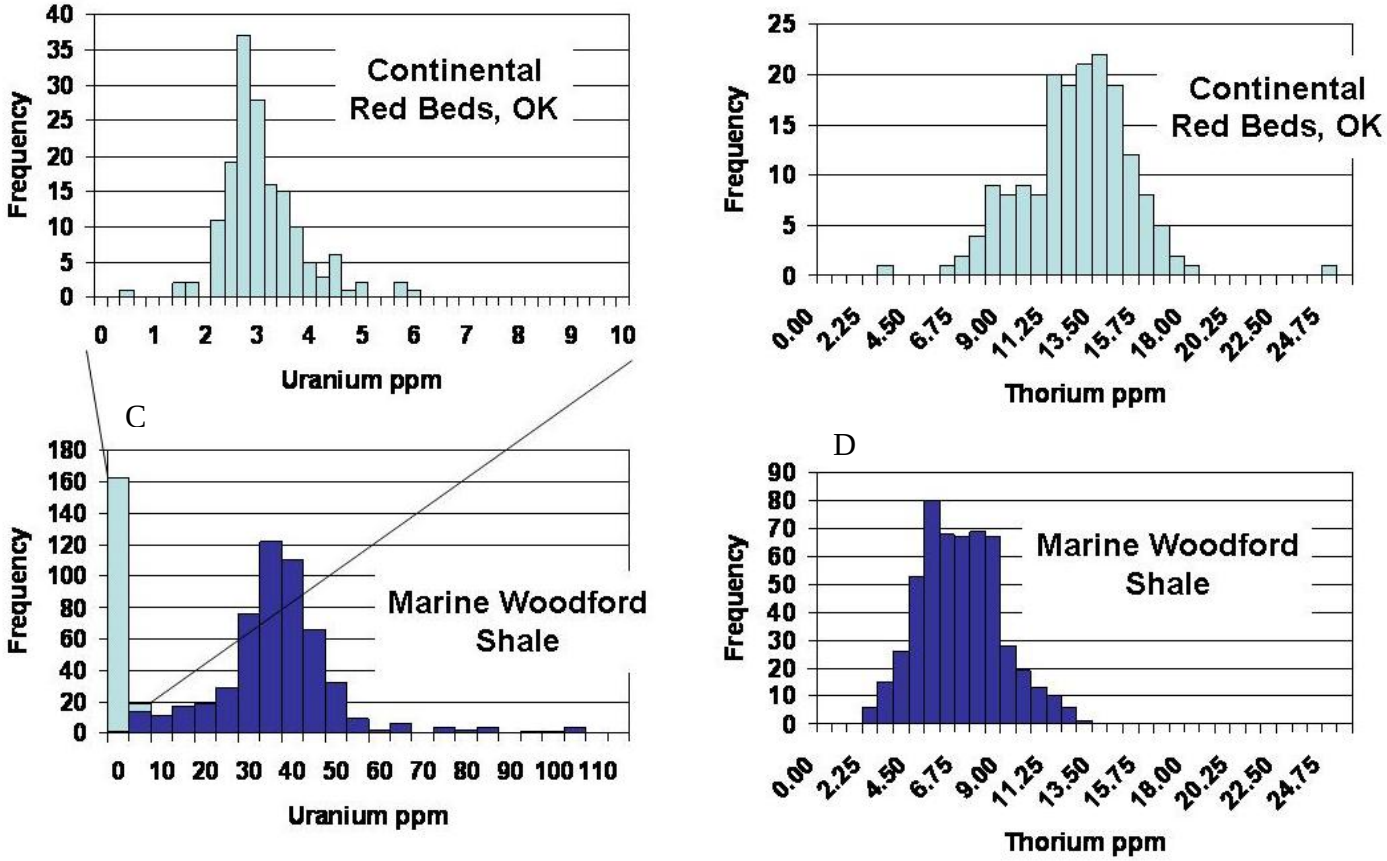

Figure 20. Marine Woodford in comparison with Gromadzki's continental red beds of Oklahoma Note the scale change in uranium histogram (A vs. C), (Gromadzki, 2004).

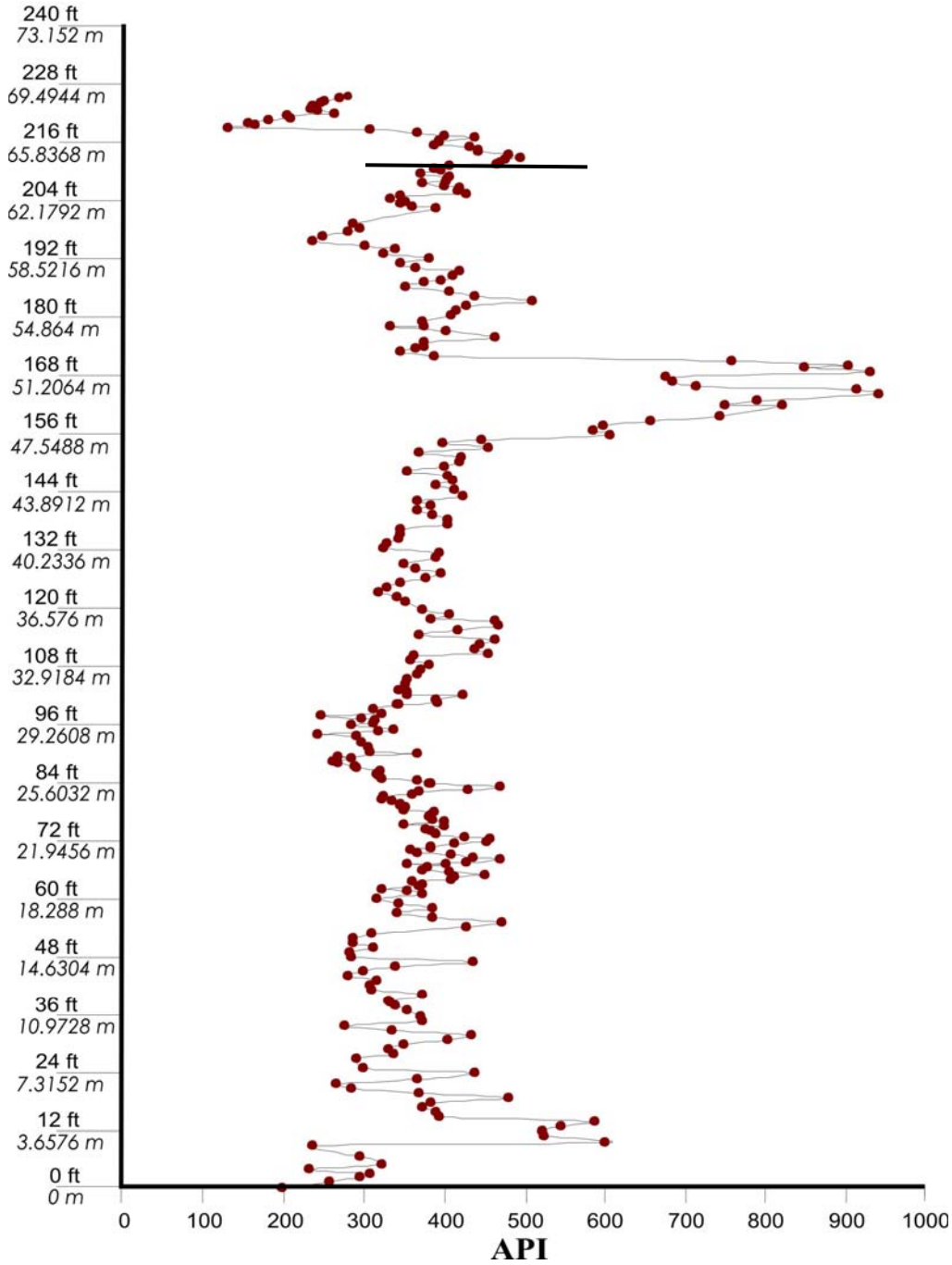

Figure 21. Outcrop derived gamma-ray profile of the Henryhouse Creek section, above the black line indicates phosphate nodule zone.

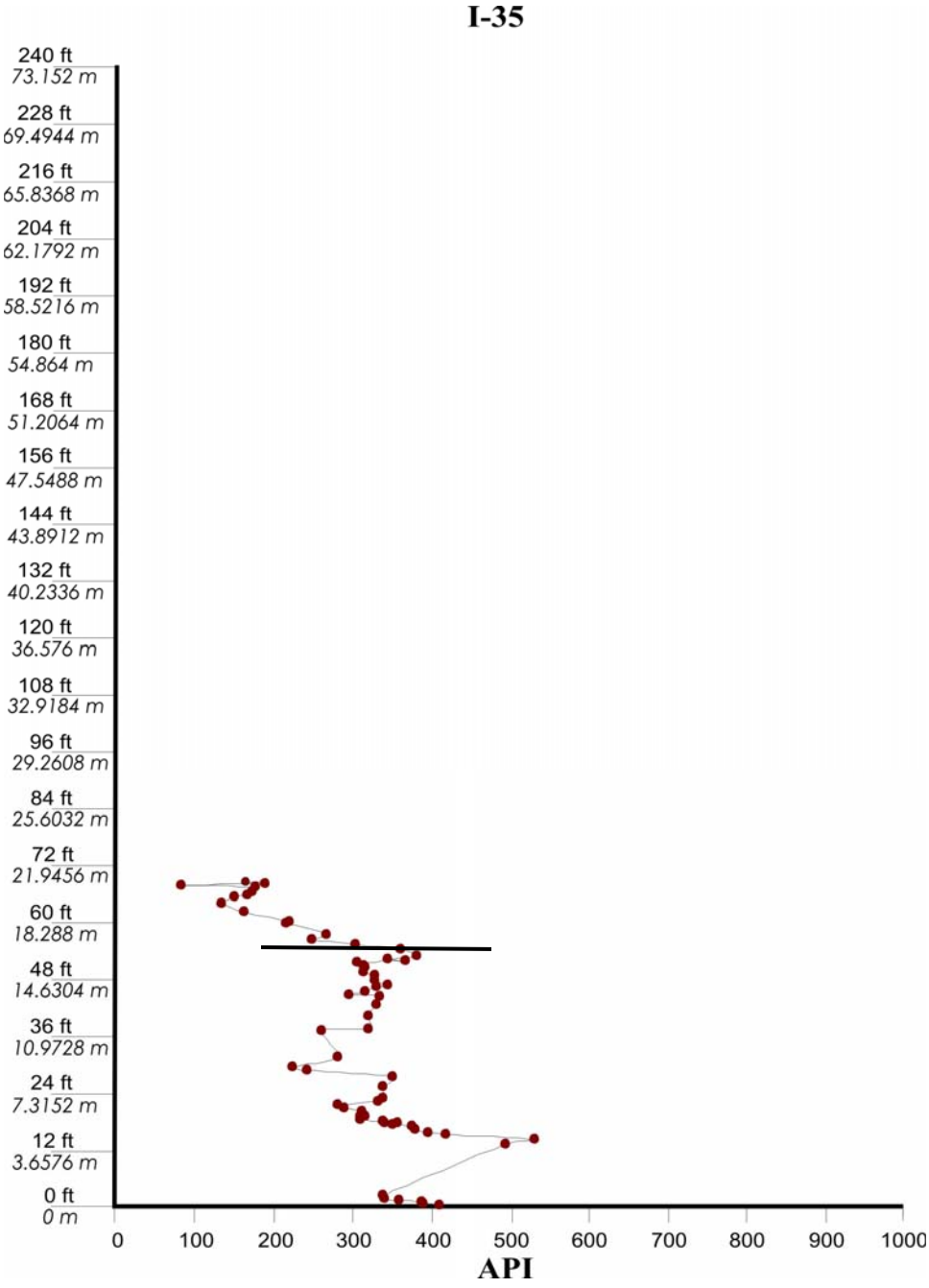

Figure 22. Outcrop derived gamma-ray profile of the I-35 outcrop, above black line indicates phosphate nodule zone.

According to Swanson (1962), the occurrence of uranium content in nodules depends on the timing of the nodule formation and is represented by four scenarios (Fig. 23). The four scenarios are as follows; (1) phosphate is not deposited and uranium is concentrated in the sediment by organic matter or by chemical reduction through the action of hydrogen sulfide, (2) scattered phosphate nodules form in the sediment but the amount of uranium that substitutes for calcium in the carbonate fluorapatite is in large part dependent on the availability of the uranium in the waters where precipitation of phosphate takes place; when considering the phosphate nodules of the upper Chatanooga Shale, Swanson concluded the uranium in these waters had already been depleted by direct hydrogen sulfide precipitation, and the resulting phosphate nodules contain little or no uranium, (3) major phosphate deposition takes place at the sea floor sufficient water circulation involved to result in phosphate nodules containing 0.01 to 0.10 percent uranium and scenario (4) a minor amount of phosphate is precipitated, the phosphatic particles may have a high uranium content, but the rocks that house the nodules rarely contain more than a few parts per million uranium (Swanson, 1962). The Woodford Shale phosphate nodules probably represent scenario 2 and may be indicative of a lesser amount of uranium accumulation. If sulfide had not reached the location of phosphate precipitation, and uranium was available in the waters, the phosphate nodules in the upper Woodford deposited during scenario 2 could have the potential to contain several hundredths percent uranium (Swanson, 1962). Siy, (1988) determined that certain elements other than uranium are enriched in the phosphate nodules of the Woodford Shale. Sr, Y, La, Ce, and Sc are some elements that are enriched in the I-35 phosphate

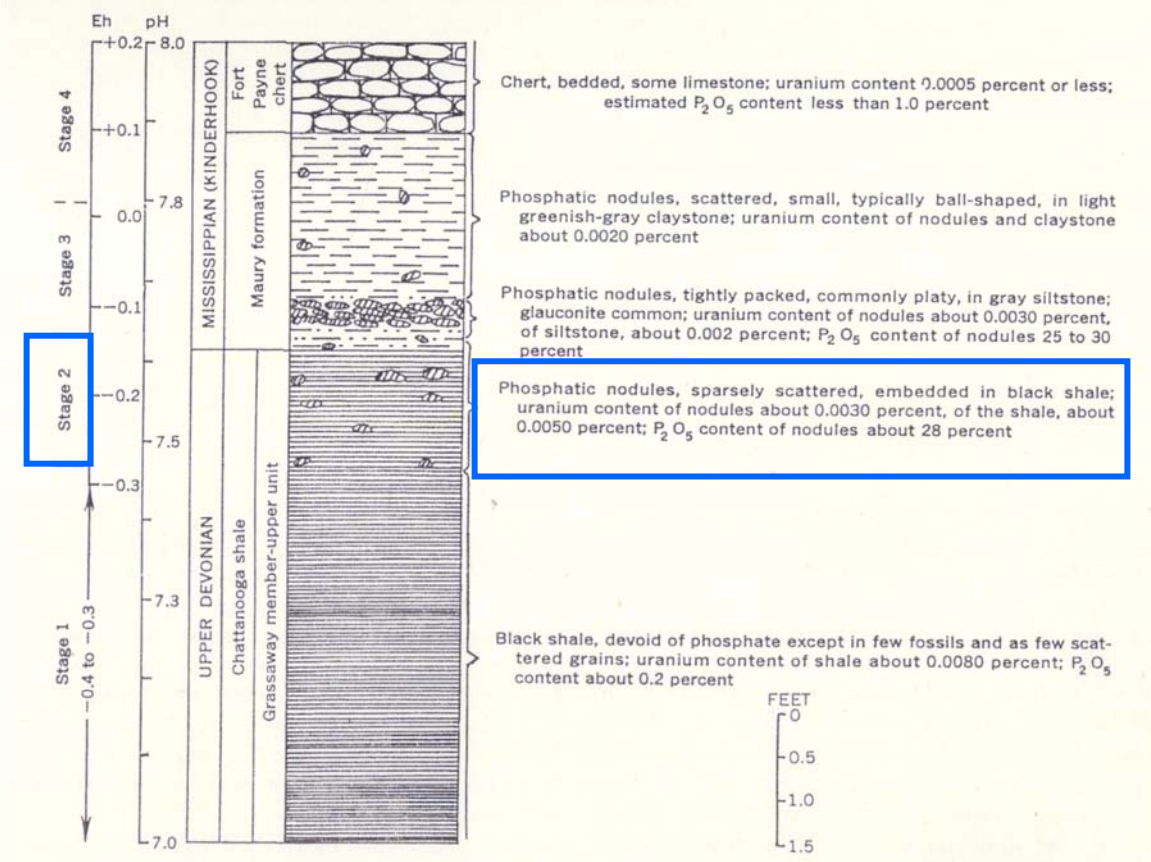

Figure 23. Stratigraphic section representing the four stages as related to the distribution of phosphate in the Chattanooga Shale with interpreted pH and Eh that existed in the time of deposition in upper Devonian-Mississippian black shales (modified after Swanson, 1962).

nodules either by substitution of calcium or by association with specific apatite morphologies (La, Ce, and Nb), (Siy, 1988).

Correlation

The three shale members of the Woodford as defined by Hester et al., (1988), for the Permian basin, by Lambert (1992) in Kansas, and by Dennis (2004) for Logan County, Oklahoma are clearly visible on the outcrop based gamma-ray profiles of the Woodford Shale constructed for this study (Fig. 24). These three shale members are informally named the lower, middle, and upper members, nomenclature adopted by Lambert, (1992). The Henryhouse outcrop profile is used to highlight these three members because at this location the entire Woodford Shale is exposed. The lower Woodford Shale at Henryhouse is about 60 feet (18 m) thick and is represented by uranium readings from 19.8 to 66 ppm with an average of 36.9 ppm. API units in the lower Woodford Shale member fall between 198-602 API units with an API average of 355. The middle shale member is about 120 feet (36 m) thick with uranium readings that fall between 22.4 to 106 ppm with an average of 43.4 ppm. API units in the middle Woodford Shale range from 242-943 API with an average of 410 API units. The upper Woodford Shale is about 60 feet (18 m) thick and is represented by uranium readings from 13.3 to 57.5 ppm with an average of 39.2 ppm. The API units in the upper Woodford range from 130 to 510 API units with an average API of 355. The outcrop-based gamma-ray profile suggests that the upper Woodford Shale can further be divided into a fourth member. This member is based upon the occurrence of abundant phosphate nodules at Henryhouse (Fig. 24) and is represented by the upper 14 feet (4 m) of the

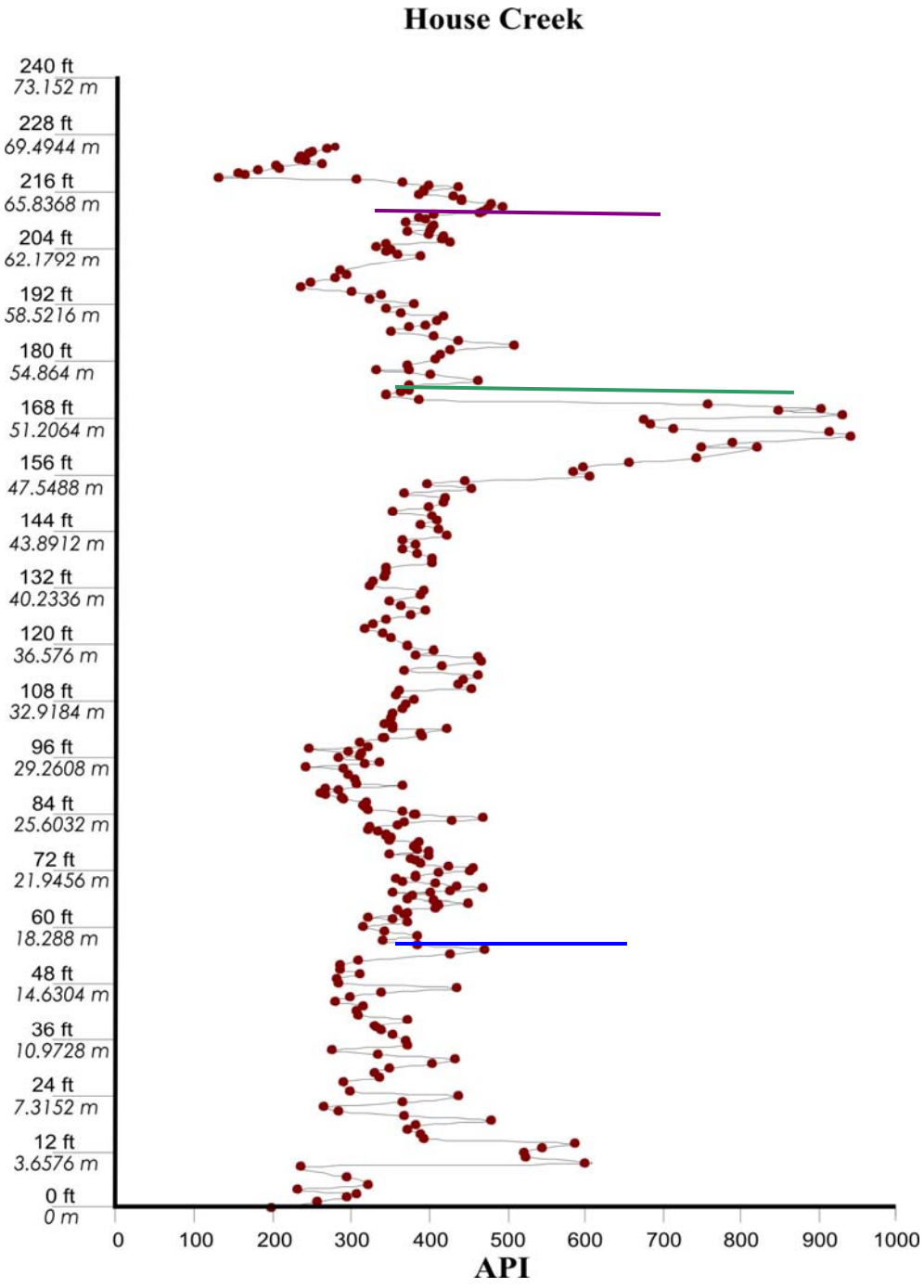

Figure 24. Henryhouse section showing the lower, middle and upper shale members. The blue line indicates the top of the lower shale member and the bottom of the middle shale member. The green line indicates the top of the middle shale member and the bottom of the upper shale member. The purple line indicates the bottom of the fourth member (zone where the phosphate nodules appear).

Woodford Shale. Uranium readings from this zone are from 13.3 to 57 ppm with an average of 36.3. API units in the phosphate zone range from 130-496 API units with an average of 329 API.

The shale members in the outcrop-based gamma-ray profile of the Henryhouse section can then be correlated to the other four studied outcrops in south-central Oklahoma (Plate. 3). The upper 30 feet (9 m) of the Woodford Shale from the Henryhouse section can be correlated to the 68 foot (20 m) of the I-35 section where only the upper Woodford is exposed. The I-35 section can then be correlated to the Brimley residence outcrop where the upper Woodford Shale is 17 feet (5 m) thick. A portion of the middle shale member from 81 feet (24 m) to 147 feet (45 m) of the Henryhouse section can be correlated to McAlester Cemetery shale pit from about 23 feet (7 m) to about 85 feet (26 m). The McAlester outcrop from about 21 feet (6 m) to about 81 feet (24 m) can be correlated to the Hunton quarry outcrop from about 6 feet (1.8 m) to about 54 feet (16 m).

These members along with outcrop-based gamma-ray profiles can also be used to correlate outcrops into the subsurface (Plate. 4) Because gamma-ray logs are continuous curves, in contrast to the sequences of closely spaced, connected points composing a vertical outcrop profile, gamma-ray logs and outcrop profiles are not identical (Ettensohn, 1979). That outcrop-based gamma-ray profiles of the Woodford can be correlated into the subsurface has economic significance. The ability to correlate between outcrop profiles provides an important context for which rock properties can be projected into the subsurface. These properties provide insight as to the potential zones that may be the most economically viable for gas in the subsurface. For instance,

viewing what the siliceous shales look like in outcrop and making comparisons to subsurface, potentially can help exploration geologists locate portions of the section that are; 1) easily fractured and 2) difficult to drill through, particularly in the case of horizontal drilling.

Chapter 5
Petrology Results

Lithofacies in Outcrop

The Woodford Shale of south-central Oklahoma is an organic-rich black shale that also contains phosphatic shale, siliceous shale, rare chert, rare bedded limestone, bedded dolomite and phosphate nodules. The bulk of the shale in the Woodford has two main habits, fissile and non-fissile (Fig. 25**)**. The non-fissile habit contains phosphatic shale, rare chert, siliceous shale, phosphate nodules (housed in the fissile shale) and (occasionally) a carbonate bed. Lithofacies found within the fissile shales category are the more highly organic-rich shales, phosphatic shales and phosphate nodules. The fissile lithofacies are composed of laminations that are between 1-4 centimeters thick (Fig. 26) and are occasionally silty (<.065mm). Portions of these organic-rich fissile shales are very finely laminated (<3mm). Siliceous shale has a blocky appearance and ranges between 1-6 centimeters **(**Fig. 27) in thickness. On occasion both siliceous and fissile shales are interlaminated on about a 1-2 cm scale, suggesting lateral gradation changes occur between these two lithofacies and are noted in outcrop.

Dark gray to black shales are commonly found at the base of the Woodford just above the carbonates of the Hunton Group. The lower basal Woodford is represented by a maximum flooding surface that is common on the gamma-ray profile (Fig. 17). For wells located to the east of the study area, the base of the Woodford just above the Hunton Group carbonates contains dolomitic rip-ups and rock fragments (Devon Study, 2004). According to the Henryhouse outcrop, the lower Woodford Shale is about

Figure 25. Woodford Shale along I-35, green arrow indicates siliceous shale, pink arrow indicates fissile shale (penny for scale).

Figure 26. Woodford Shale along I-35, yellow circle indicates fissile shale that is laminated <1 cm thick.

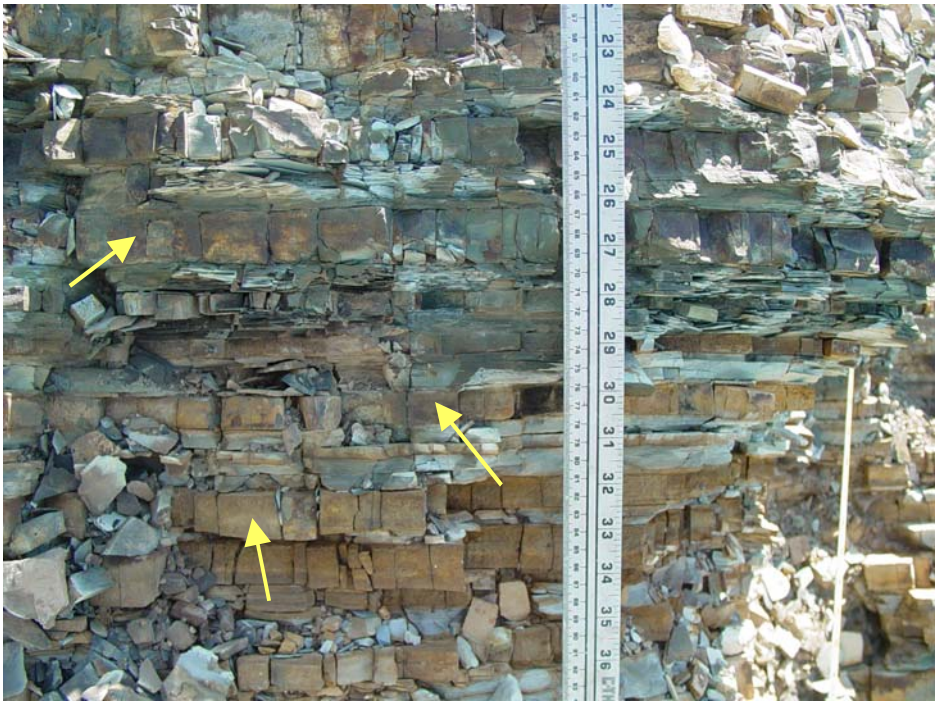

Figure 27. Woodford Shale at Brimley residence; yellow arrows indicate siliceous, blocky shale.

60 feet (18 m) thick. The middle section of the Woodford Shale is 120 feet (36 m) thick in outcrop and contains both a fissile and a gray to black silty shale that is horizontally laminated. Diagenetic nodular pyrite, marcasite and detrital mica are visible in outcrop. The pyrite concretions are the result of anaerobic oxidation of organic matter by sulfate reducing bacteria (D.W. Kirkland et al., 1992). The upper section of the Woodford Shale is 60 feet (18 m) thick in outcrop and is much lighter in color than the base and the middle Woodford, and is generally light grey to sometimes white. Phosphate, siliceous phosphate, phosphate nodules and occasionally chert compose the upper portion of the Woodford Shale (Fig. 28). Dolomite beds are found in the lower, middle and upper Woodford (Fig. 29) Organic-rich beds that have a coal-like appearance occur in the upper Woodford at the Henryhouse outcrop.

Thin-section Analysis

Thin sections were collected from the upper Woodford Shale from the I-35 and House Creek localities and thin sections from the lower Woodford Shale were analyzed by TerraTek in Salt Lake City, Utah. A 2004 Devon Study revealed that the base of the Woodford is made up of dolomitic rip-up clasts, rock fragments, including reworked sandstone clasts and other mineral grains: glauconite, quartz and chert (Fig. 30). Glauconite is usually a result of locally reducing conditions in an oxidizing environment and is commonly found in the basal portions of Transgressive System Tracts (Devon Study, 2004). Importantly, a high gamma-ray well log response is common to the base of the Woodford, over the top of the pre-Woodford unconformity. The lower Woodford

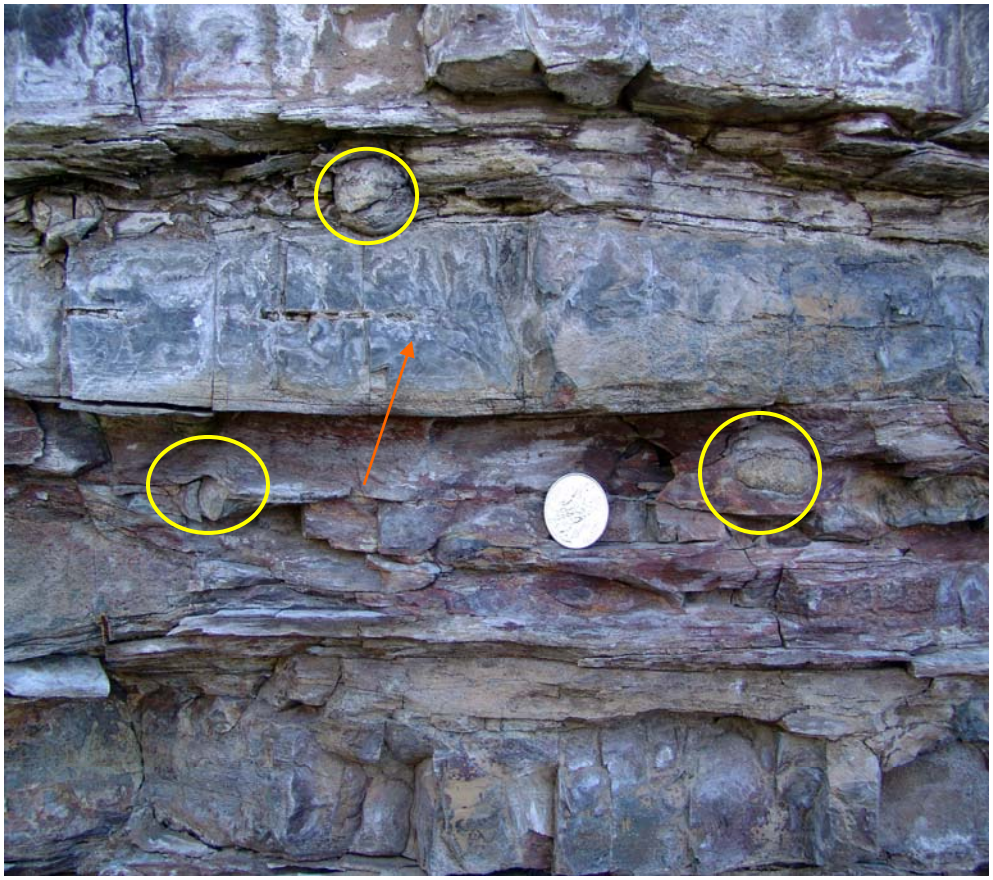

Figure 28. Woodford Shale at Henryhouse Creek; yellow circle indicates phosphate nodules. Orange arrow indicates siliceous shale bed.

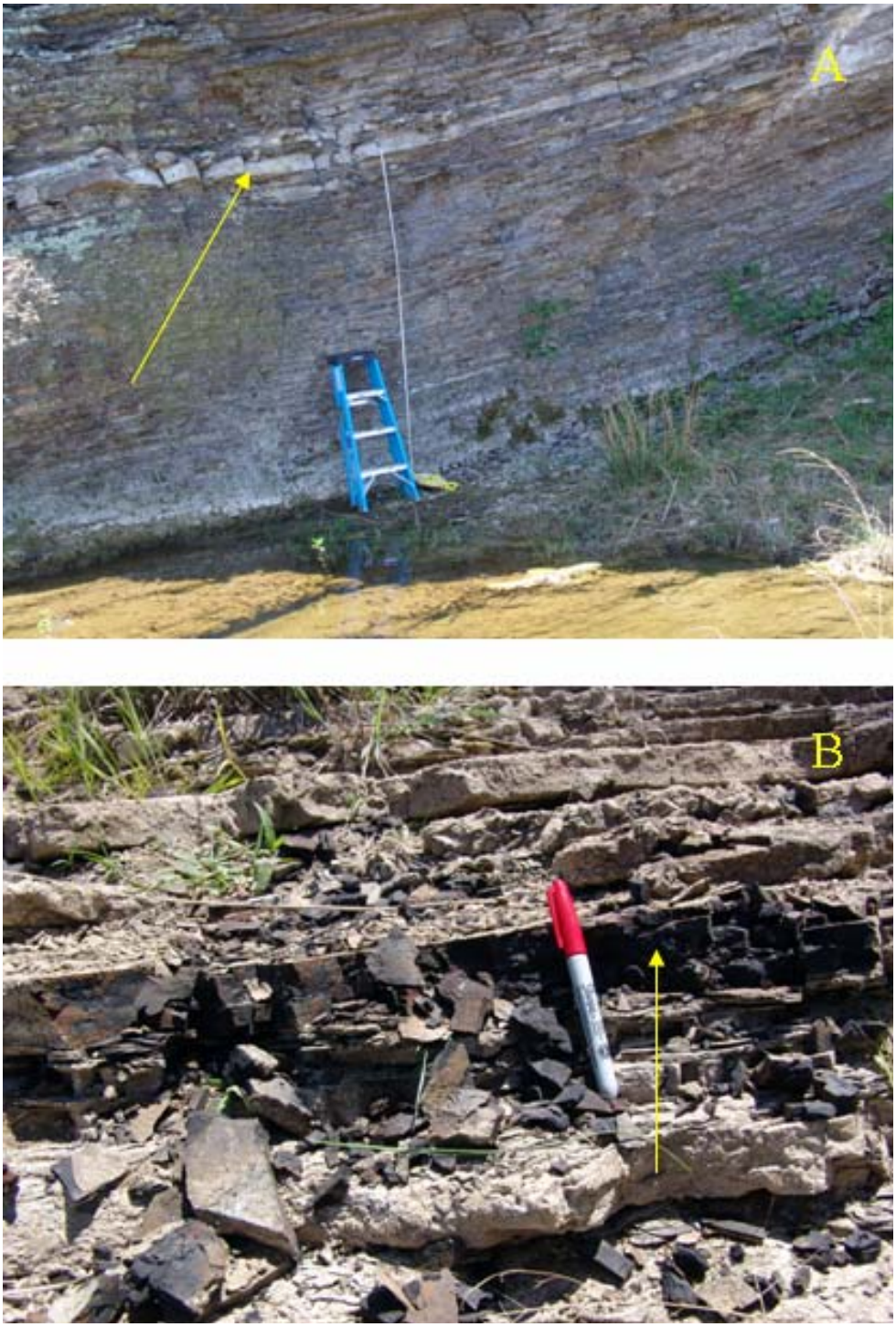

Figure 29. (A) Hydrocarbon-bearing dolomite bed found in the upper Woodford Shale at Henryhouse (yellow arrow). (B) Organic-rich shale that has a coaly-like appearance found in the upper Woodford at Henryhouse Creek (yellow arrow).

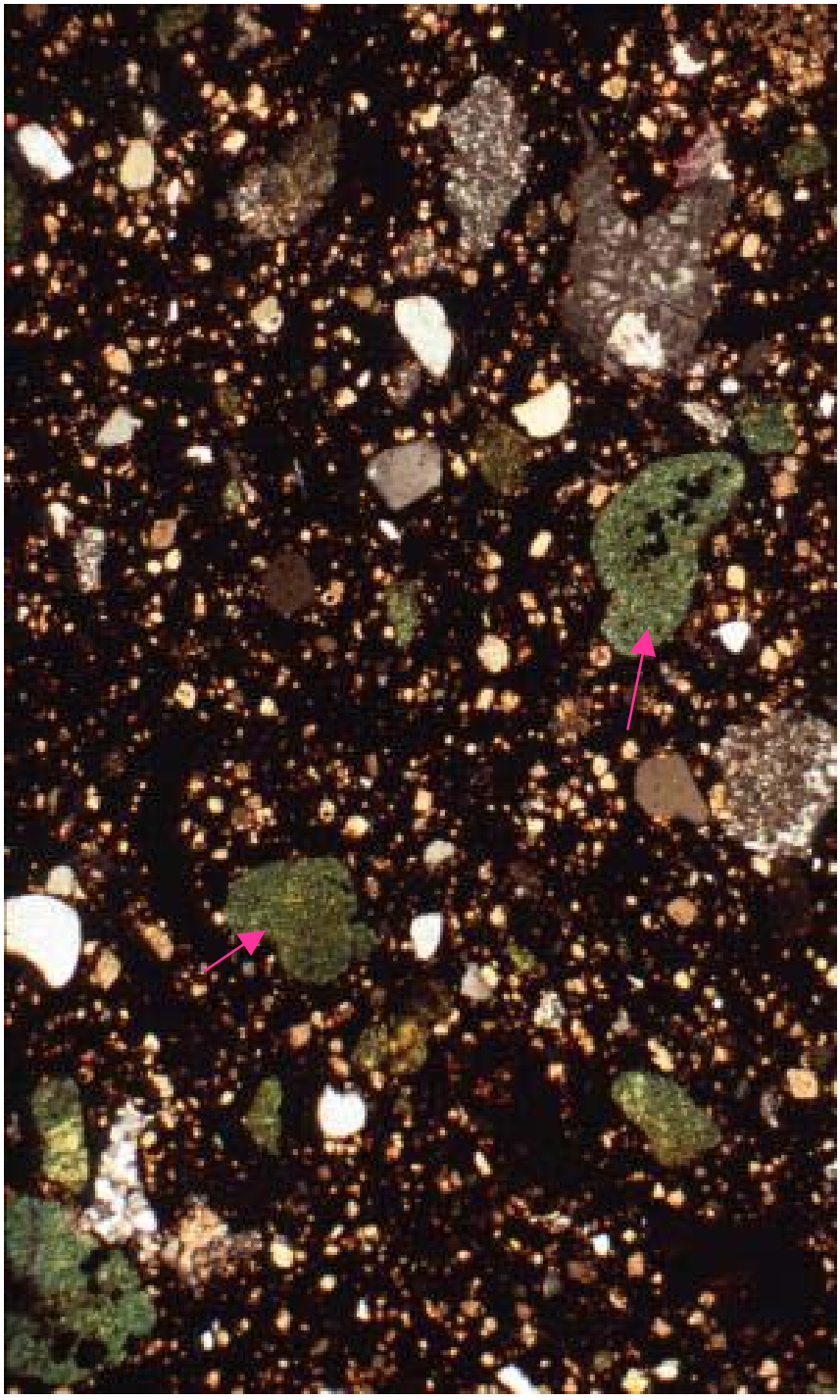

Figure 30. Thin section photograph magnified 40x of the lower Woodford Shale near the contact with the underlying Hunton Group. Thin section shows The presence of glauconite (pink arrows) rounded quartz grains, and rock fragments.

shale is composed of repetitive siliceous shale beds that are 1-4 centimeters thick and fissile shale that is 1-4 centimeters thick.

The middle section of the Woodford Shale is largely composed of fissile shale with some siliceous shale. Nodular pyrite and marcasite in the form of concretions is also found weathering out of the fissile shale. There were no inspections of the thin sections from the middle section of the Woodford Shale.

Inspection of thin sections of the lower portion of the upper Woodford Shale indicates that the shale is composed of biogenic quartz (chalcedony) derived from radiolarians, pyrite, phosphate, and clay (Fig. 31). Thin sections made from fissile shale portions indicate that it is an organic-rich part of the Woodford. Radiolarians in the fissile portion of the shale are compacted and wisps of phosphate are apparent (Fig. 32). Alginite, tasmanities, crushed foraminifers, bituminite and framboidal pyrite is also commonly found in the lower portion of the Woodford Shale (Fig.33). Alginite is a type of kerogen that is made from decomposed algae and other plant material. Alginite is also known as “amorphous organic matter” (Szabo, 2003). Thin sections indicate that this portion of the Woodford is very organic-rich. This observation is based upon the increasing reddish-brown color of the thin sections (common color of some organic matter types). Phosphate nodules are also becoming much more distinct in thin section. Fragments of bivalves and crushed foraminifers are also represented in the lower portion of the upper Woodford (Fig. 34). Small dolomite beds ranging from 1 – 2 centimeters are also occasionally found in this portion of the section and phosphate stringers are found within the dolomite beds.

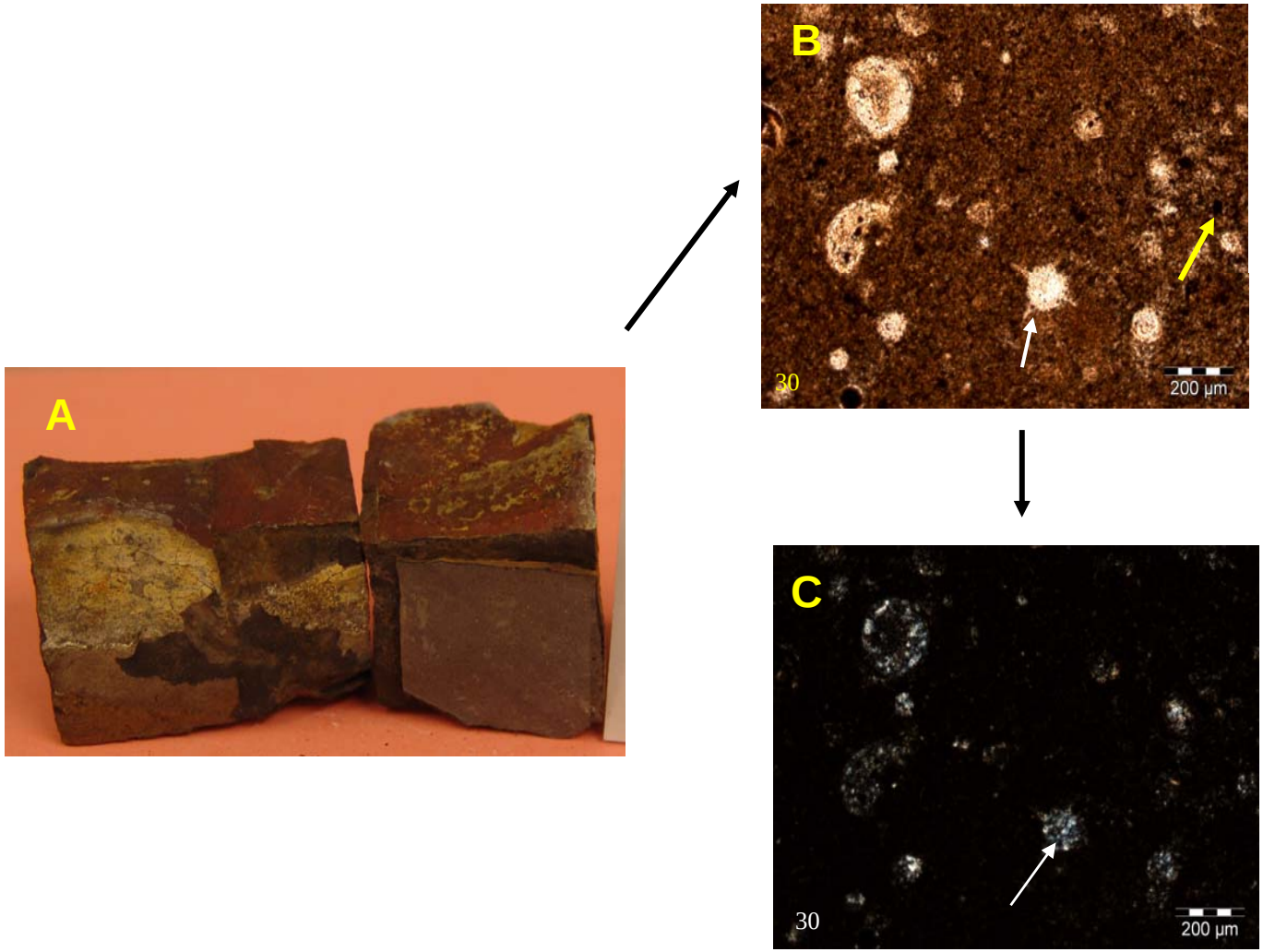

Figure 31. (A) Siliceous sample from the middle Woodford Shale at the Henryhouse location. (B) White arrows indicate radiolarians, yellow arrows indicate pyrite. (C) White arrows indicate chalcedony (thin section photographs are perpendicular to bedding).

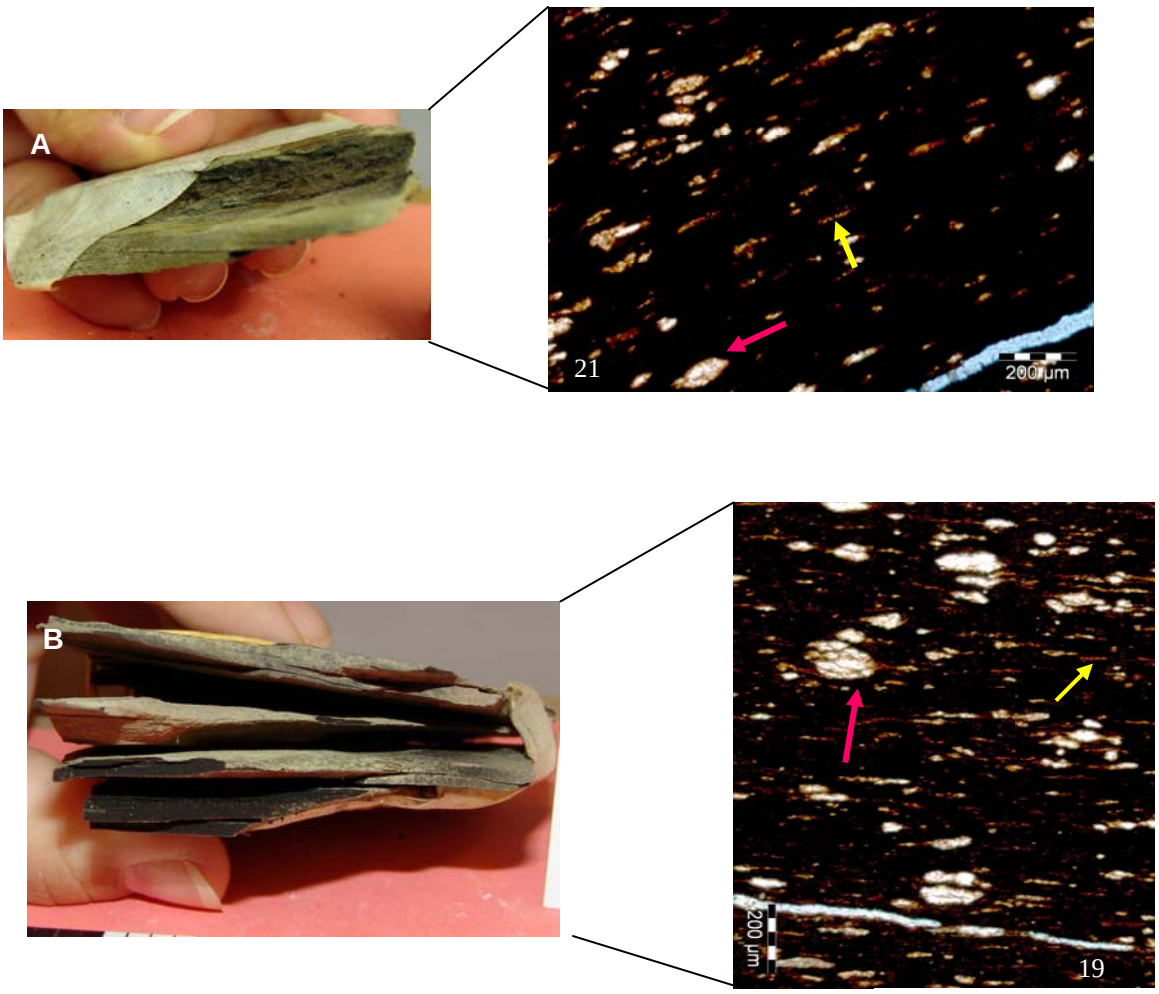

Figure 32. Fissile shale samples taken from the middle of the Woodford Shale at the Henryhouse outcrop. (A) and (B), pink arrows indicate radiolarians, yellow arrows indicate wisps of phosphate.

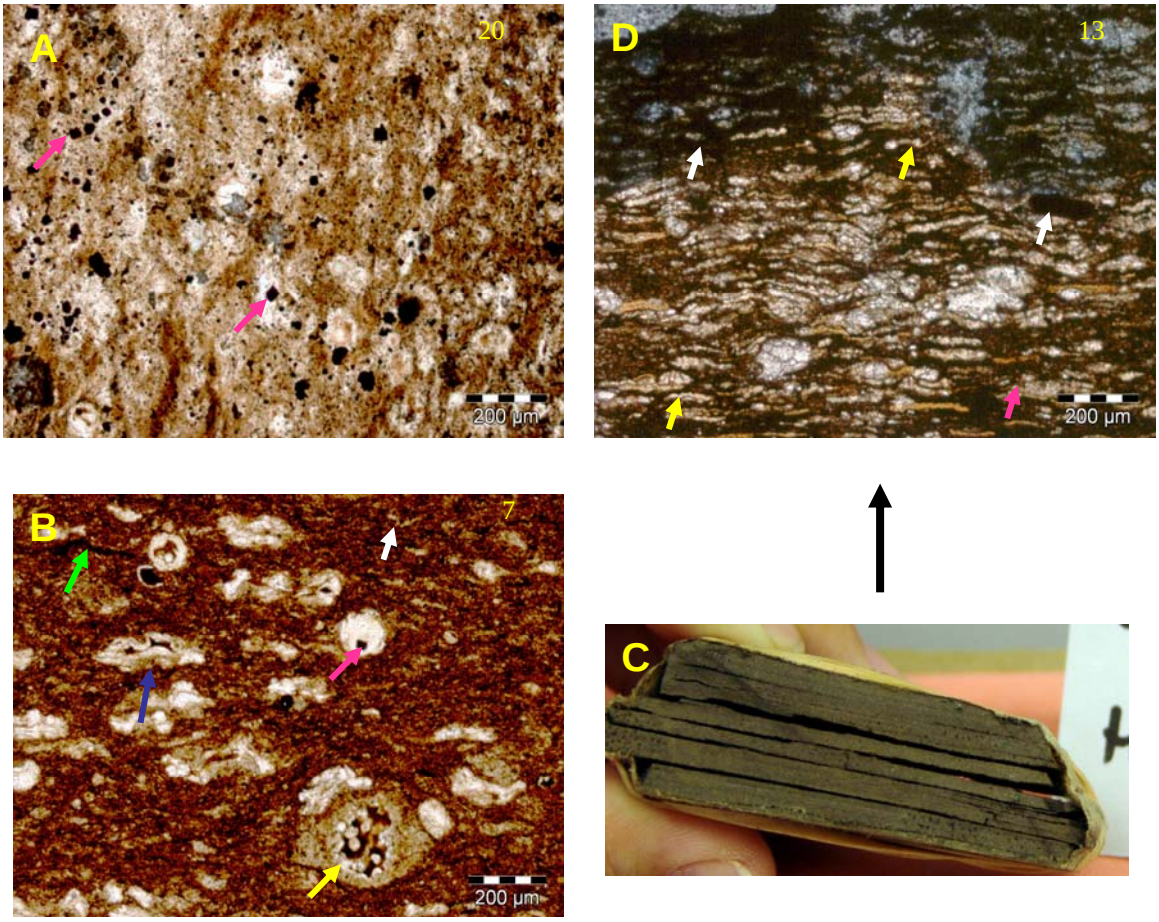

Figure 33. Photographs are from fissile Woodford Shale. (A) Thin section photograph, pink arrows indicate pyrite (thin section photograph is perpendicular to bedding). (B) Green arrows show wisps of bituminite, blue arrow represents a crushed foraminifer, yellow arrow indicates tasmanities and white arrow shows alginite. (C) Hand sample from Henryhouse used to prepare thin section in D. (D) Thin section photograph from hand sample C, white arrow indicate bituminite, yellow arrows indicate alginite. Note, the discontinuous algal mat type appearance of thin section D.

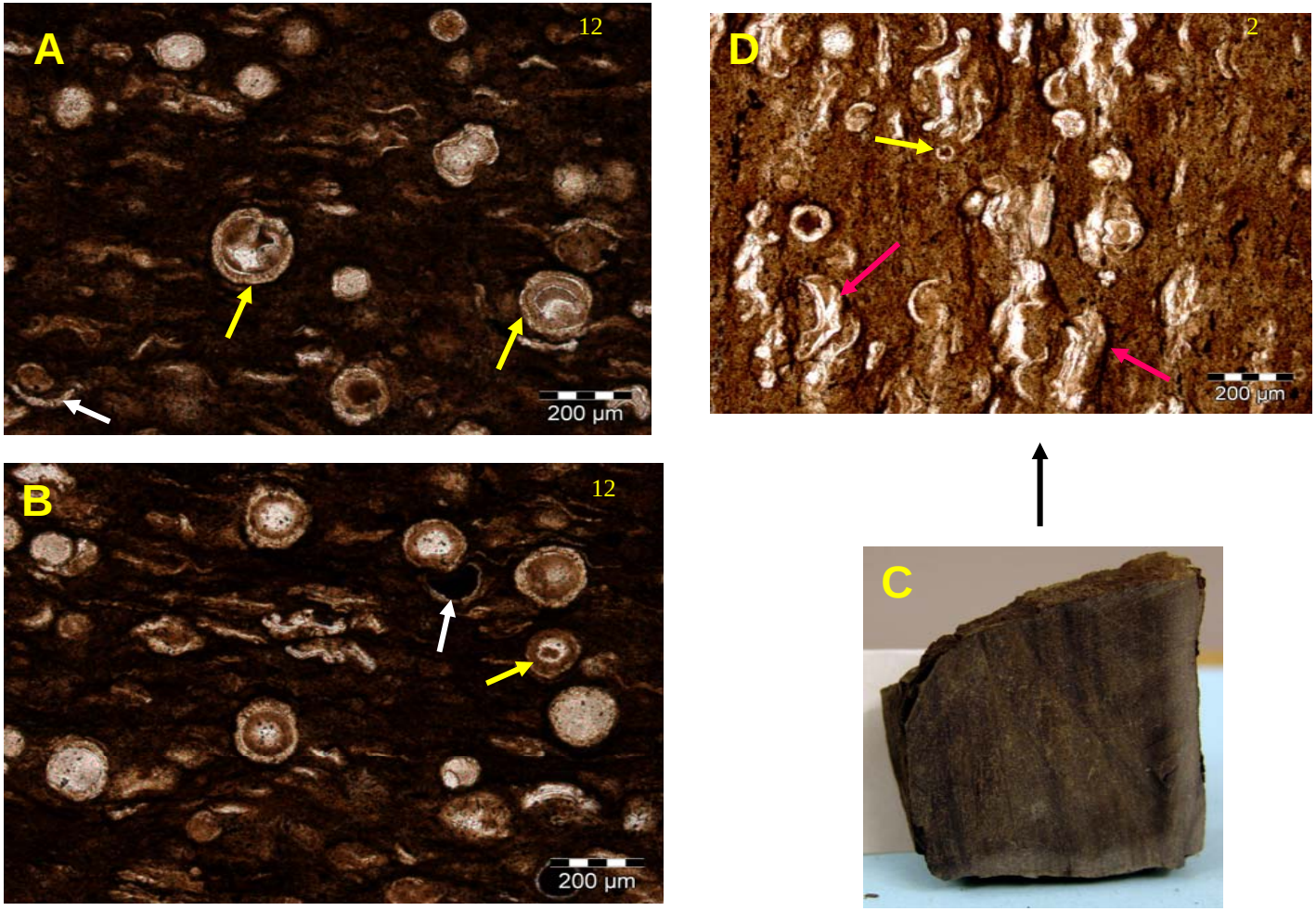

Figure 34. (A) Phosphatic shale thin section of the Woodford Shale from Henryhouse. Yellow arrows indicate phosphate nodules. (B) White arrows indicate bivalve shell fragments, yellow arrows show concentric phosphate ring in nodule. (C) Woodford Shale hand sample from Henryhouse. (D) Yellow arrow indicates pyrite, pink arrows indicate crushed foraminifers (thin section photograph is oriented perpendicular to bedding).

Progressing up stratigraphic section in the upper Woodford, shales are composed of repetitive siliceous shale beds that are 1-3 centimeters thick and fissile shale that is 1-3 centimeters thick. Minerals visible in siliceous shale hand samples are detrital quartz and diagenetic pyrite. Thin sections (siliceous samples) indicate the presence of radiolarians, phosphate, clays, pyrite and amorphous organic material (Fig. 35). Distinctive laminations of clay materials are apparent in thin section as well. Dolomite beds are also found in outcrop (Fig. 36). Dolomite beds are much more noticeable in thin section than in outcrop (Fig. 37) because of their physical similarities to siliceous shales. These dolomite beds are potentially the result of diagenetic replacement of shaly limestones. The occurrence of pelagic organisms such as radiolarians and the organic-rich environment supports a deep marine depositional setting for shaly limestones.

Continuing up stratigraphic section, the upper Woodford Shale consists of siliceous and phosphatic shales and nodules. Inspection of thin-sections reveals that the upper Woodford contains silt sized particles, phosphates, clays and disseminated pyrite (Fig. 38). The shales of the upper Woodford are becoming more silty and phosphatic than the shales found in the lower portion of the upper Woodford (Fig. 39). According to Schieber (2000), the quartz found in the upper Woodford is not detrital but instead precipitated very early in diagenesis in algal cysts and other pore spaces, with silica derived from the dissolution of radiolarians or diatomic opal.

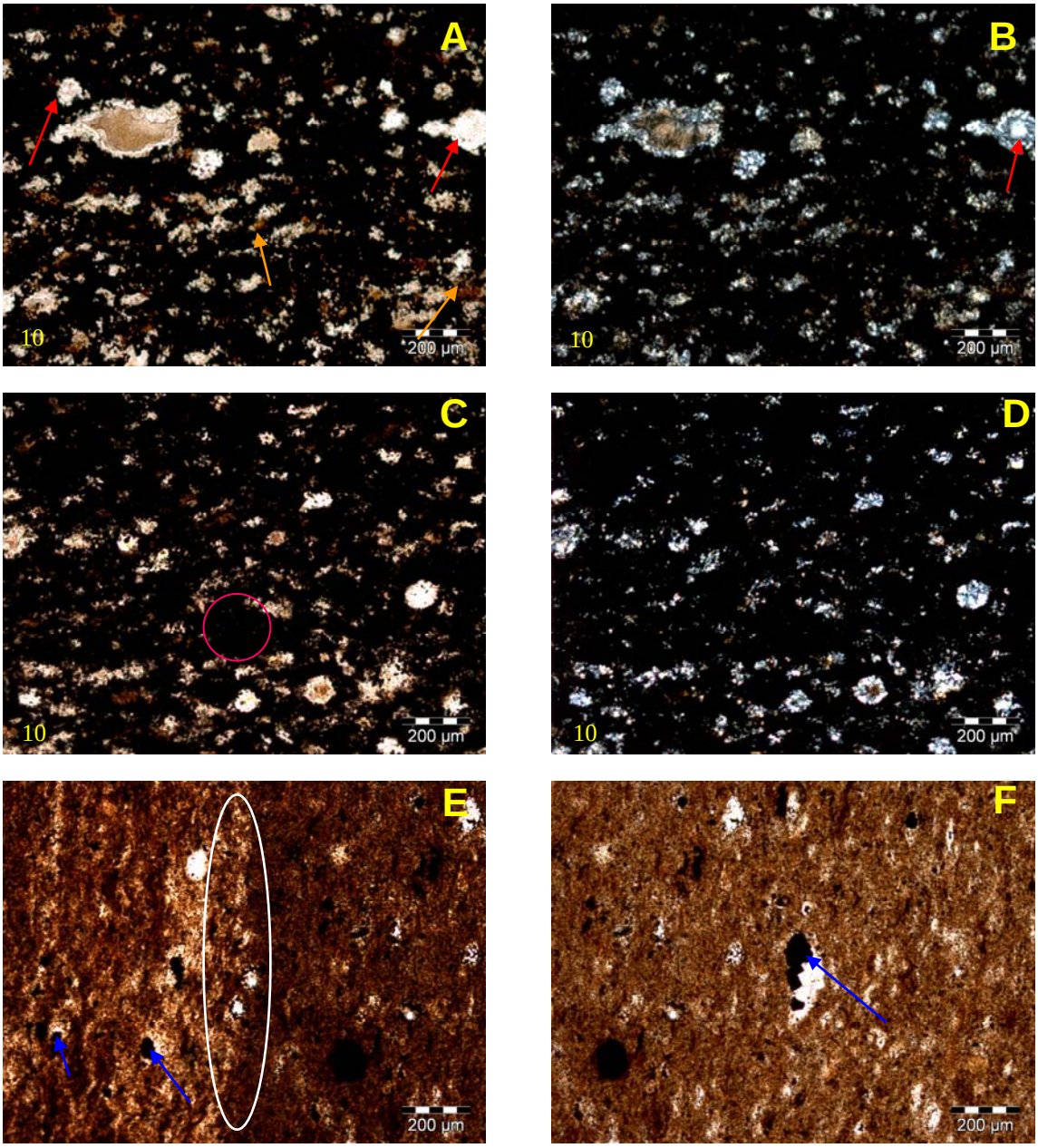

Figure 35. Thin sections of siliceous shale samples collected from the I-35 outcrop. (A) Transmitted light, red arrows indicate radiolarians, orange arrows indicate phosphate. (B) Previous slide with cross polarization, red arrows indicate chalcedony. (C) Pink circle is representative of amorphous organic material, (D) previous slide with cross polarization / note the abundance of chalcedony. (E) Clay-rich thin section, white circle represents layers between clays and phosphate; blue arrows indicate framboidal and pyrite blebs (thin section photograph is perpendicular to bedding). (F) Blue arrow is pointing to pyrite (thin section photograph is perpendicular to bedding).

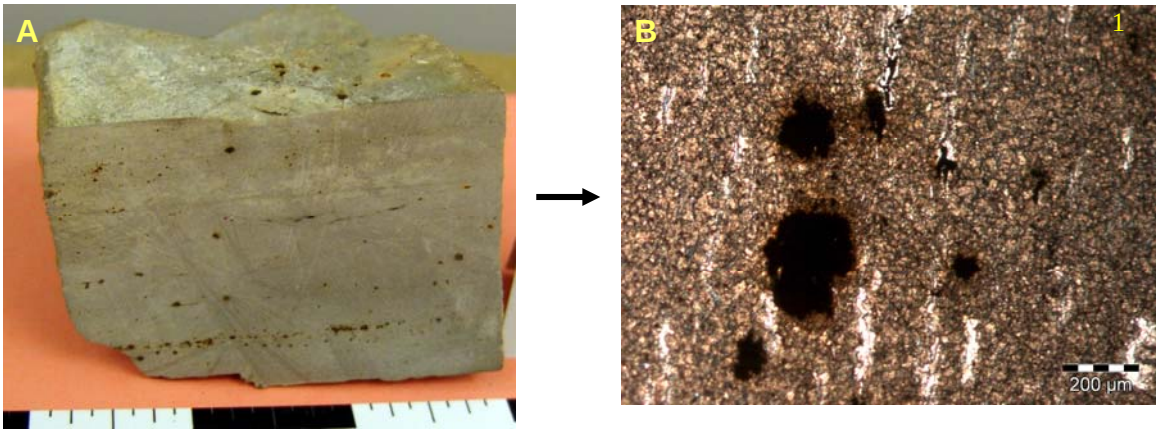

Figure 36. (A) Hand Sample of dolomite bed from McAlester shale pit. (B) Thin section made from hand sample, showing the presence of dolomite (thin section photograph is oriented perpendicular to bedding).

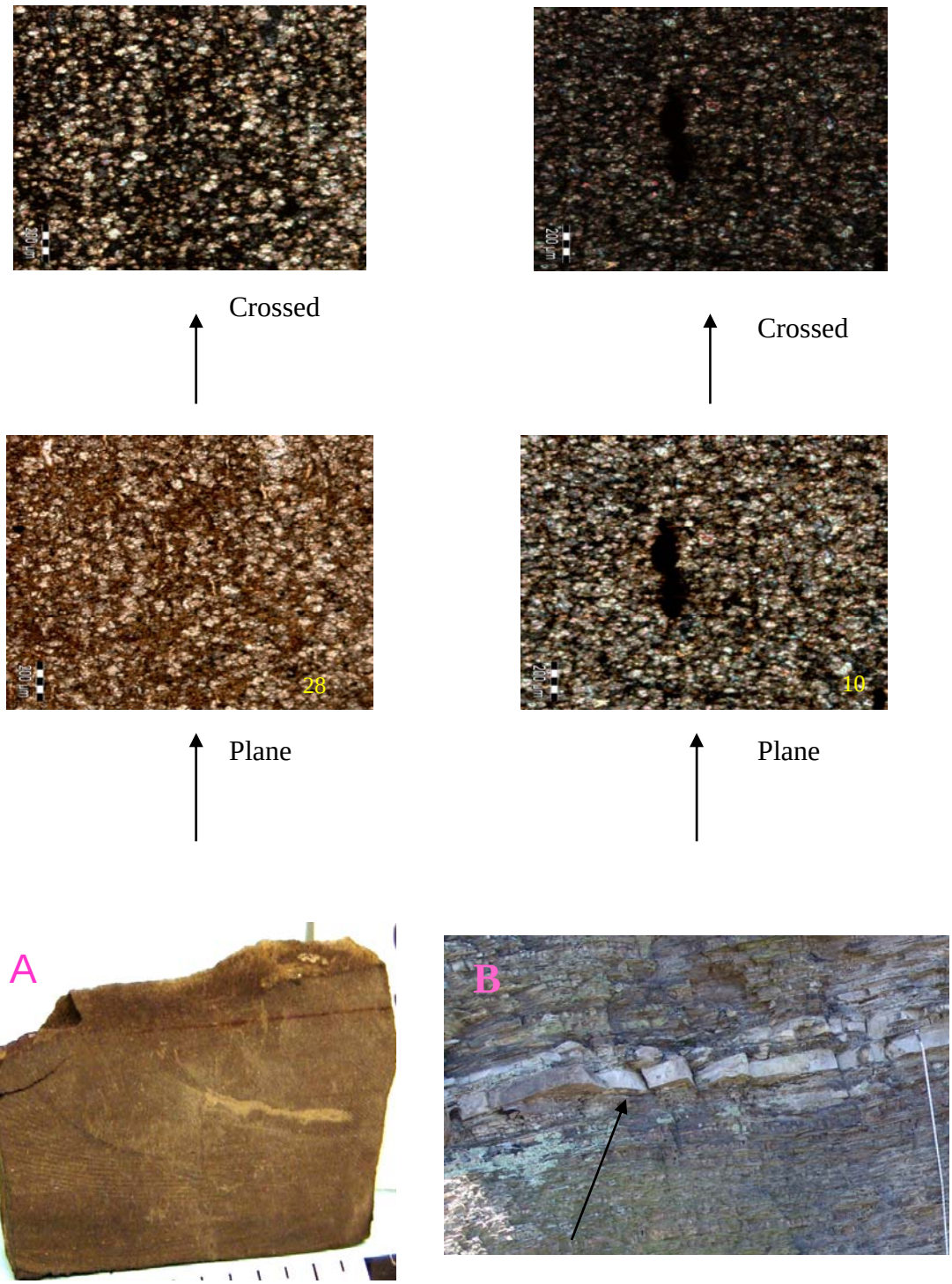

Figure 37. (A) Shale from Henryhouse containing small dolomite beds, noticeable only in thin section. (B) Dolomite bed found in the upper Woodford Shale at Henryhouse. The thin section photographs are oriented perpendicular to bedding.

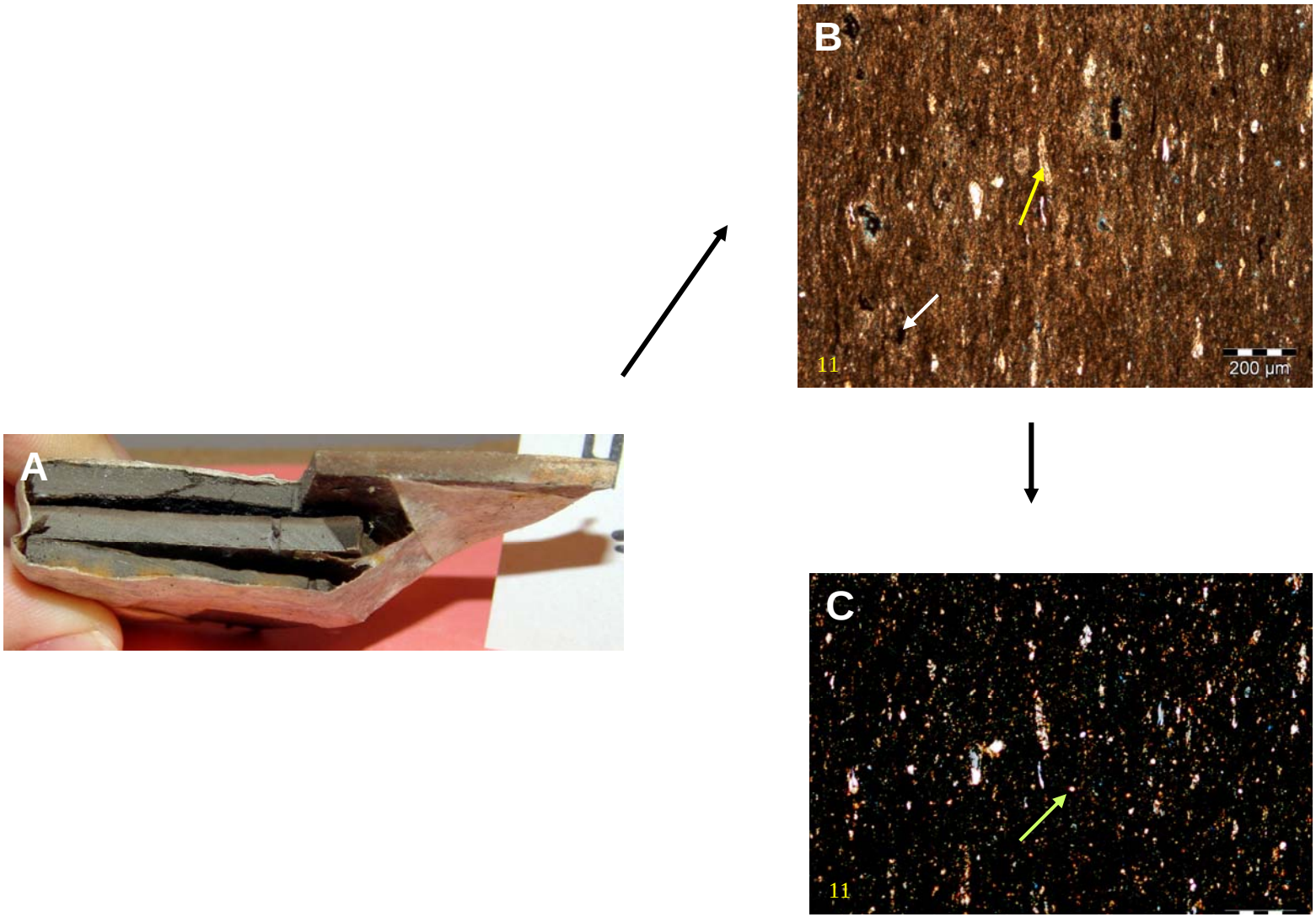

Figure 38. (A) Fissile hand sample from Henryhouse location. (B) White arrow indicates disseminated pyrite, yellow arrow indicates phosphate. (C) Thin section with cross-polarization, yellow arrow indicates silt grains (view is perpendicular to bedding.

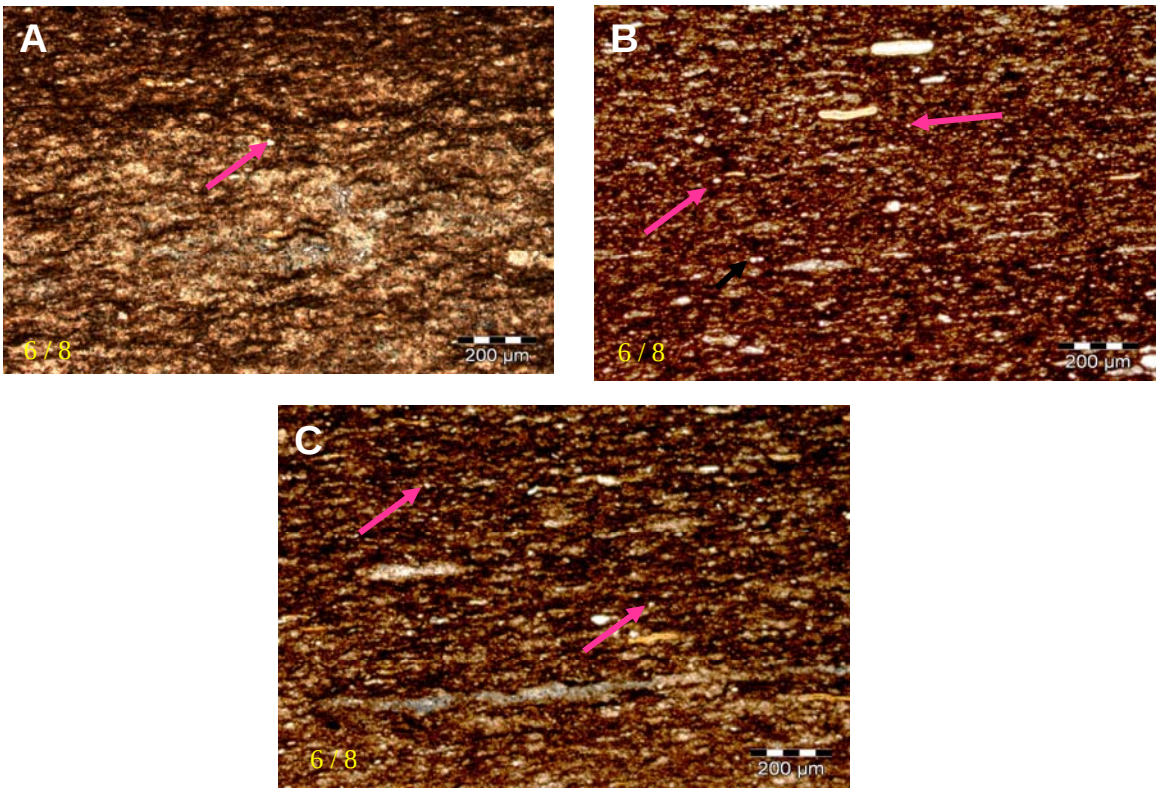

Figure 39. (A), (B) and (C) Woodford Shale thin sections from the upper Woodford Shale at I-35 representing the increase in silica (radiolarian remains).

Organic-rich black shales that have a coal-like appearance are also found in the upper sections of the Woodford Shale. Schieber (2001) suggests that organic-rich black shales with a coal-like appearance originated in the following manner: (1) accumulation of layers of organic debris that is stabilized by microbial slime, (2) compaction and further maturation of these layers follows, thus leading to streaks of bituminite. Therefore, these coal-like streaks may actually represent compressed layers of essentially pure organic debris (Schieber, 2001).

Rare occurrences of chert occur in the upper Woodford. Thin section analyses of samples reveal a high concentration of chalcedony (Fig.40). The chalcedony is the result of dissolving radiolarian tests, which are originally composed of opaline silica and provided the silica for initial chalcedony precipitation (Schieber, 2000). Upon burial of the radiolarians, opaline silica undergoes transformation. The transformation of opaline silica is generally a two step process. First, siliceous oozes are altered to porcellanite (represented in the upper Woodford at McAlester Cemetery shale Pit), which is composed primarily as cristobalite. The cristobalite is then converted to a chert containing mainly micro quartz and chalcedony (Scholle and Arthur, 1983).

Phosphate nodules are found in the upper Woodford shale. Phosphate nodules weather light to gray to white and are easily recognized in the darker shales. The majority is pebble-sized, but diameters range from 0.5-9 centimeters (Siy, 1988). According to Siy, (1988) phosphate nodules are early diagenetic, in situ features which formed in the upper few centimeters of the Woodford Shale. Sufficient concentrations of phosphorous and euxinic, (anaerobic) conditions in the lower water column enhanced the inorganic

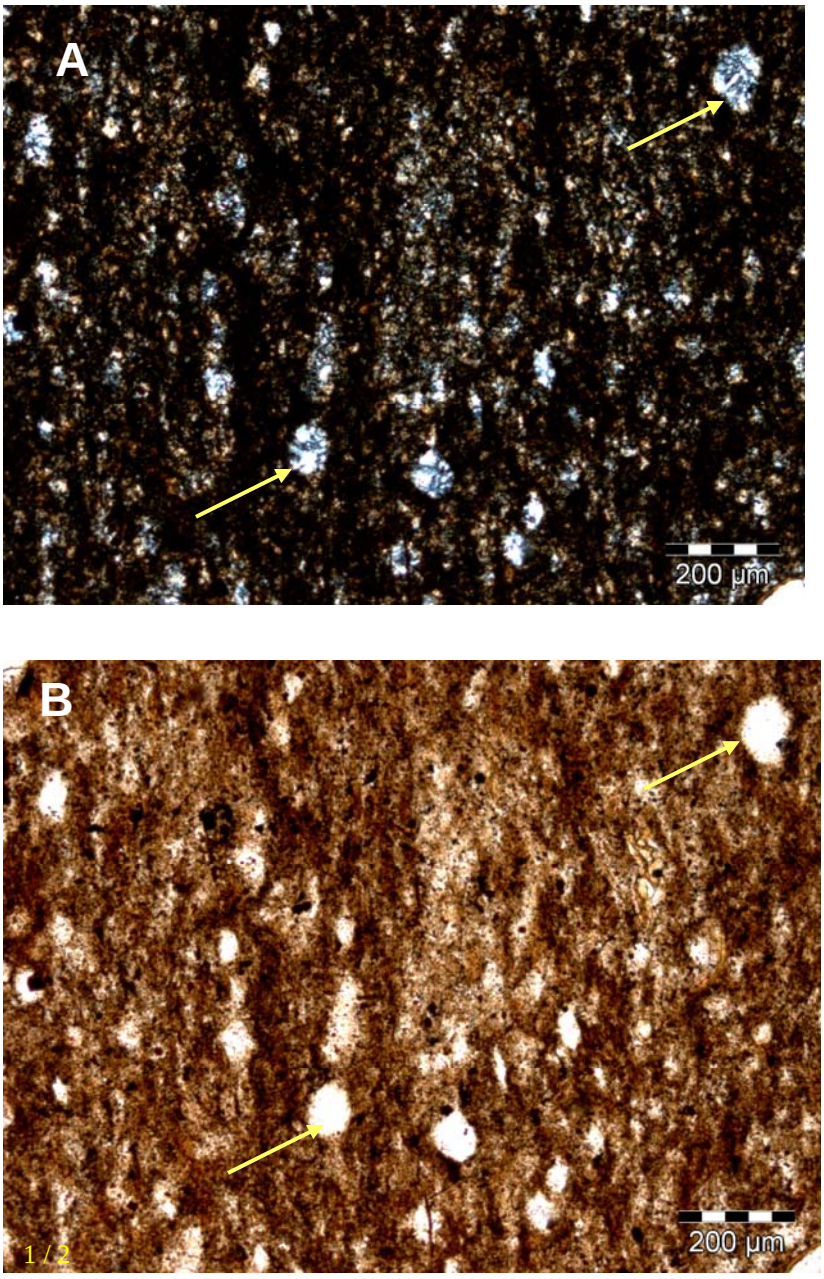

Figure 40. (A) Cross-polarization of thin sections from siliceous shale found at McAlester Cemetery shale pit show the abundance of chalcedony (yellow arrow). (B) Thin section in transmitted light, showing radiolarians (yellow arrow).

precipitation of apatite during a major transgressive episode (Siy, 1988). The Woodford Shale phosphatic nodules are composed of carbonate fluorapatite resulting from varying amounts of diagenetic alterations of the apatite (Siy, 1988). Nodules of this interval contain 15-38 wt % P_2O_5, which is high enough to permit classification of the shale phosphorites (Siy, 1988). All shales are compressed around phosphate nodules. This confirms that phosphogenesis preceded shale compaction (Fig. 41), (Siy, 1988). Thin section analysis confirms the phosphatic composition of the nodules and the presence of phosphate minerals such as wavellite (Fig. 42).

XRD Data

XRD (X-Ray diffraction) data from siliceous and fissile samples reveals that the upper Woodford Shale is composed of between 5% - 19% mixed layered illite / smectite. Quartz constitutes between 40-76% of the sample. Jarosite percentages lie within the 2-5% range with occasional trace amounts. Jarosite is not a common mineral and occurs as a crust of crystals on the surface of the rock. Jarosite is classified as a potassium iron sulfate hydroxide. The presence of jarosite is probably the result of a pyrite-oxidizing environment (modern weathering). Na-plagioclase, calcite and dolomite are also found as trace amounts within the samples.

Figure 41. Fissile shale compaction around phosphate nodules found at the Henryhouse outcrop.

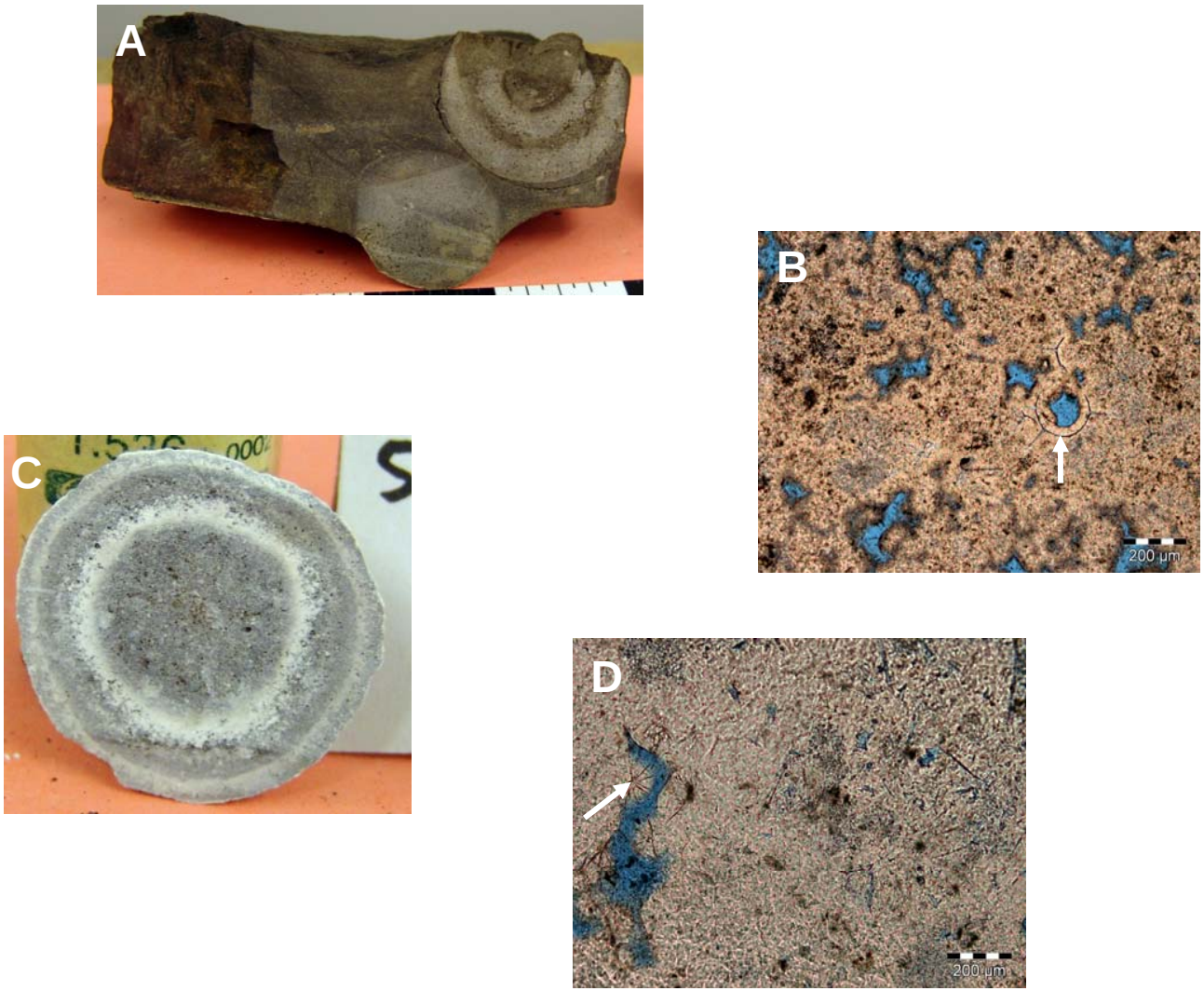

Figure 42. (A) Siliceous sample of phosphate nodules from I-35. (B) Thin section showing phosphate, white arrow indicates radiolarian. (C) Phosphate nodule from McAlester shale pit. (D) Thin section of phosphate nodule, white arrow is pointing to mineral wavellite (phosphate mineral).

TOC Data

Thirty eight samples were analyzed for TOC by Humble Geochemical in Houston, Texas. The samples were collected at the I-35 Outcrop on the southern flank of the Arbuckle Mountains. The sample interval is from the base of the outcrop to 52ft towards the top of the outcrop (up stratigraphic section). TOC results reveal that there is distinct variation in total organic carbon within the measured section. Samples were organized according to increasing TOC and range from about 0.8 -17.0 wt%, with an average of 10 wt% (Fig. 42). TOC analysis in coordination with hand samples (Fig. 43), reveals lower TOC values, 0.6 – $\leq$ 6 wt % are characteristic of the siliceous, blocky, lithofacies. Samples with TOC values in the middle range 6-$\leq$ 14 wt% are slightly siliceous and fissile. The highest TOC values correspond with fissile organic-rich shales. This organic-rich fissile shale has TOC values of >14 wt %. D.W. Kirkland others (1992) completed a TOC study from the McAlester outcrop. This previous study had TOC values between (0.3-17.0%) and an average of 8.0%. The high percentages of TOC are potentially the result of dissolved organic molecules (common in seawater) being absorbed into the crystal lattice of smectite clay minerals. The organic matter that is associated with the clays is protected from oxidization and metabolization (Kennedy, Pevear, and Hill, 1992). Schmoker (1980) showed a relationship for TOC based on color of Devonian Shales in the western Appalachian Basin. Schmoker used a Munsell color system to show that high TOC content is associated with dark-medium to gray colored shales. An attempt was made to

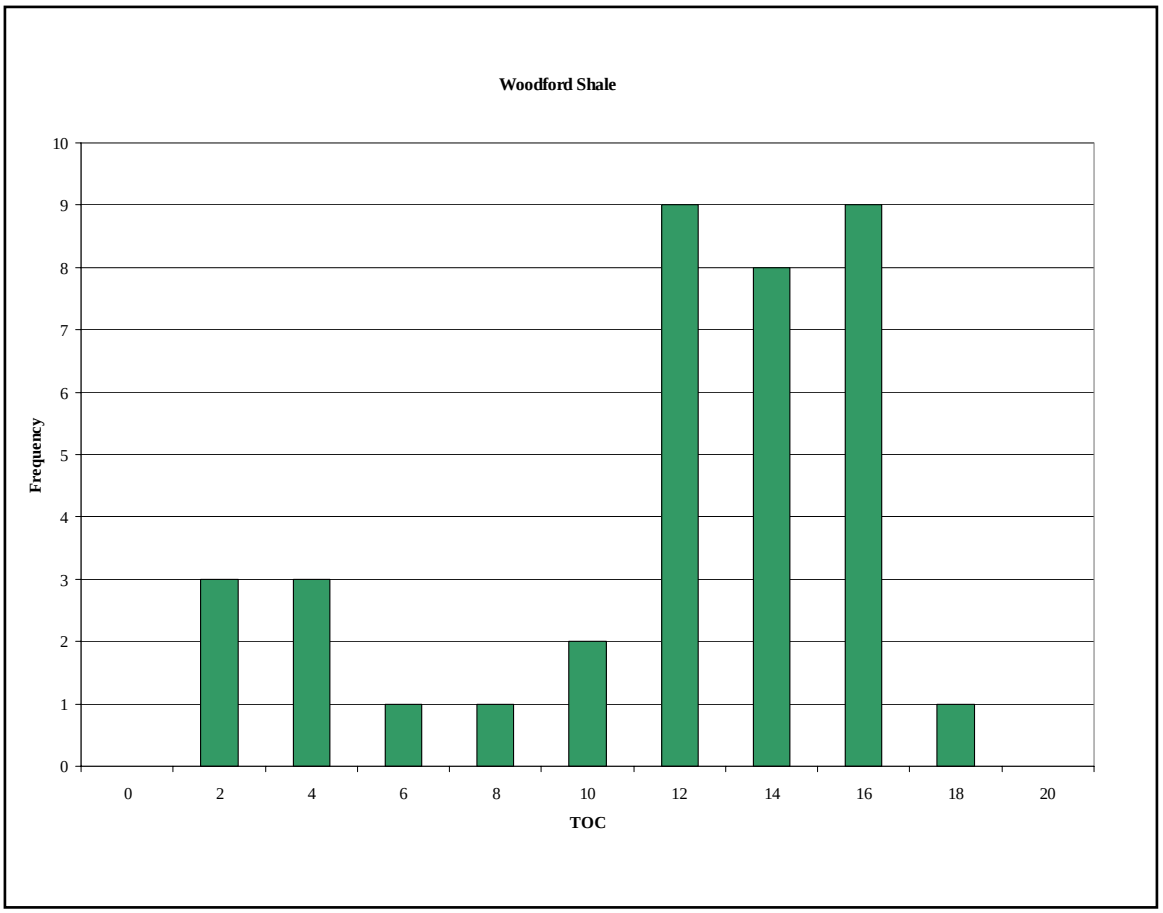

Figure 43. Frequency distribution of the TOC content in outcrop samples from the I-35 location (n=38).

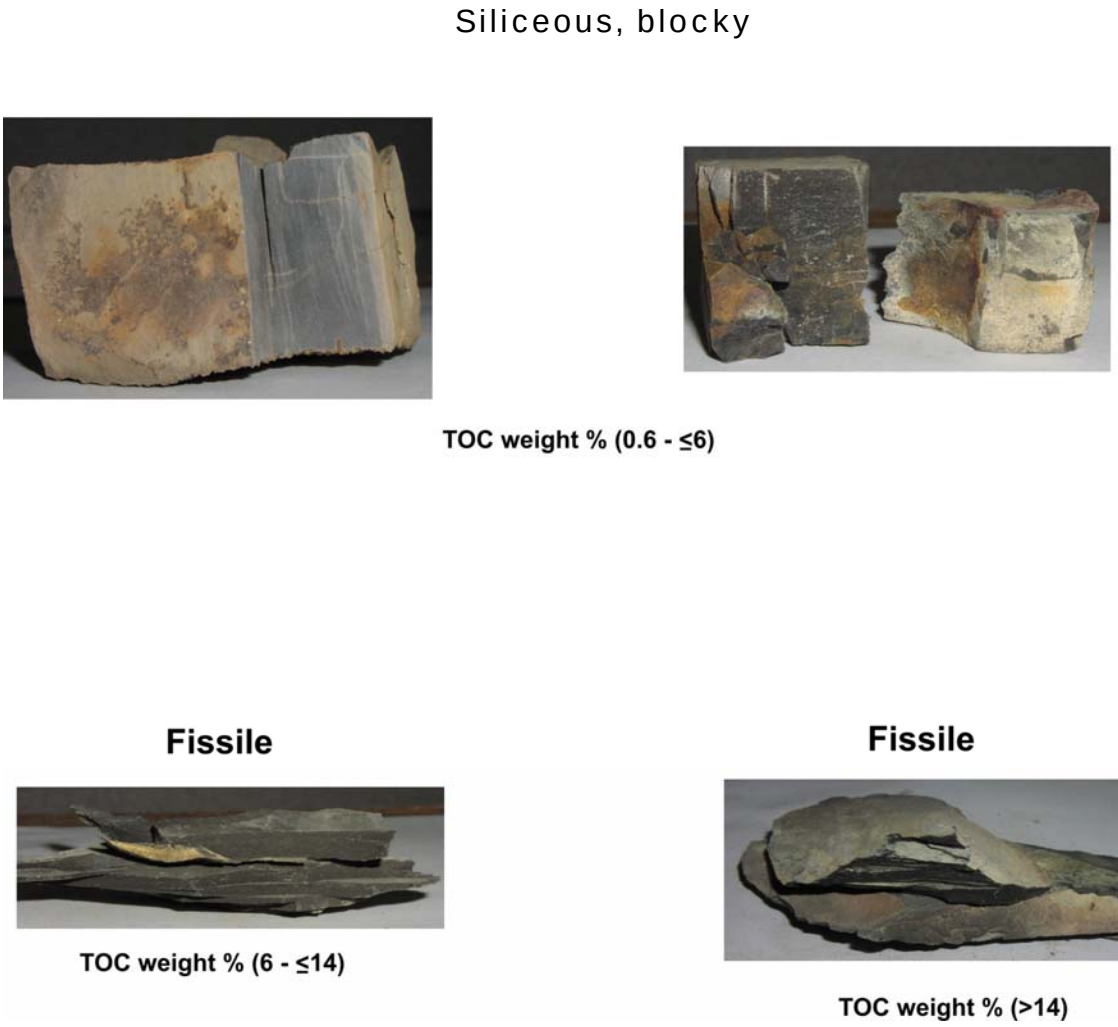

Figure 44. Samples of the Woodford Shale from the I-35 location representing the three categorized TOC values.

establish a similar relationship within the TOC samples from the I-35 outcrop. Samples were categorized according to the Munsell color charts and then graphed to determine if a relationship exists between TOC and color. A relationship can be determined within the fissile lithofacies because fresh, non-weathered samples are represented by high TOC values and dark colors. However, a direct relationship between TOC and siliceous samples cannot be determined. Siliceous samples are represented by both light and dark colors, yet the dark colors have low TOC values, thus there is not enough strong evidence to establish the relationship between TOC and color in the Woodford Shale.

Humble Geochemical in Houston, Texas conducted calculations on four outcrop samples from the I-35 location to determine vitrinite reflectance for estimating (%/Ro) thermal maturity. Vitrinite reflectance estimates are important because they reveal the thermal maturity of an area and the potential zones for oil and gas. Vitrinite reflectance ranges from the I-35 outcrop are between 0.70% and 0.72%. This data suggests that the thermal maturity of the four samples lies in the early "Oil window maturity zone". This categorization is based upon the following data; (1) <0.60% immature oil window, (2) 0.60-1.00 oil window, (3) 1.00-1.40 condensate / wet gas window and >1.40 dry gas window. Producible gas may be found at about 1.0%Ro (Jarvie, 2004). Amorphous kerogen is a dominating characteristic within the samples. Humble Geochemical (2005) also noted the presence of tasmanities and bitumen. The amounts of bitumen indicate that some liquid hydrocarbons were generated in the past. Cardott (2001) determined the thermal maturity of the Woodford Shale by measuring vitrinite reflectance of well cuttings. Cardott (2001) determined that the average vitrinite reflectance of the Woodford

Shale ranges from about 0.5% - 6.4%. Cardott (2001) also indicates that the thermal maturation of the Woodford Shale increases from west to east and with increasing depth in the Arkoma basin. Olson (1982) determined that thermal maturation of the Woodford Shale increased from immature in the central portion of Oklahoma (current depth of burial less than 6000 feet) to advanced maturity in the Anadarko Basin (current depth of burial greater than 14,000 feet) and Ouachita Mountains (Fig. 44).

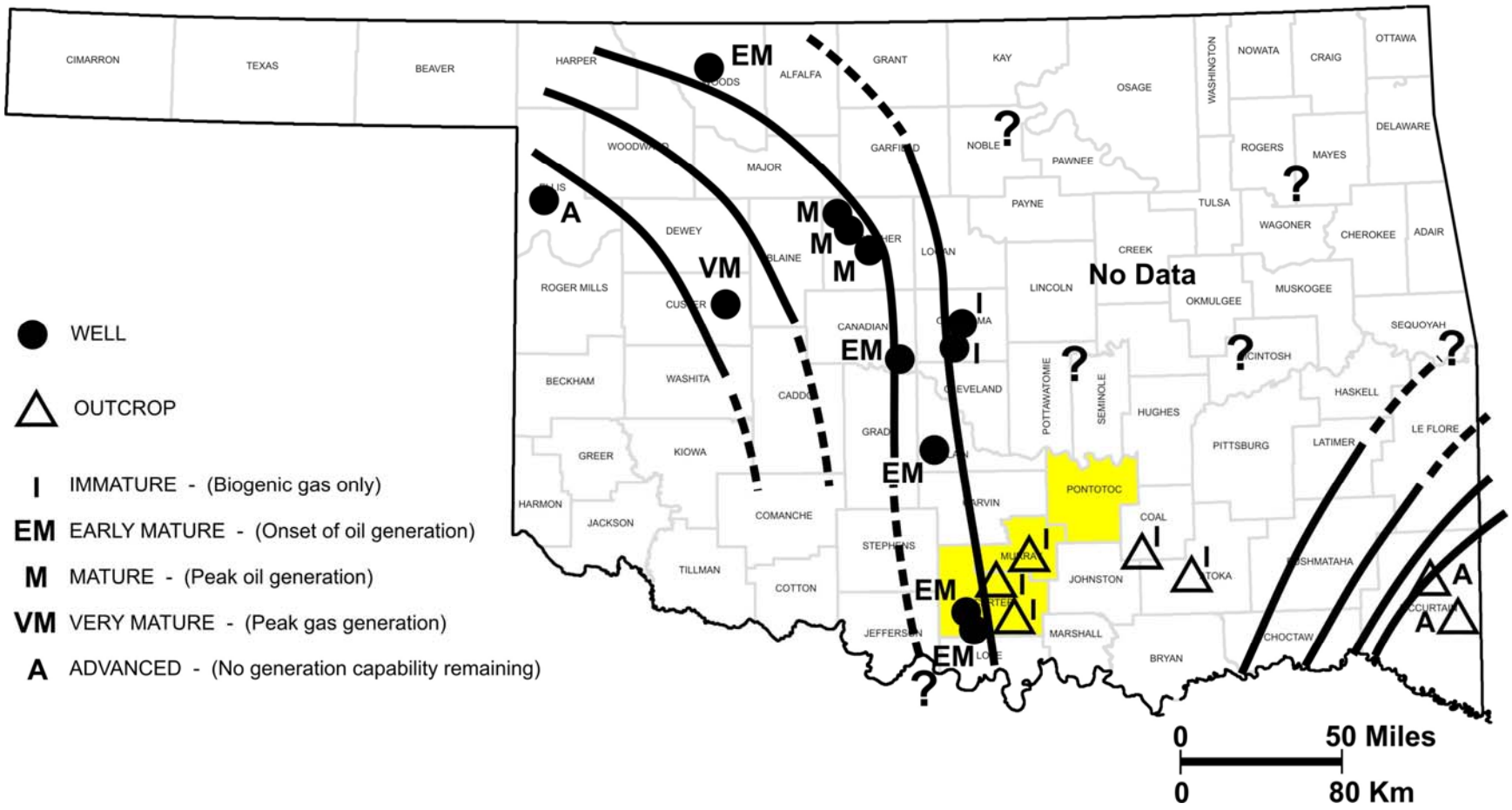

Figure 45. Modified after Olson (1982), thermal maturity distribution of the Woodford Shale. Yellow area indicates author's field area.

Chapter 6

Summary and Conclusions

The current rise in oil prices has led many companies to consider unconventional gas-shale plays. One such possibility that may prove economically viable is the Woodford Shale of south-central Oklahoma. The Woodford Shale is an organic-rich black shale that is upper Devonian- lower Mississippian in age. On well logs, the Woodford has API gamma-ray readings of 150 and higher and is therefore classified as a "hot" shale.

A detailed study of the Woodford Shale would result in a better conceptual understanding of hydrocarbon source rocks and their role as possible unconventional gas-shale plays. For instance, to evaluate this possibility, relationships between lithofacies both in outcrop and the subsurface can be established relative to outcrop-based gamma-ray profiles in correspondence with potassium (K %), uranium, (U ppm) and thorium (Th ppm) along with subsurface gamma-ray logs.

This study was conducted to determine if a relationship exists between outcrop lithofacies and gamma-ray response and if ultimately this relationship can be extended into the subsurface. This data, along with data collected through the examination of five outcrops, in conjunction with thin-section analyses, TOC and XRD data allows for the potential to improve our ability to predict the properties of black shales and project them into the subsurface.

On the basis of the above data, the following conclusions are drawn for the Woodford Shale of south-central Oklahoma.

1. The bulk of the Woodford contains two main shale habits, fissile and non-fissile. Lithofacies found in or associated with the non-fissile category are phosphatic shale, siliceous shale, dolomite beds, phosphate nodules and rare occurrences of chert and limestone. Siliceous shales are generally blocky and range from 1-10 cm in thickness. The siliceous beds are found to be thicker and less common in the lower Woodford Shale and thinner and more prevalent in the upper Woodford Shale. Siliceous shale is commonly absent in the middle Woodford. Phosphate nodules and phosphatic shale is found in the upper 20-40 feet (6-12 m) of Woodford. Some dolomite beds are found in the lower and upper Woodford Shale. Dolomite beds are from 7-15 cm in thickness. A 12 cm thick limestone bed was found in the upper Woodford at the I-35 locations, but was not found in any of the other studied outcrops. According to past conodont work, this limestone is probably Mississippian (Kinderhookian) in age.

The fissile shale habits are composed of laminations that are <1cm thick and are the most organic-rich of the Woodford Shales. The fissile shales are dominantly found in the middle Woodford, but are also in the upper and lower Woodford. The fissile shales in the upper and lower Woodford are interlaminated with siliceous shales on the 1-2 cm scale. The association of siliceous and fissile shale is suggestive of local, lateral facies changes on the sea floor.

2. The occurrence of pelagic organisms such as radiolarians and the organic-rich carbonate environment supports a deep marine depositional setting for shaly limestones. Dolomite beds are apparent in outcrop, but may be more abundant than previously noted. The reason for this is because in some instances, dolomite in outcrop is internally black

and appears similar to siliceous shale. The dolomite does not readily react with acid in the field, but is obvious in thin-section.

3. Thin-section analysis of the upper Woodford indicates that radiolarians are the main source for silica in the Woodford. Radiolarian tests can be seen in thin sections cut from siliceous shale samples.. Analysis of thin-sections of the upper Woodford also indicates that the upper Woodford is composed of silty and phosphatic shales. Thin-sections cut from phosphate nodules and surrounding shales suggests that radiolarians provide the nuclei for phosphate development.

4. Thirty-eight samples analyzed for total organic carbon (TOC) from the upper Woodford at I-35 have values that are about 0.8-17 wt%. The fissile shales have the greatest weight percentage of TOC. Values for the fissile shale fall between 5-17 wt %. The average TOC found within the I-35 outcrop is 10.5 wt% with a standard deviation of 4.4. In contrast to reports in the literature, the degree of TOC content could not be determined by color alone. Some samples of Woodford Shale are dark to almost black in color and would appear to be organic-rich, yet thin-section analysis reveals them to be highly siliceous or even dolomitic in composition. These dark colored siliceous samples yield TOC values as low as 0.83-3.5 wt%.

5. Thirty-eight samples analyzed using x-ray diffraction (XRD) from the upper Woodford at I-35 reveals that the upper Woodford Shale is composed of 5-19% mixed layered illite / smectite. Quartz constitutes between 40-76% of the samples. Jarosite percentages lie within the 2-5% range with occasional trace amounts. The presence of jarosite is the result of a pyrite-oxidizing environment (weathering). Na-plagioclase, calcite and dolomite are also found as trace amounts within the collected samples.

6. The Woodford Shale falls into the uraniferous shale category (>20 ppm) with uranium readings as high as 106 ppm. Uranium is the main constituent controlling gamma-ray character. The amount of uranium in ppm along with its variation and occurrence in the outcrop is well documented. The greatest occurrence of uranium occurs in the lower Woodford and in the top of the middle Woodford. The lower Woodford Shale is 60 feet (18 m) thick has uranium values from 19.8-66 ppm and an average uranium content of 36.9 ppm. API units in the lower Woodford range from 198-602 API with an average of 355. The middle Woodford Shale is 120 (36 m) thick with uranium values that fall between 22.4-106 ppm and an average of 43.4 ppm. API units in the middle Woodford range from 242-943 API with an average of 410. The upper Woodford Shale is 60 feet (18 m) thick and is represented by uranium readings from 13.3-57 ppm with an average of 39.2 ppm. API units in the upper Woodford range from 130-510 API with an average of 355. The phosphate zone found in the upper 14 feet (4.2 m) of the upper Woodford Shale contains uranium that ranges from 13.3-57 ppm with an average of 36.3. API units in the phosphate zone are from 130-496 API with an average of 329.

7. The phosphate nodules found in the upper Woodford Shale represent an interval in which the availability of uranium in the sea waters where phosphate precipitation takes place was low. The uranium appears to have already been depleted by chemically reducing waters associated with hydrogen sulfide precipitation. Consequently, the phosphate nodules have little or no uranium.

8. The Woodford outcrop-based gamma-ray profiles can be correlated into the subsurface. This correlation is based upon pattern recognition of the connected points

that compose a gamma-ray profile in comparison with the gamma-ray logs which are continuous curves.

Future Work

The Woodford Shale has been and remains an extensively studied organic-rich marine black shale. Despite this fact, there is still much more work that needs to be completed in order to develop a conceptual understanding of this unit. This work could be addressed by the following procedures: (1) Creation of detailed maps indicating locations of the Woodford Shale outcrops in Oklahoma along with their thicknesses. This will enhance future researchers in their search for outcrops to study. (2) Collect gamma-ray measurements from additional outcrops along with a detailed lithofacies description of the Woodford. This data can then be correlated and mapped into the subsurface to determine the extent of thickness and the members of the Woodford Shale on a more regional basis. (3) Collect samples for paleontology, TOC and XRD analysis. In particular, samples should be collected every six inches from the Henryhouse Creek location. The entire Woodford Shale is exposed at Henryhouse Creek, thus this data has the potential to lead to a more accurate assessment of hydrocarbon potential. This could also lead to information regarding depositional environments, time of deposition, and environmental factors, such as climate. (4) Well and outcrop fracture characterization of the Woodford Shale. Understanding the fracture patterns and their relationship to lithofacies has the ability to aid in the gas recovery of horizontal wells.

References

Adams, S. J. A., and Weaver, C. E. 1958. Thorium-to-Uranium Ratios as Indicators of Sedimentary Processes: Examples of Concept of Geochemical Facies. Bulletin of the American Association of Petroleum Geologist, vol. 42, no. 2, pp. 387 – 430.

Amsden, T., 1975, Hunton Group (Late Ordovician, Silurian, and Early Devonian) in the Anadarko basin of Oklahoma: Oklahoma Geological Survey Bulletin 121, 214 p.

Amsden, T., and Klapper, G., 1972, Misener Sandstone (Middle-Upper Devonian), north-central Oklahoma: AAPG Bulletin, v. 56, p. 2323-2334.

Burke, K., 1977, Aulacogens and continental breakup: Annual Review of Earth and Planetary Sciences, v. 5, p. 371-396

_____and J.F. Dewey, 1973, Plume-generated triple junctions: key indicators in applying plate tectonics to old rocks: Journal of Geology, v. 81, p. 406-433.

Cardott, B. J. 2001. Thermal Maturation of the Woodford Shale in Eastern Oklahoma. Oklahoma Geological Survey Circular 106.

Cardott, B. J., and Lambert, M. W. 1985. Thermal Maturation by Vitrinite Reflectance of Woodford Shale, Anadarko Basin, Oklahoma. The American Association of Petroleum Geologists Bulletin, v. 69, no. 11, pp. 1982 –1998.

Champlin, S. C. 1959. A Stratigraphic Study of the Sycamore and Related Formations in the Eastern Arbuckle Mountains. Unpublished Masters Thesis, University of Oklahoma, pp. 66.

Coffey, W.S., 2000. The Diagenetic History and Depositional System of the Sycamore Formation (Mississippian), Carter-Knox Field, Grady and Stephens Counties, Oklahoma. Doctorate of Philosophy dissertation, 167 pp. Oklahoma State University, Stillwater, Oklahoma.

Cole, T. 1988. A Surface to Subsurface Study of the Sycamore Limestone (Mississippian) Along the North Flank of the Arbuckle Anticline. Unpublished Masters Thesis, University of Oklahoma, pp. 99.

Conant, L., C., and V. E. Swanson, 1961, Chattanooga Shale and related rocks of central Tennessee and nearby areas: U.S. Geological Survey Professional Paper 357, 91p.

Comer, J. B., and Hinch, H. H. 1987. Recognizing and Quantifying Expulsion of Oil from the Woodford Formation and Age-Equivalent Rocks in Oklahoma and Arkansas. The American Association of Petroleum Geologists Bulletin, v. 71, no. 7, pp. 844 –858.

Curtis, J. B. 2002. Fractures Shale-Gas Systems. American Association of Petroleum Geologist Bulletin, vol. 86, no. 11, pp. 1921 – 1938.

Davis, D. K., and Vessell, R. K. 2002. Gas Production from Shales. Gulf Coast Association of Geological Societies Transactions, vol. 52, pp. 1079 – 1091.

Dennis, L. F. N. 2004. The Woodford Shale in Portions of Logan County, Oklahoma: Feasibility of Defining an Algorithm for Mapping and Exploration. Unpublished Masters Thesis, Oklahoma State University, pp. 73.

Denison, R.E., 1982, Geologic cross section from the Arbuckle Mountains to the Muenster arch, southern Oklahoma and Texas: GSA Map and Chart Series MC-28R, 1 sheet, 8 p.

Devon Study, 2004: Proprietary

Ettensohn, F. R., Fulton, L. P., and Kepferle, R. C. 1979. Use of Scintillometer and Gamma-ray Logs for Correlation and Stratigraphy in Homogeneous Black Shales: Summary. Geological Society of America Bulletin, Part I, vol. 90, pp. 421 – 423.

Garner, D.L., and D.L. Turcotte, 1984, The thermal and mechanical evolution of the Anadarko basin: Tectonophysics, v. 107, p. 1-24

Gromadzki, G. A., 2004. Outcrop-Based Gamma-Ray Characterization of Arsenic-Bearing Lithofacies in the Garber-Wellington Formation, Cetral Oklahoma Aquifer (COA), Cleveland County, Oklahoma. Unpublished Masters Thesis, Oklahoma State University, pp. 232.

Ham, W.E., and J.L. Wilson, 1967, Paleozoic epeirogeny in the central United States: American Journal of Science, v. 265, no. 5, p. 332-407

Herron, S.L., and M.L. Herron, 1996 Quantitative Lithology: An Application for Open and Cased Hole Spectroscopy: Transactions of the SPWLA thirty-seventh annual Logging Symposium, New Orleans, LA, June 16-19, 1996. Paper E.

Hester, T., Sahl, H., and Schmoker, J., 1988, Cross sections based on gamma-ray, density, and resistivity logs showing stratigraphic units of the Woodford Shale, Anadarko basin, Oklahoma: United States Geological Survey Miscellaneous Field Studies Map 2054, 2 plates.

Hilpman, P., 1967, Devonian Stratigraphy in Kansas: a progress report: Tulsa Geological Society Digest, v. 35, p. 88-98

Hoffman, P., J. F. Dewey, and K. Burke, 1974, Aulacogens and their genetic relation to geosynclines, with a Proterozoic example from Great Slave Lake, Canada, in

Modern, U.S.A., in Aspects of diagenesis: SEPM Special Publication 19, p. 38-55.

Jarvie, D., 2004 Evaluation of Hydrocarbon Generation and Storage in the Barnett Shale, Ft. Worth Basin, Texas. Humble Geochemical Website www.humble-inc.com/

Johnson, G. J., Klapper, G., and Sandberg, A. C., 1985. Devonian Eustatic Fluctuations in Euramerica. Geological Society of America Bulletin, v. 96, pp. 567 – 587.

Johnson, K., 1989, Geologic evolution of the Anadarko basin, in K. Johnson, ed., Anadarko basin symposium, 1988: Oklahoma Geological Survey Circular 90, p. 3-12.

Jolly, G. D. 1988. Correlation of the Woodford Formation in South-Central Oklahoma Using Gamma-ray Scintillation Measurements of the Natural Background Radiation. Unpublished Masters Thesis, Stephen F. Austin State University, pp. 154.

Kennedy, M. J., Pevear, D. R., and Hill, R. J. 2002. Mineral Surface Control of Organic Carbon in Black Shale. Science, v. 295, pp. 657 – 660.

Kirkland, W. D., Denison, E. R., Summers, M. D and Gormly, R. J. 1992. Geology and Organic Geochemistry of the Woodford Shale in the Criner Hills and Western Arbuckle Mountains, Oklahoma. Oklahoma Geological Survey Circular 93, pp. 38 – 69.

Lambert, M., 1993. Internal Stratigraphy and Organic Facies of the Devonian-Mississippian Chattanooga (Woodford) Shale in Oklahoma and Kansas. AAPG Studies in Geology, v. 37, pp 163-176.

Lee, W., 1956, Stratigraphy and structural development of the Salina basin area: Kansas Geological Survey Bulletin 121, 167 p.

Newell, K., 1989, Salina basin: distribution of the Upper Devonian-Lower Mississippian Misener Sandstone (superimposed on sub-Chattanooga subcrop map): Kansas Geological Survey Open File Report 89-18, 1 plate.

Olson, R.K., 1982, Factors Controlling Uranium Distribution in Upper Devonian-Lower Mississippian Black Shales of Oklahoma and Arkansas, Doctoral, University of Tulsa, Tulsa, Oklahoma, 224 p.

Over, J. D. 1992. Conodonts and the Devonian-Carboniferous Boundary in the Upper Woodford Shale, Arbuckle Mountains, South-Central Oklahoma. Journal of Paleontology, v. 66, no. 2, pp. 293 –311.

Over, J. D., and Barrick, J. E. 1990. The Devonian / Carboniferous Boundary in the Woodford Shale, Lawrence Uplift, South-Central Oklahoma. Oklahoma Geological Survey Guidebook, pp. 63 – 73.

Raymond, Loren. A., 2002. Petrology: The Study of Igneous, Sedimentary and Metamorphic Rocks. 2nd Edition. New York, New York. McGraw Hill., 720pp.

Rottmann, K., 2000. Defining the role of Woodford-Hunton depositional relationships in Hunton stratigraphic traps of western Oklahoma, in Johnson, K. S. (ed.), Platform carbonates in the southern Midcontinent, 1996 symposium: Oklahoma Geological Survey Circular 101, p. 139-146.

Schieber, J. 2001. A Role for Organic Petrology in Integrated Studies of Mudrocks: Examples from Devonian Black Shales of the Eastern US. International Journal of Coal Geology, v. 47, issues 3-4, pp. 171 – 187.

Siy, S. E. 1988. Geochemical and Petrographic Study of Phosphate Nodules of the Woodford Shale (Upper Devonian – Lower Mississippian) of Southern Oklahoma. Unpublished Masters Thesis, Texas Tech University, pp. 170.

Sloss, L., 1963, Sequencesin the cratonic interior of North America: Geological Society of America Bulletin, v. 74, p. 93-114.

Spears, D. A. 1980. Towards a Classification of Shales. The Geological Society of London, vol. 137, pp. 125 – 129.

Sullivan, K., 1985, Organic facies variation of the Woodford Shale in western Oklahoma: Shale Shaker, v. 35, p. 76-89.

Swanson, V. E. 1961. Geology and Geochemistry of Uranium in Marine Black Shales. Geological Survey Professional Paper 356-C.

Swanson, V.E. and E.R. Landis, 1962, Geology of a uranium-bearing black shale of late Devonian age in north-central Arkansas: Arkansas Geol. And Conservation Comm. Inform. Circ. No. 22.

Tourtelot, H. A. 1979 Black Shale – Its Deposition and Diagenesis. Clays and Clay Minerals, vol. 27, no. 5, pp. 313 – 321.

U.S. Department of Energy, Morgantown Energy Technology Center, 1981, Evaluation of Devonian shale potential in (New York: DOE/METC-118) (Pennsylvania: DOE/METC-119) (West Virginia: DOE/METC-120, available from NTIS) (Eastern Kentucky/Tennessee: DOE/METC-121) (Ohio: DOE/METC-124): prepared for publication by Tetra Tech, Columbus, Ohio.

Woodrow, D., Fletcher, F., and Ahrnsbrak, W., 1973, Paleogeography and paleoclimate at the deposition sites of the Devonian Catskill and Old Red Sandstone Facies: Geological Society of America Bulletin, v. 84, p. 3051-3064.

APPENDIX A

Outcrop-Based Gamma-Ray Data

McAlester Cemetery Shale Pit

U (ppm)	TH(ppm)	K (%)	API	API (+)	API(-)	DEPTH (in)
40.8	5.8	1.0	365.60	455.00	276.20	1870
30.5	6.8	1.3	292.00	362.40	221.60	1824
39.0	7.9	1.4	366.00	454.70	277.30	1805
36.1	5.9	1.5	336.40	417.50	255.30	1769
41.2	6.4	1.5	379.20	471.00	287.40	1757
37.7	7.1	1.8	358.80	444.90	272.70	1745
41.5	5.5	1.9	384.40	476.70	292.10	1738
35.8	7.8	1.4	340.00	422.20	257.80	1702
33.2	6.5	1.5	315.60	391.50	239.70	1690
34.8	6.3	0.8	316.40	393.90	238.90	1678
38.4	6.1	0.8	344.40	428.90	259.90	1666
39.2	10.7	1.3	377.20	468.90	285.50	1654
39.8	5.8	1.5	365.60	454.00	277.20	1610
36.7	6.3	1.8	347.60	430.90	264.30	1577
38.7	5.5	1.7	358.80	445.10	272.50	1551
38.3	6.9	1.4	356.40	442.70	270.10	1524
36.5	4.2	1.7	336.00	416.60	255.40	1506
33.9	4.7	1.9	320.40	396.70	244.10	1452
29.3	5.4	1.8	284.80	352.40	217.20	1428
29.1	5.0	1.4	275.20	341.20	209.20	1188
35.0	5.5	1.1	319.60	397.30	241.90	1166
35.7	4.4	1.6	328.80	407.80	249.80	1151
30.5	6.3	1.9	299.60	370.70	228.50	1124
35.2	7.3	1.3	331.60	411.90	251.30	1112
38.2	6.6	1.3	352.80	438.40	267.20	1078
33.4	5.1	1.6	313.20	388.30	238.10	1057
32.9	4.7	1.2	301.20	374.10	228.30	1016
30.7	6.0	1.4	292.00	362.20	221.80	992
33.2	7.0	1.1	311.20	386.80	235.60	950
33.2	4.6	1.5	308.00	382.00	234.00	936
31.1	7.5	1.5	302.80	375.50	230.10	920
35.8	7.9	1.6	343.60	426.30	260.90	890
38.3	7.2	1.5	359.20	446.00	272.40	874
36.8	8.4	1.4	350.40	435.20	265.60	848
37.4	7.5	0.9	343.60	427.70	259.50	839
31.3	5.6	1.6	298.40	369.80	227.00	824
38.1	4.3	1.2	341.20	424.10	258.30	803
36.8	5.2	1.1	332.80	413.80	251.80	761
36.8	4.2	1.6	336.80	417.80	255.80	740
35.2	6.2	0.8	319.20	397.40	241.00	713
28.4	5.2	1.2	267.20	331.60	202.80	668
31.8	5.5	1.1	294.00	365.30	222.70	638
29.2	4.1	1.0	266.00	330.50	201.50	620
26.6	3.5	0.8	239.60	297.90	181.30	584
29.2	5.0	1.1	271.20	336.80	205.60	540

McAlester Cemetery Shale Pit Continued

U (ppm)	TH(ppm)	K (%)	API	API (+)	API(-)	DEPTH (in)
40.5	5.4	1.6	371.20	460.80	281.60	516
34.3	7.4	1.7	331.20	410.60	251.80	492
33.1	4.8	1.1	301.60	374.80	228.40	471
28.6	6.1	1.4	275.60	341.70	209.50	454
45.0	5.1	1.3	401.20	498.90	303.50	437
32.8	7.7	1.6	318.80	395.30	242.30	420
31.6	5.3	0.6	283.60	353.30	213.90	396
29.2	4.2	0.9	264.80	329.20	200.40	384
23.5	3.0	0.4	206.40	257.20	155.60	372
24.8	3.8	0.6	223.20	277.80	168.60	360
27.1	5.6	0.9	253.60	315.20	192.00	348
21.9	4.6	0.9	208.00	258.20	157.80	336
21.2	4.6	0.8	200.80	249.40	152.20	324
21.7	3.2	0.5	194.40	242.00	146.80	312
21.5	2.7	0.6	192.40	239.30	145.50	282
24.6	4.0	0.7	224.00	278.60	169.40	264
29.2	6.0	0.9	272.00	338.20	205.80	192
28.6	4.2	0.6	255.20	317.80	192.60	180
34.0	4.3	0.9	303.60	377.70	229.50	127
32.3	6.7	1.1	302.80	376.30	229.30	96
28.0	5.2	0.5	252.80	315.00	190.60	82
30.2	4.9	0.7	272.40	339.10	205.70	48
23.1	8.1	1.2	236.40	293.10	179.70	16

U (ppm)	TH(ppm)	K (%)	API	API (+)	API(-)	DEPTH (in)
17.3	3.5	0.5	160.40	199.50	121.30	820
20.0	3.5	0.8	186.80	231.90	141.70	814
6.9	2.4	0.9	79.20	97.20	61.20	808.5
18.7	4.2	0.5	174.40	217.00	131.80	804.5
17.9	3.9	0.6	168.40	209.30	127.50	793
16.3	5.2	0.7	162.40	201.60	123.20	785.5
14.9	4.6	0.6	147.20	182.80	111.60	782
12.5	4.1	0.9	130.80	161.70	99.90	765
16.5	4.1	0.7	159.60	198.10	121.10	745
23.6	4.9	0.5	216.40	269.50	163.30	720
23.6	4.2	0.5	213.60	266.00	161.20	713
29.7	3.3	0.9	265.20	329.70	200.70	684
26.8	4.6	0.8	245.60	305.40	185.80	672
34.8	5.5	0.1	302.00	377.30	226.70	660
40.6	5.5	0.8	359.60	447.90	271.30	649
44.1	5.7	0.3	380.40	474.90	285.90	632
37.3	6.2	1.3	344.00	427.40	260.60	625
40.1	7.4	0.9	364.80	454.20	275.40	618
34.9	4.5	0.4	303.60	378.70	228.50	615
34.9	4.9	0.8	311.60	387.90	235.30	608.5
36.1	3.7	0.7	314.80	392.10	237.50	604.5
34.4	5.7	0.9	312.40	388.70	236.10	590
36.2	4.4	1.2	326.40	405.60	247.20	583
36.3	5.6	0.8	325.60	405.40	245.80	570
37.9	4.7	1.3	342.80	425.90	259.70	559
36.8	4.3	1.0	327.60	407.50	247.70	554
33.2	6.9	1.3	314.00	389.90	238.10	542.5
32.0	5.3	1.0	293.20	364.50	221.90	531
36.6	5.4	1.1	332.00	412.80	251.20	528
36.8	4.1	1.1	328.40	408.30	248.50	508
33.0	6.9	1.6	317.20	393.30	241.10	478
35.0	5.4	1.0	317.60	395.00	240.20	447
27.7	4.9	1.1	258.80	321.30	196.30	441
30.0	6.0	0.9	278.40	346.20	210.60	378
23.1	5.0	1.0	220.80	274.00	167.60	352
25.3	5.4	1.0	240.00	298.00	182.00	343
38.4	6.5	1.0	349.20	434.50	263.90	328
36.7	7.7	0.8	337.20	419.90	254.50	303
37.2	6.6	0.8	336.80	419.40	254.20	272
36.0	4.9	1.4	330.00	409.70	250.30	266
29.6	5.0	1.4	279.20	346.20	212.20	255
30.9	4.9	1.3	287.60	356.90	218.30	248
33.7	6.2	1.0	310.40	386.00	234.80	241.5
34.1	6.0	1.1	314.40	390.80	238.00	229
34.6	4.5	0.8	307.60	382.90	232.30	225.5

I-35 Continued

U (ppm)	TH(ppm)	K (%)	API	API (+)	API(-)	DEPTH (in)
33.6	4.9	1.2	307.60	382.10	233.10	220
37.1	4.7	1.3	336.40	417.90	254.90	216
37.4	4.5	1.4	339.60	421.70	257.50	212.5
40.9	4.9	0.6	356.40	444.30	268.50	211.5
38.1	6.5	1.2	350.00	435.10	264.90	207
41.0	6.1	1.4	374.80	465.70	283.90	204
42.4	5.2	1.1	377.60	469.80	285.40	193.5
43.1	7.9	1.2	395.60	492.10	299.10	186
45.5	7.5	1.4	416.40	517.70	315.10	180
57.4	10.7	1.8	530.80	659.90	401.70	168
55.5	8.4	1.0	493.60	615.00	372.20	157.5
35.9	7.0	1.4	337.60	419.20	256.00	27.5
35.5	7.5	1.6	339.60	421.30	257.90	22.5
37.4	7.6	1.7	356.80	442.60	271.00	18
40.7	7.9	1.8	386.00	478.90	293.10	13.5
41.2	8.1	1.6	387.60	481.30	293.90	8.5
42.8	8.7	2.0	409.20	507.50	310.90	4

Hunton Quarry

U (ppm)	TH(ppm)	K (%)	API	API (+)	API(-)	DEPTH (in)
37.7	6.1	1.1	343.60	427.30	259.90	1163
37.0	4.6	1.2	333.60	414.60	252.60	1155
44.4	4.4	1.1	390.40	485.80	295.00	1137
43.6	5.0	0.9	383.20	477.20	289.20	1126
49.5	8.3	1.7	456.40	567.10	345.70	1112
51.8	7.5	1.6	470.00	584.30	355.70	1100
49.7	8.6	1.6	457.60	568.80	346.40	1084
46.0	8.6	1.8	431.20	535.40	327.00	1072
44.0	7.2	1.6	406.40	504.80	308.00	1058
48.0	7.4	2.1	447.20	554.80	339.60	1041
53.5	6.2	1.8	481.60	598.40	364.80	1028
34.3	5.0	1.1	312.00	387.80	236.20	1024
32.7	4.2	0.8	291.20	362.40	220.00	1020
31.3	3.1	0.8	275.60	342.90	208.30	920
30.0	4.0	0.7	267.20	332.60	201.80	907
50.8	5.7	0.9	443.60	552.70	334.50	840
46.3	4.4	0.9	402.40	501.20	303.60	821
45.7	5.6	0.6	397.60	495.80	299.40	812
42.9	4.6	1.0	377.60	470.00	285.20	806
41.4	7.5	1.0	377.20	469.50	284.90	773
41.8	6.3	0.9	374.00	465.70	282.30	760
44.7	4.4	0.8	388.00	483.40	292.60	747
40.6	3.5	0.5	346.80	432.50	261.10	721
42.5	5.3	1.2	380.40	473.10	287.70	695
35.0	4.5	0.9	312.40	388.70	236.10	671
32.3	4.5	1.0	292.40	363.50	221.30	663
34.6	5.8	1.2	319.20	396.60	241.80	647
39.0	3.8	0.4	333.60	416.20	251.00	579
36.0	6.1	1.3	333.20	413.90	252.50	566
40.7	6.0	0.9	364.00	453.20	274.80	539
51.5	6.4	1.0	453.60	565.00	342.20	512
49.6	7.0	0.8	437.60	545.40	329.80	494
46.0	4.6	1.1	404.00	502.80	305.20	476
35.4	5.9	1.2	326.00	405.10	246.90	437
37.5	6.3	0.7	336.40	419.10	253.70	425
44.7	5.7	1.3	401.20	498.90	303.50	380
40.3	7.5	1.5	376.40	467.50	285.30	360
45.7	7.3	0.9	409.20	509.70	308.70	350
43.7	4.9	0.8	382.00	475.90	288.10	349
39.5	5.7	1.1	356.40	443.30	269.50	343
38.0	5.2	1.4	347.20	431.20	263.20	331
37.2	5.5	1.1	337.20	419.30	255.10	318
28.2	6.3	0.8	263.60	327.90	199.30	282
28.3	5.5	0.9	262.80	326.70	198.90	268
33.7	5.5	1.7	318.80	395.10	242.50	247

Hunton Quarry Continued

U (ppm)	TH(ppm)	K (%)	API	API (+)	API(-)	DEPTH (in)
35.9	7.4	1.5	340.80	423.00	258.60	232
45.6	6.7	1.5	415.60	516.50	314.70	217
42.0	5.4	1.3	378.40	470.40	286.40	213
42.6	5.4	1.9	392.80	487.20	298.40	186
38.9	7.8	1.4	364.80	453.20	276.40	174
43.0	7.5	1.7	401.20	498.10	304.30	121
48.6	7.4	2.1	452.00	560.80	343.20	120
63.2	11.5	2.2	586.80	729.10	444.50	111
50.6	10.4	1.7	473.60	588.60	358.60	103
51.0	11.2	2.8	497.60	616.40	378.80	98
53.7	10.1	2.2	505.20	627.10	383.30	91
46.0	8.8	2.8	448.00	554.40	341.60	84
40.5	10.7	2.8	411.60	508.90	314.30	73
40.9	10.4	2.0	400.80	497.00	304.60	63
35.8	9.9	2.2	361.20	447.10	275.30	50
36.0	10.6	2.5	370.40	458.00	282.80	42
36.7	7.9	1.9	355.60	440.70	270.50	16
45.6	7.4	2.4	432.80	536.20	329.40	0

Brimley Residence

U (ppm)	TH(ppm)	K (%)	API	API (+)	API(-)	DEPTH (in)
11.8	7.8	1.9	156.00	191.20	120.80	183
15.0	5.5	1.6	167.60	206.30	128.90	168
14.2	7.6	1.6	169.60	208.80	130.40	158
14.1	5.9	2.1	170.00	208.30	131.70	139
18.4	7.5	2.1	210.80	259.30	162.30	125
19.5	6.5	1.9	212.40	261.70	163.10	120
21.5	4.7	2.1	224.40	276.30	172.50	111
25.0	5.8	1.5	247.20	306.00	188.40	91
26.9	5.9	1.4	261.20	323.70	198.70	74
29.3	8.4	1.9	298.40	369.20	227.60	61
28.1	6.3	1.9	280.40	346.70	214.10	48
31.8	5.5	1.5	300.40	372.50	228.30	41
30.0	5.9	1.5	287.60	356.50	218.70	36
32.0	5.3	1.7	304.40	377.10	231.70	28
35.3	6.6	1.2	328.00	407.60	248.40	23
35.0	3.9	1.3	316.40	392.90	239.90	21
34.4	8.0	1.1	324.80	403.80	245.80	0

Henryhouse Creek

U (ppm)	TH(ppm)	K (%)	API	API (+)	API(-)	DEPTH (in)
31.8	2.8	0.9	280.00	348.20	211.80	2709
29.8	4.5	0.8	269.20	334.90	203.50	2703
27.4	3.7	1.1	251.60	312.30	190.90	2697
28.0	3.1	0.7	247.60	308.10	187.10	2691
26.5	3.1	0.8	237.20	294.90	179.50	2685
26.1	3.7	0.6	233.20	290.30	176.10	2679
27.4	3.0	0.7	242.40	301.60	183.20	2673
29.8	4.1	0.5	262.80	327.50	198.10	2667
22.6	3.7	0.5	203.60	253.50	153.70	2661
22.0	5.0	0.8	208.80	259.40	158.20	2655
19.9	2.8	0.7	181.60	225.60	137.60	2649
15.9	3.7	0.9	156.40	193.70	119.10	2643
17.1	4.3	0.6	163.60	203.30	123.90	2637
13.3	3.2	0.7	130.40	161.60	99.20	2631
34.2	4.6	1.0	308.00	383.00	233.00	2625
39.6	7.4	1.3	367.20	456.40	278.00	2618
45.8	4.5	1.0	400.40	498.50	302.30	2612
49.4	7.5	0.9	439.60	547.70	331.50	2606
43.5	7.0	1.1	393.60	489.80	297.40	2600
43.8	6.2	1.2	394.40	490.60	298.20	2594
42.8	6.1	1.3	387.60	481.90	293.30	2588
47.6	6.5	1.6	432.40	537.30	327.50	2582
49.2	6.5	1.4	442.00	549.70	334.30	2576
50.2	6.4	1.0	443.20	552.00	334.40	2570
54.6	5.1	1.5	481.20	598.50	363.90	2564
57.0	6.5	0.9	496.40	618.70	374.10	2558
52.8	7.1	1.6	476.40	592.30	360.50	2552
52.4	8.3	1.1	470.00	585.30	354.70	2546
51.8	5.9	1.7	465.20	578.10	352.30	2540
44.5	6.0	1.7	407.20	505.60	308.80	2537
42.1	6.6	1.5	387.20	481.00	293.40	2529
43.6	4.6	1.8	396.00	491.40	300.60	2523
40.0	7.0	1.5	372.00	462.00	282.00	2517
45.0	7.2	1.2	408.00	507.60	308.40	2511
45.3	5.3	1.3	404.40	502.90	305.90	2505
44.2	7.2	1.3	403.20	501.40	305.00	2499
41.5	5.5	1.2	373.20	464.10	282.30	2493
45.4	5.3	1.0	400.40	498.50	302.30	2487
45.3	6.9	1.8	418.80	519.90	317.70	2481
46.7	5.9	1.3	418.00	519.90	316.10	2475
46.7	6.8	1.7	428.00	531.60	324.40	2467
38.9	5.0	0.9	345.60	430.20	261.00	2464
36.1	5.8	1.3	332.80	413.40	252.20	2455
38.2	5.7	1.5	352.40	437.50	267.30	2448
38.2	5.9	1.1	346.80	431.30	262.30	2442

Henryhouse Creek Continued

U (ppm)	TH(ppm)	K (%)	API	API (+)	API(-)	DEPTH (in)
38.2	5.9	1.1	346.80	431.30	262.30	2442
38.7	7.7	1.3	361.20	448.90	273.50	2436
42.9	6.1	1.4	390.00	484.70	295.30	2433
31.3	5.3	1.0	287.60	357.50	217.70	2392
31.9	6.6	0.8	294.40	366.40	222.40	2380
30.4	4.8	1.2	281.60	349.60	213.60	2374
26.2	5.1	1.2	249.20	309.10	189.30	2362
24.7	5.7	1.0	236.40	293.50	179.30	2350
32.7	5.6	1.1	301.60	374.80	228.40	2338
36.3	6.9	1.3	338.80	420.90	256.70	2329
35.0	5.9	1.3	324.40	402.90	245.90	2317
41.7	7.1	1.3	382.80	475.90	289.70	2305
37.3	6.5	1.4	346.80	430.70	262.90	2293
39.9	5.7	1.4	364.40	452.70	276.10	2281
46.2	6.7	1.4	418.80	520.70	316.90	2275
43.9	7.7	1.8	410.80	509.90	311.70	2263
44.5	2.8	1.8	396.00	491.40	300.60	2251
41.5	5.6	1.3	375.20	466.40	284.00	2248
38.3	4.5	1.7	351.60	436.10	267.10	2236
44.9	7.6	1.1	407.20	506.80	307.60	2224
50.0	4.4	1.3	438.40	545.40	331.40	2212
57.5	7.0	1.4	510.40	635.20	385.60	2200
48.6	5.1	1.2	428.40	533.10	323.70	2188
46.9	5.7	1.1	415.60	517.30	313.90	2176
45.1	6.0	1.5	408.80	508.00	309.60	2164
40.6	5.5	1.6	372.40	462.30	282.50	2152
42.0	5.4	1.1	375.20	466.80	283.60	2140
36.8	4.6	1.3	333.60	414.40	252.80	2137
44.1	5.5	1.8	403.60	500.90	306.30	2125
50.1	7.6	2.1	464.80	576.80	352.80	2113
40.4	6.4	1.7	376.00	466.60	285.40	2101
42.1	5.8	1.0	376.00	468.00	284.00	2089
39.8	6.4	1.3	364.80	453.40	276.20	2083
38.5	5.1	1.1	346.00	430.30	261.70	2077
43.9	5.0	1.1	388.80	483.80	293.80	2065
87.2	8.1	1.8	758.80	944.90	572.70	2053
102.5	12.2	2.3	905.60	1127.40	683.80	2041
100.2	7.7	1.1	850.00	1060.30	639.70	2038
106.3	8.3	3.1	933.20	1160.30	706.10	2026
77.0	7.2	2.0	676.80	842.00	511.60	2014
77.3	7.9	2.2	685.20	852.10	518.30	2002
80.9	10.0	1.8	716.00	891.40	540.60	1990
103.5	12.0	2.5	916.00	1140.00	692.00	1981
105.9	12.1	3.0	943.60	1173.50	713.70	1969

Henryhouse Creek Continued

U (ppm)	TH(ppm)	K (%)	API	API (+)	API(-)	DEPTH (in)
86.9	10.7	3.3	790.80	981.90	599.70	1957
82.5	11.4	2.9	752.00	934.20	569.80	1945
93.5	10.9	1.9	822.00	1023.70	620.30	1942
81.8	11.1	2.9	745.20	925.70	564.70	1918
72.7	9.1	2.5	658.00	817.50	498.50	1906
65.9	8.8	2.3	599.20	744.40	454.00	1894
62.9	11.4	2.3	585.60	727.40	443.80	1882
65.5	12.3	2.1	606.80	754.30	459.30	1870
47.7	9.0	1.8	446.40	554.40	338.40	1858
40.9	8.8	2.3	399.20	494.40	304.00	1851
46.1	11.5	2.6	456.40	565.30	347.50	1839
38.0	6.7	2.4	369.20	456.70	281.70	1827
44.5	8.3	2.0	421.20	522.50	319.90	1815
43.7	9.7	1.9	418.80	519.70	317.90	1803
41.6	8.8	2.0	400.00	496.00	304.00	1791
36.2	6.3	2.5	354.80	438.50	271.10	1779
41.6	8.8	2.3	404.80	501.40	308.20	1767
42.9	7.9	2.3	411.60	509.90	313.30	1755
39.6	8.4	2.5	390.40	483.00	297.80	1743
42.4	9.0	2.4	413.60	512.20	315.00	1731
45.4	6.1	2.3	424.40	525.90	322.90	1719
36.2	10.0	2.4	368.00	455.20	280.80	1707
39.6	7.1	2.4	383.60	474.70	292.50	1695
37.8	7.1	2.3	367.60	454.90	280.30	1683
39.6	8.4	2.2	385.60	477.60	293.60	1671
41.6	8.7	2.4	406.00	502.70	309.30	1659
41.7	8.1	2.5	406.00	502.50	309.50	1647
35.1	7.2	2.3	346.40	428.40	264.40	1635
35.0	8.5	2.0	346.00	428.50	263.50	1623
35.6	7.9	1.7	343.60	426.10	261.10	1611
33.2	8.8	1.8	329.60	408.40	250.80	1599
32.3	7.2	2.4	325.60	402.20	249.00	1587
42.1	7.6	1.7	394.40	489.60	299.20	1575
42.8	5.8	1.6	391.20	485.80	296.60	1563
37.1	5.5	1.9	349.20	432.70	265.70	1551
37.9	6.3	2.3	365.20	451.90	278.50	1539
42.2	7.4	1.8	396.00	491.40	300.60	1527
38.5	8.6	2.2	377.60	467.60	287.60	1515
36.7	6.3	1.7	346.00	429.10	262.90	1503
32.3	9.1	2.1	328.40	406.30	250.50	1491
32.7	5.1	2.3	318.80	393.90	243.70	1479
34.7	7.5	2.2	342.80	424.10	261.50	1467

42.3	8.5	2.8	417.20	515.90	318.50	1386
37.8	7.9	2.2	369.20	457.10	281.30	1374
48.3	10.1	2.3	463.60	574.90	352.30	1362
46.6	9.5	2.2	446.00	553.10	338.90	1350
45.6	8.3	2.6	439.60	544.30	334.90	1338
46.4	11.1	2.5	455.60	564.50	346.70	1326
35.9	8.7	2.6	363.60	449.30	277.90	1323
37.7	7.4	1.7	358.40	444.60	272.20	1311
39.6	8.1	2.1	382.80	474.30	291.30	1299
35.9	11.2	2.4	370.40	458.20	282.60	1287
36.0	9.4	2.6	367.20	453.80	280.60	1275
36.2	7.9	2.1	354.80	439.30	270.30	1263
35.0	8.3	2.4	351.60	434.70	268.50	1251
34.8	7.1	2.3	343.60	424.90	262.30	1239
35.6	9.2	2.0	353.60	438.00	269.20	1233
35.2	8.3	2.5	354.80	438.50	271.10	1227
41.1	12.3	2.9	424.40	524.70	324.10	1224
40.0	7.5	2.5	390.00	482.50	297.50	1212
38.7	8.6	3.0	392.00	484.00	300.00	1206
35.3	7.9	1.9	344.40	426.70	262.10	1203
34.8	8.1	2.0	342.80	424.50	261.10	1201
31.4	6.6	2.2	312.80	386.60	239.00	1189
31.7	8.3	2.2	322.00	398.10	245.90	1177
22.4	9.3	1.9	246.80	304.70	188.90	1174
28.5	7.9	2.4	298.00	367.70	228.30	1168
31.0	7.6	2.2	313.60	387.60	239.60	1162
31.9	6.7	1.9	312.40	386.70	238.10	1156
27.9	7.6	1.9	284.00	351.20	216.80	1152
33.3	9.2	2.2	338.40	418.60	258.20	1140
32.4	7.8	1.7	317.60	393.60	241.60	1134
22.4	7.9	2.0	242.80	299.50	186.10	1126
26.8	10.6	2.1	290.40	358.80	222.00	1122
27.7	10.1	2.2	297.20	367.10	227.30	1110
30.2	7.5	2.2	306.80	379.10	234.50	1098
32.4	5.1	1.8	308.40	381.90	234.90	1086
36.9	9.6	2.1	367.20	454.80	279.60	1080
26.6	7.6	1.6	268.80	332.80	204.80	1074
30.7	4.5	1.3	284.40	352.90	215.90	1068
27.0	4.8	1.7	262.40	324.60	200.20	1062
27.8	5.2	1.5	267.20	331.00	203.40	1056
29.6	5.6	1.8	288.00	356.40	219.60	1050
28.5	8.3	1.9	291.60	360.70	222.50	1044
33.8	5.7	1.7	320.40	397.10	243.70	1038
32.0	8.4	1.7	316.80	392.60	241.00	1032
33.6	5.4	1.8	319.20	395.40	243.00	1026
33.7	5.5	1.9	322.00	398.70	245.30	1020

38.2	8.0	1.8	366.40	454.40	278.40	1014
39.8	8.1	1.9	381.20	472.70	289.70	1008
41.0	6.3	1.9	383.60	475.70	291.50	1005
50.9	8.5	1.8	470.00	583.90	356.10	999
45.8	8.6	1.8	429.60	533.40	325.80	993
38.9	7.4	1.8	369.60	458.40	280.80	987
38.5	6.6	1.6	360.00	446.80	273.20	981
33.9	7.2	1.5	324.00	402.00	246.00	975
33.3	6.9	1.8	322.80	399.90	245.70	969
36.2	6.3	1.3	335.60	416.90	254.30	963
38.0	5.5	1.3	346.80	430.90	262.70	957
37.0	5.9	1.7	346.80	430.10	263.50	954
36.1	8.6	1.8	352.00	436.40	267.60	948
36.5	6.5	2.0	350.00	433.50	266.50	942
41.0	7.7	1.9	389.20	482.70	295.70	936
40.2	9.0	1.7	384.80	477.60	292.00	930
40.9	7.8	1.5	382.40	475.00	289.80	924
41.3	6.8	1.8	386.40	479.40	293.40	918
43.8	6.0	1.6	400.00	496.80	303.20	912
36.7	7.8	1.6	350.40	434.80	266.00	906
43.3	7.5	1.5	400.40	497.50	303.30	900
38.4	7.6	2.5	377.60	467.00	288.20	894
39.2	8.3	2.3	383.60	474.90	292.30	888
40.1	8.8	2.1	389.60	482.80	296.40	882
44.6	7.5	2.4	425.20	526.70	323.70	876
49.2	7.8	2.1	458.40	568.80	348.00	870
48.8	8.0	2.0	454.40	564.00	344.80	864
43.2	10.2	1.7	413.60	513.60	313.60	858
42.1	5.8	1.5	384.00	477.00	291.00	852
40.4	8.4	1.7	384.00	476.60	291.40	846
36.4	9.9	1.7	358.00	444.10	271.90	843
38.3	8.3	1.7	366.80	455.10	278.50	837
44.5	7.0	1.6	409.60	508.80	310.40	831
47.0	8.4	1.7	436.80	542.60	331.00	825
50.6	9.0	1.9	471.20	585.20	357.20	819
47.2	5.8	1.7	428.00	531.60	324.40	813
37.2	6.4	2.0	355.20	440.00	270.40	807
45.1	6.4	1.1	404.00	502.80	305.20	806
42.9	5.3	0.9	378.80	471.70	285.90	800
40.9	6.6	1.3	374.40	465.40	283.40	794
43.9	8.2	1.4	406.40	505.20	307.60	788
48.2	10.3	1.5	450.80	560.50	341.10	782
44.5	8.1	1.6	414.00	514.30	313.70	776
42.3	10.3	1.8	408.40	506.90	309.90	770
38.8	6.8	1.5	361.60	449.00	274.20	764
41.0	5.2	1.6	374.40	464.80	284.00	758

Henryhouse Creek Continued

U (ppm)	TH(ppm)	K (%)	API	API (+)	API(-)	DEPTH (in)
41.4	5.1	1.1	369.20	459.30	279.10	752
35.2	6.5	0.9	322.00	400.70	243.30	746
37.4	7.5	1.6	354.80	440.30	269.30	740
39.0	8.4	1.8	374.40	464.40	284.40	734
31.5	9.3	1.7	316.40	392.10	240.70	722
34.9	8.8	1.8	343.20	425.40	261.00	710
39.6	8.5	2.2	386.00	478.10	293.90	698
34.5	8.8	1.9	341.60	423.20	260.00	686
40.0	7.7	2.2	386.00	478.10	293.90	674
47.5	11.7	2.9	473.20	585.70	360.70	662
47.5	7.0	1.3	428.80	533.40	324.20	650
32.6	6.0	1.6	310.40	384.80	236.00	638
29.1	7.6	1.5	287.20	356.00	218.40	626
29.2	7.0	1.6	287.20	355.80	218.60	614
33.6	5.8	1.2	311.20	386.60	235.80	602
28.1	7.1	1.8	282.00	348.90	215.10	590
27.4	9.3	1.8	285.20	352.90	217.50	578
44.7	9.6	2.5	436.00	540.00	332.00	566
34.8	7.4	2.0	340.00	421.00	259.00	554
29.0	8.1	2.2	299.60	370.10	229.10	542
27.8	7.2	1.8	280.00	346.40	213.60	530
32.8	6.6	1.7	316.00	391.60	240.40	518
30.6	9.9	1.5	308.40	382.50	234.30	506
31.4	7.3	1.8	309.20	382.90	235.50	494
37.8	10.0	2.0	374.40	464.00	284.80	482
34.1	8.5	1.5	330.80	410.50	251.10	470
34.7	6.3	1.9	333.20	412.70	253.70	465
33.8	8.5	2.2	339.60	420.10	259.10	455
35.4	8.4	2.4	355.20	439.20	271.20	443
39.6	7.1	1.6	370.80	460.30	281.30	431
38.6	8.8	1.8	372.80	462.40	283.20	419
28.5	6.6	1.4	276.80	343.20	210.40	407
36.9	5.3	1.2	335.60	417.10	254.10	395
48.1	6.6	1.4	433.60	539.20	328.00	383
45.5	4.8	1.4	405.60	504.20	307.00	371
37.5	8.1	1.1	350.00	435.30	264.70	359
34.5	6.6	1.8	331.20	410.40	252.00	347
36.3	5.1	1.7	338.00	419.10	256.90	335
30.1	7.2	1.3	290.40	360.40	220.40	323
30.7	7.8	1.4	299.20	371.20	227.20	299
46.5	8.0	2.2	439.20	544.60	333.80	287
38.0	8.8	1.7	366.40	454.60	278.20	275
28.0	5.8	1.1	264.80	328.80	200.80	263
28.4	8.6	1.4	284.00	352.20	215.80	251

Henryhouse Creek Continued

U (ppm)	TH(ppm)	K (%)	API	API (+)	API(-)	DEPTH (in)
37.8	8.5	2.0	368.40	456.50	280.30	239
51.1	9.0	2.3	481.60	597.40	365.80	227
41.2	7.0	1.6	383.20	475.80	290.60	215
39.8	7.1	1.6	372.40	462.30	282.50	203
42.9	7.1	1.2	390.80	486.10	295.50	191
43.4	7.6	1.0	393.60	490.00	297.20	179
65.7	11.2	1.2	589.60	734.60	444.60	167
59.6	10.0	1.9	547.20	680.20	414.20	155
56.1	9.7	2.2	522.80	649.10	396.50	143
56.4	8.7	2.5	526.00	652.50	399.50	131
66.0	10.5	2.0	602.00	748.50	455.50	119
20.4	8.5	2.4	235.60	289.70	181.50	108
27.9	10.3	2.0	296.40	366.50	226.30	81
29.6	12.9	2.1	322.00	398.30	245.70	64
20.4	9.6	1.9	232.00	286.20	177.80	51
31.3	9.4	1.3	308.80	383.40	234.20	40
28.5	9.9	1.8	296.40	366.90	225.90	33
24.3	8.0	1.9	256.80	317.20	196.40	21
19.8	5.3	1.2	198.80	246.10	151.50	3

APPENDIX B

Frequency Distributions of Compiled Outcrop Gamma-Ray Data

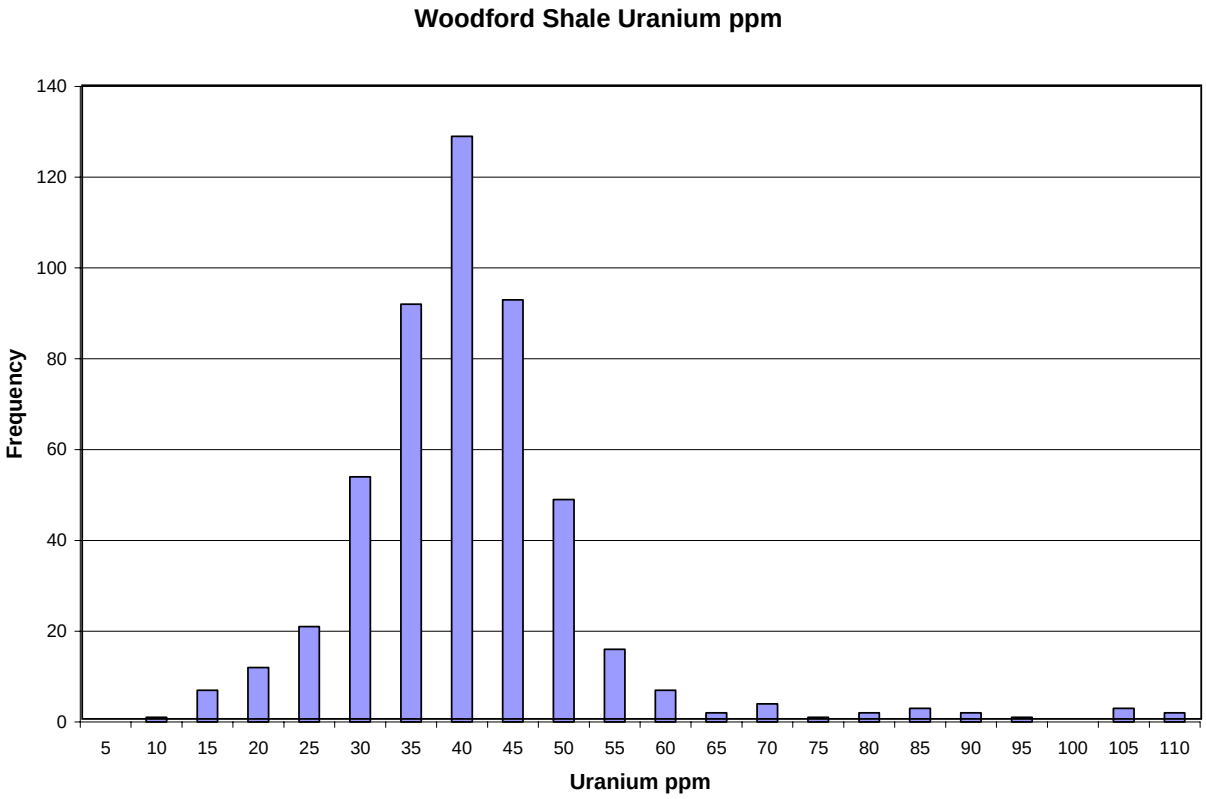

Average: 38.5 ppm
Standard deviation: 12.6

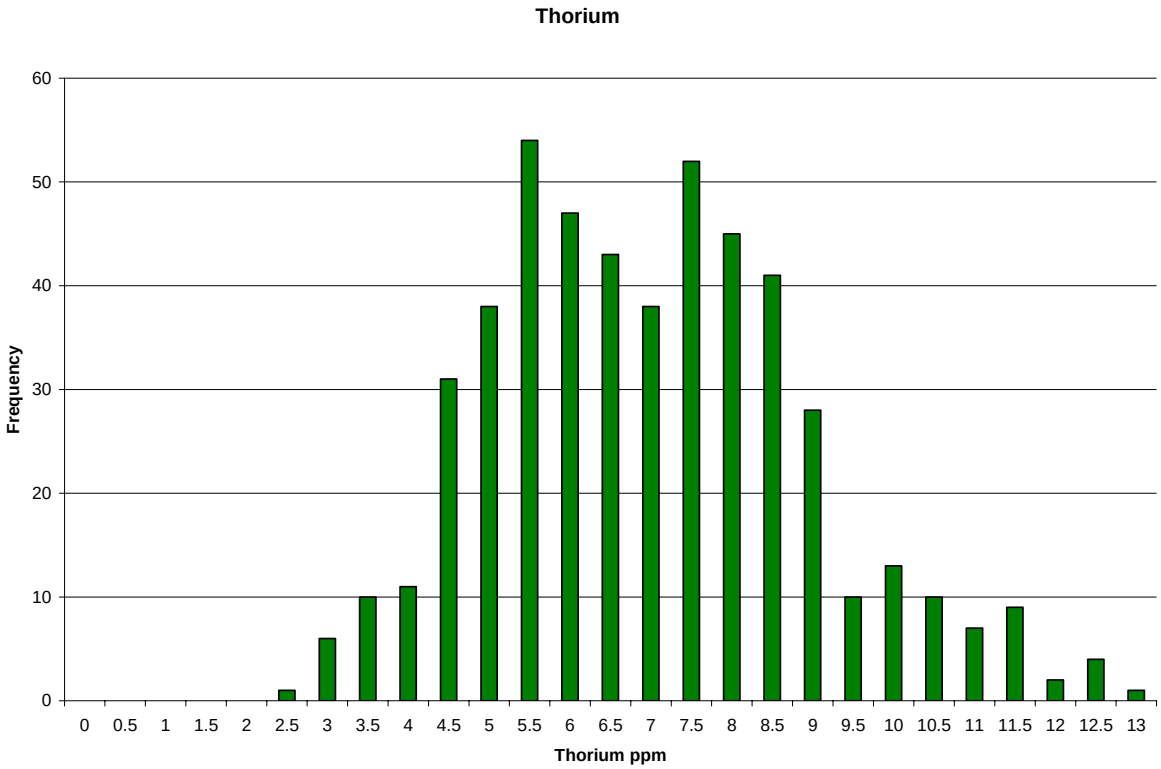

Average: 6.8 ppm
Standard deviation: 1.97

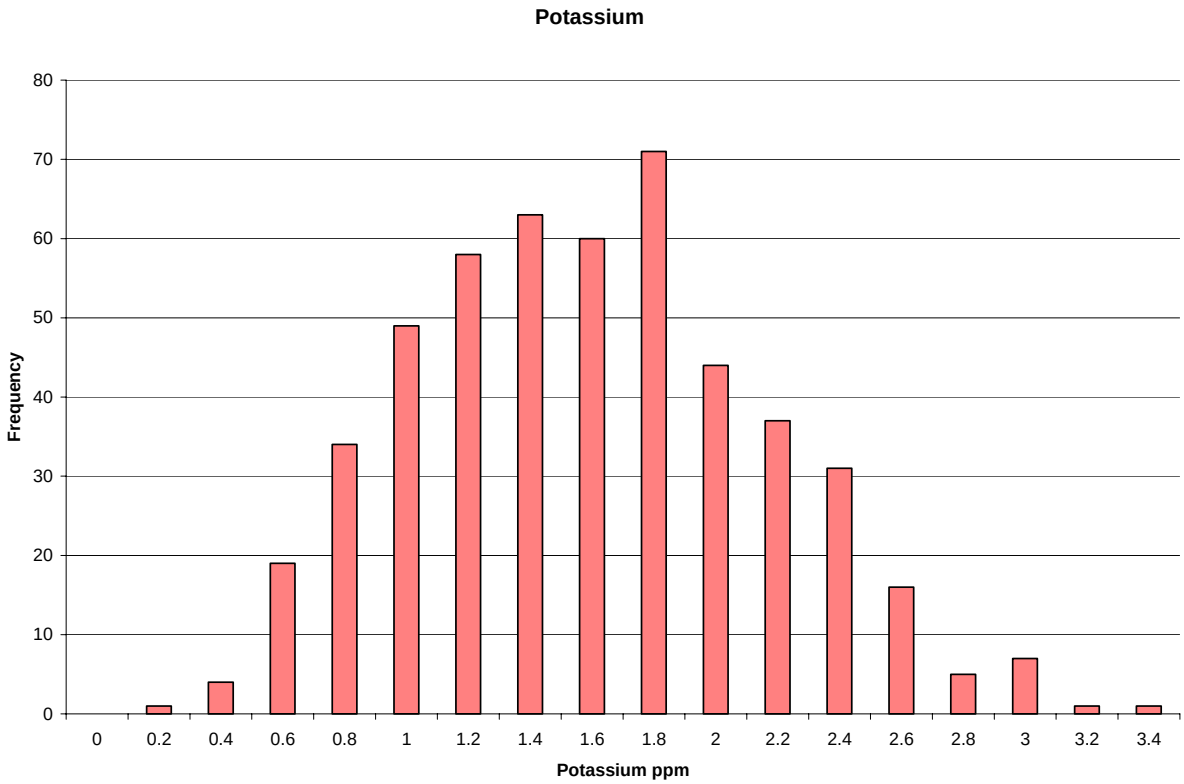

Average: 1.5 %
Standard deviation: 0.575

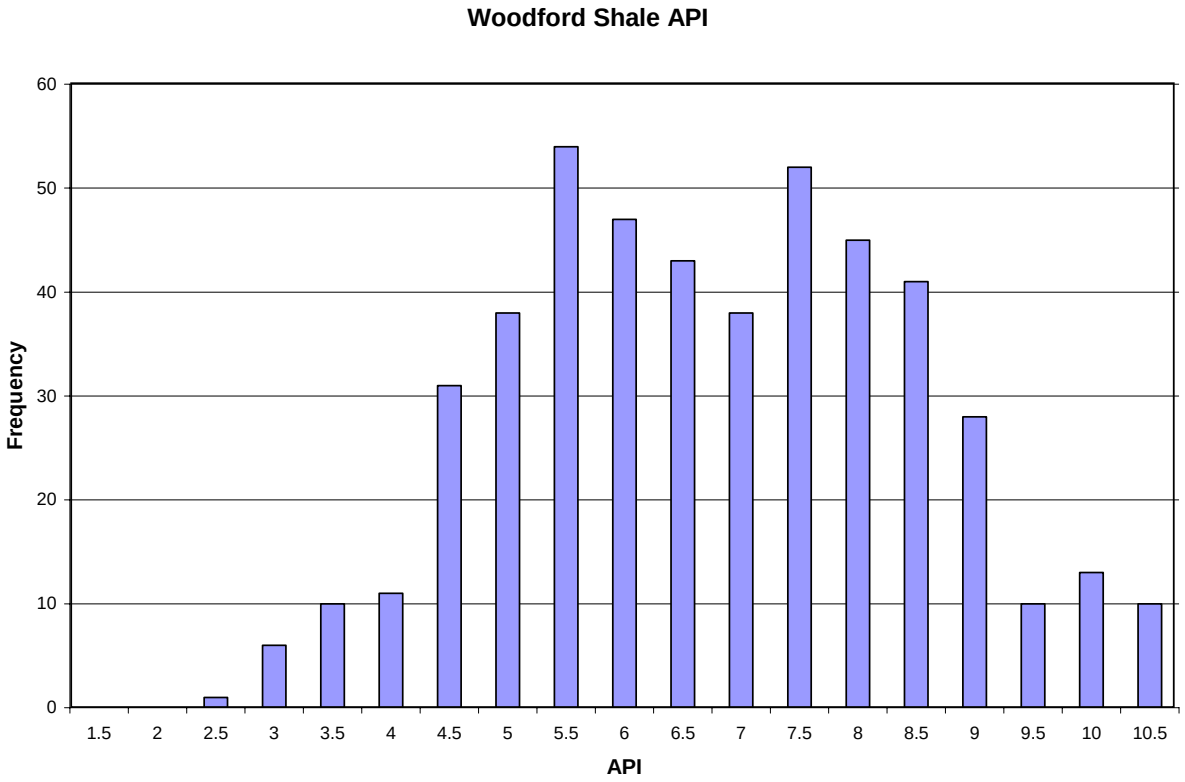

Average: 360 API
Standard deviation: 108.9

APPENDIX C

I-35 THIN-SECTION PHOTOGRAPHS

LOCATED WITHIN UNDESIGNATED AREAS OF THE OUTCROP

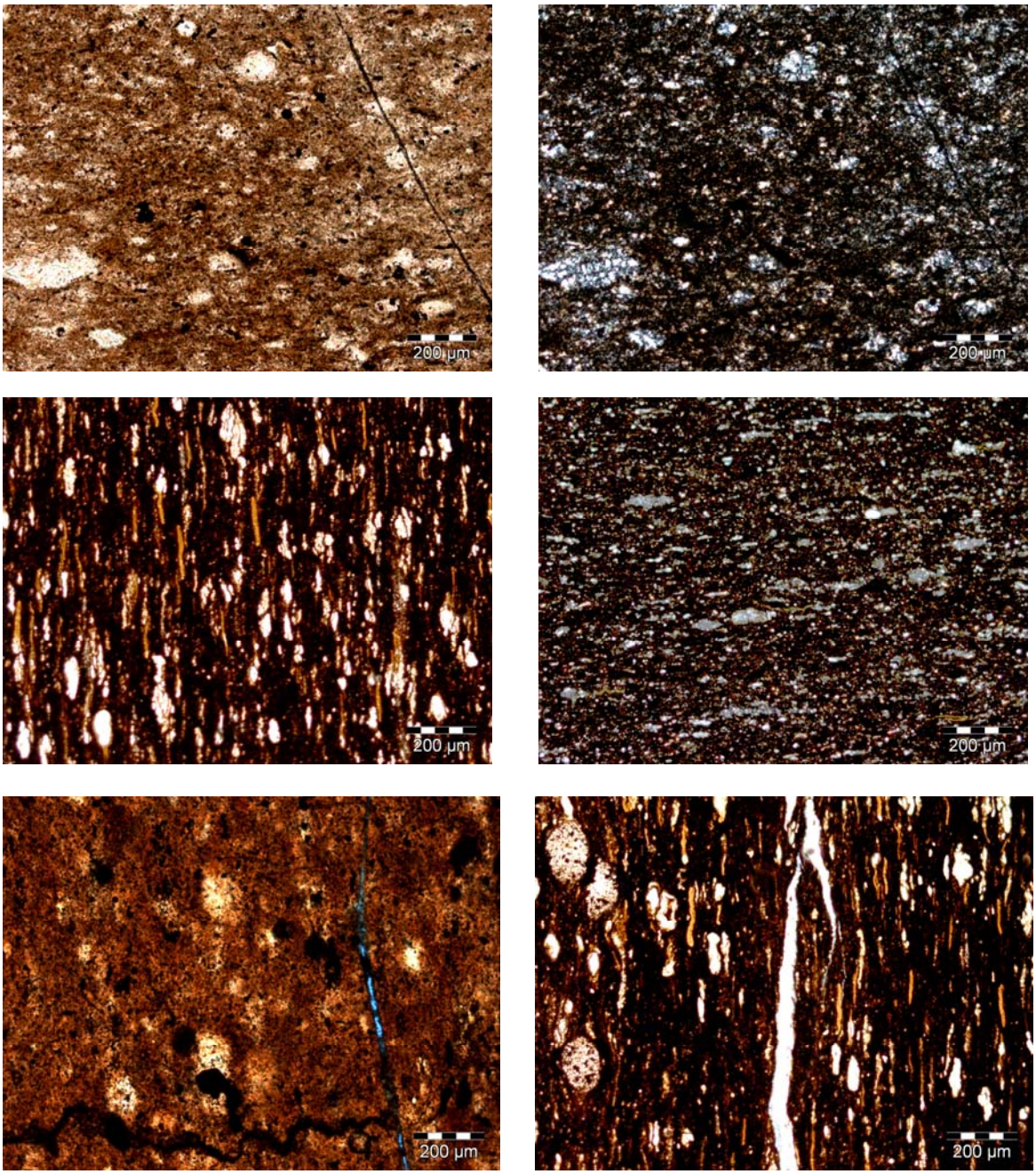

I-35 thin section photographs from undesignated areas of the outcrop.

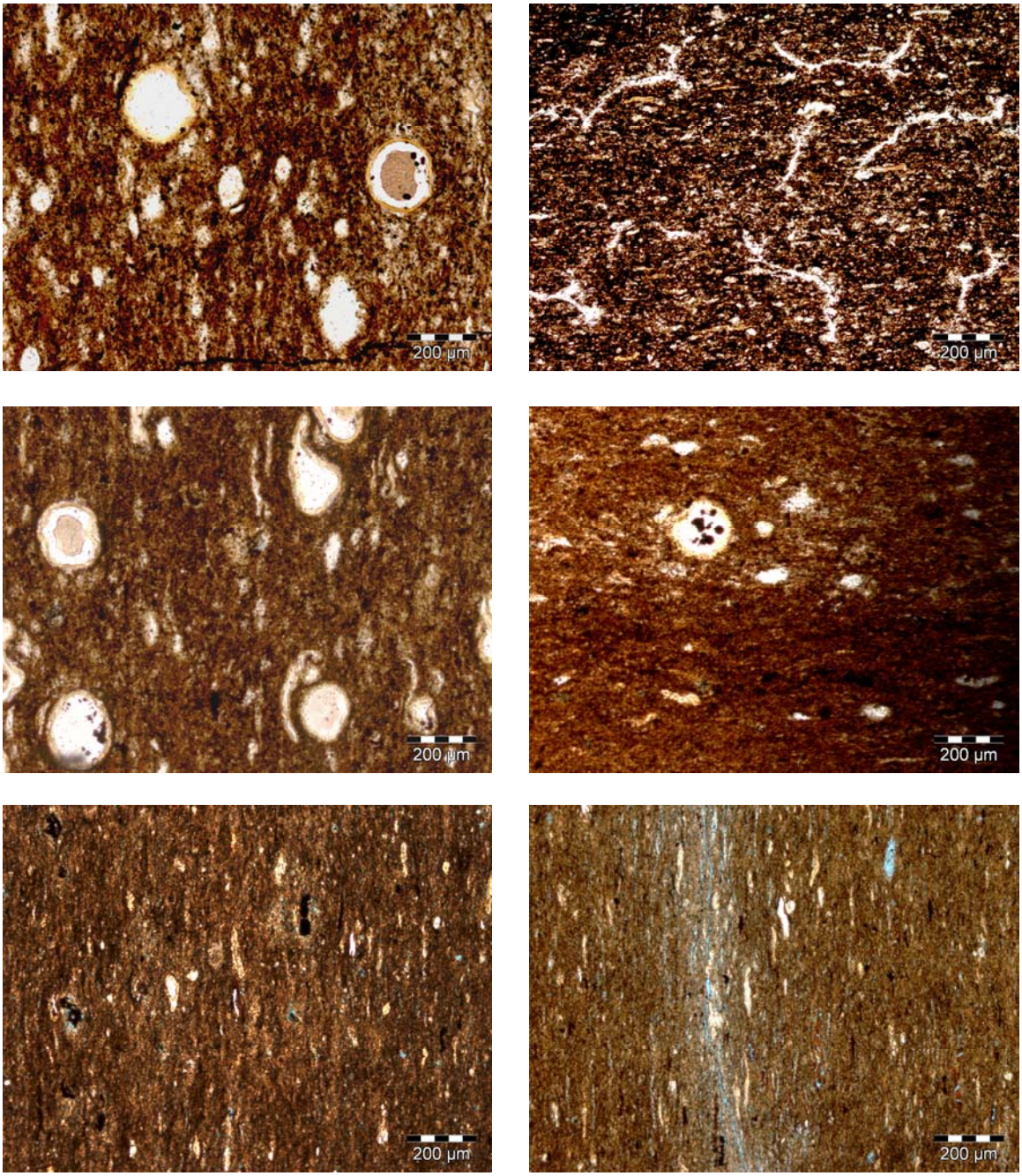

I-35 thin section photographs from undesignated areas of the outcrop.

APPENDIX C

I-35 THIN-SECTION PHOTOGRAPHS

LOCATED WITHIN DOCUMENTED AREAS OF THE OUTCROP

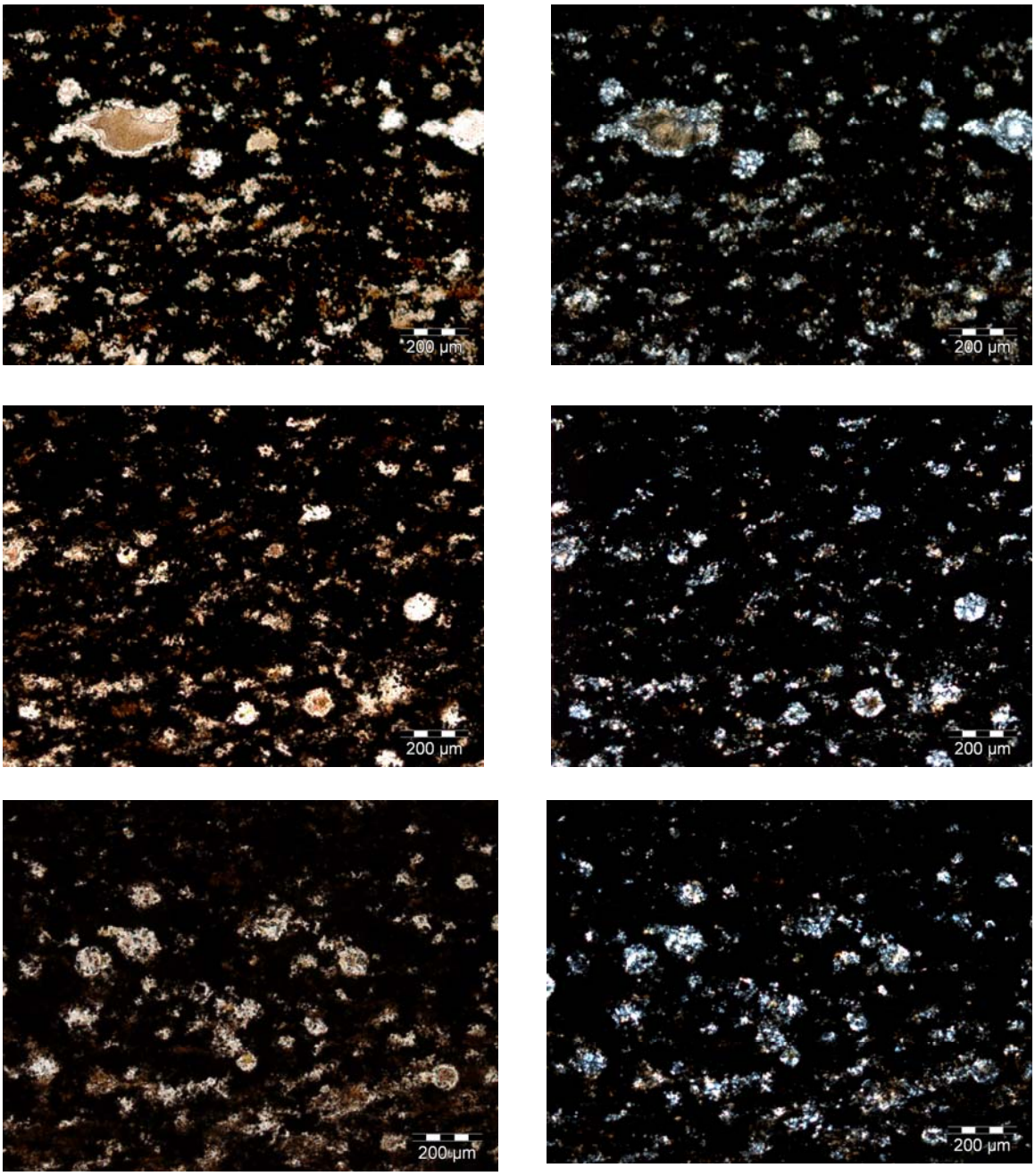

Photographs of thin sections from the upper Woodford Shale (left side represents transmitted light and the right side represents cross polarization).

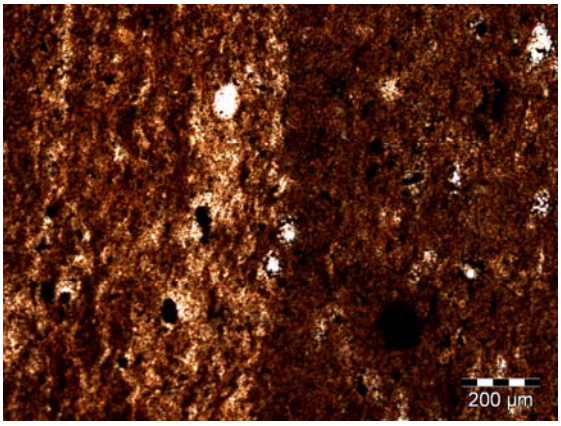

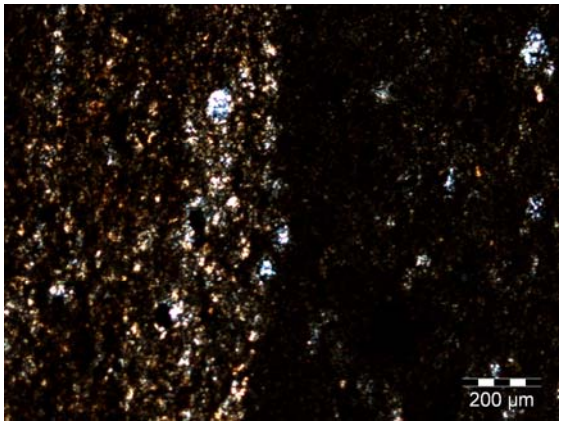

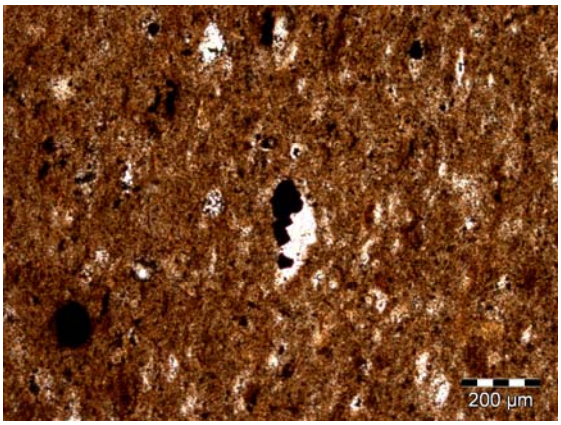

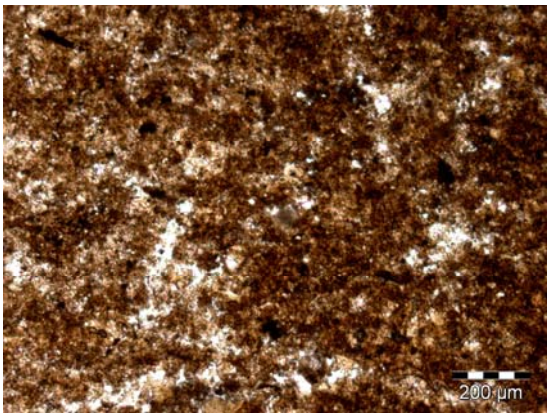

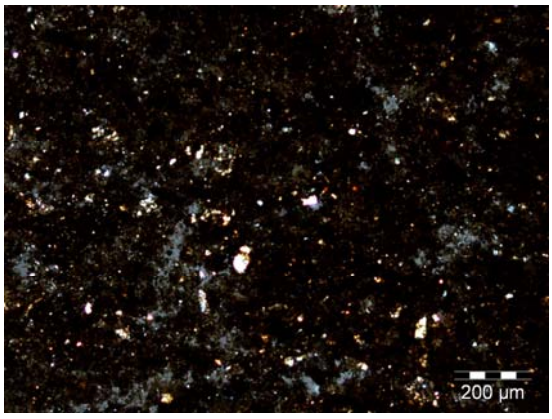

Photographs of thin sections from the upper Woodford (left side represents transmitted light and the right side represents cross polarization).

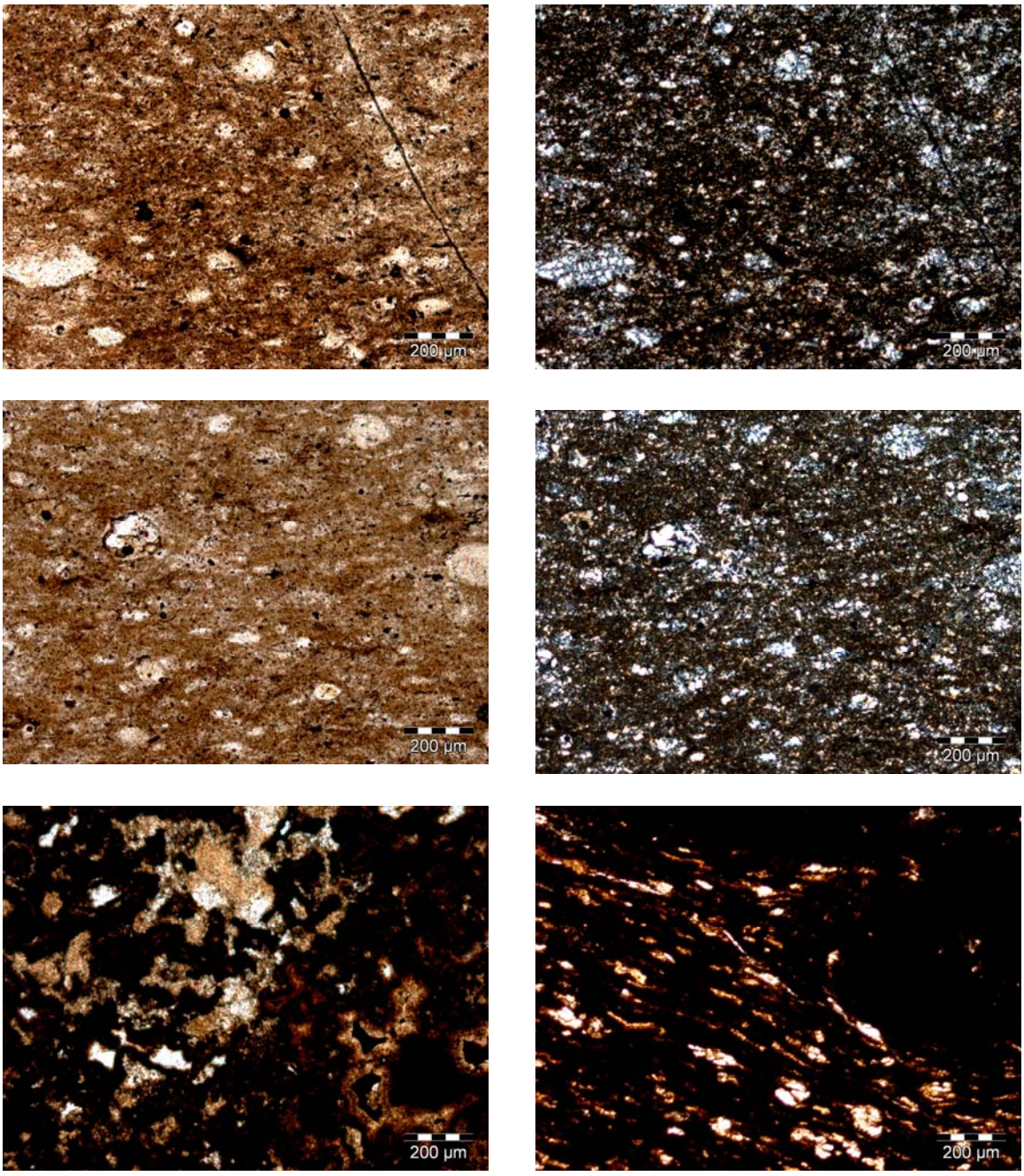

Photographs of thin sections from the upper Woodford Shale.

APPENDIX C

HENRYHOUSE CREEK ROCK SAMPLES AND THIN-SECTION PHOTOGRAPHS LOCATED WITHIN DOCUMENTED AREAS OF THE OUTCROP

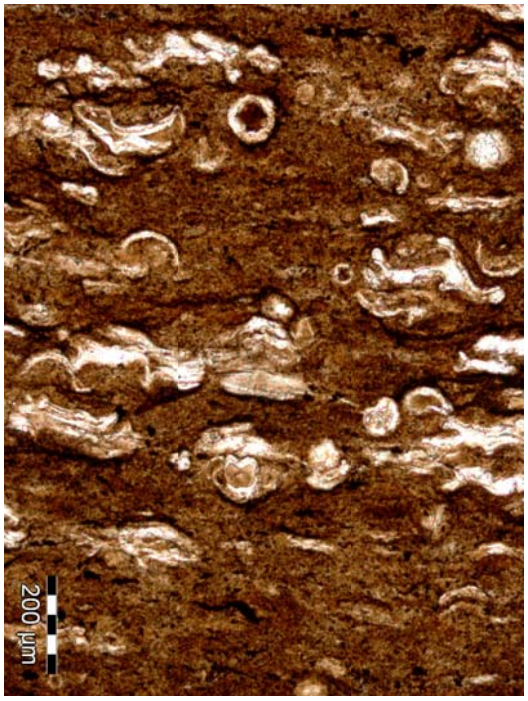

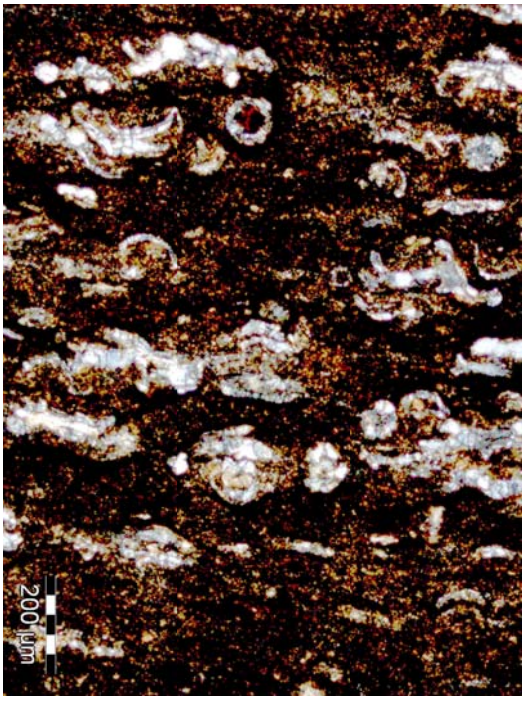

Siliceous shale sample collected from the Upper Woodford shale.

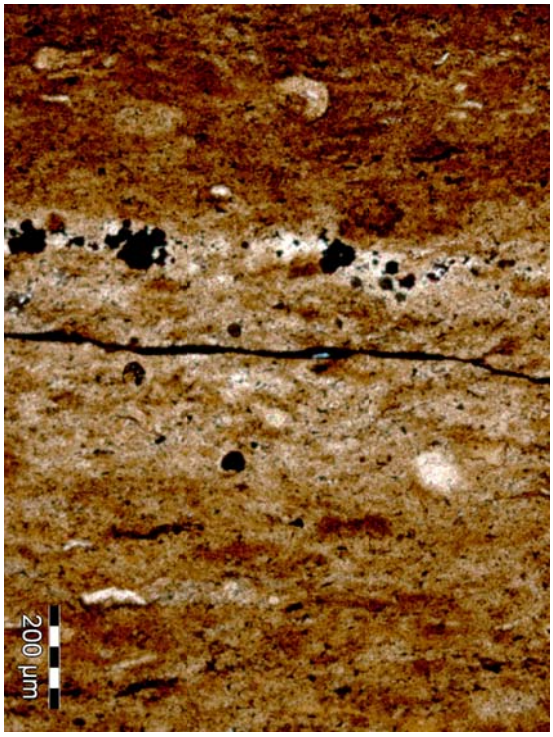

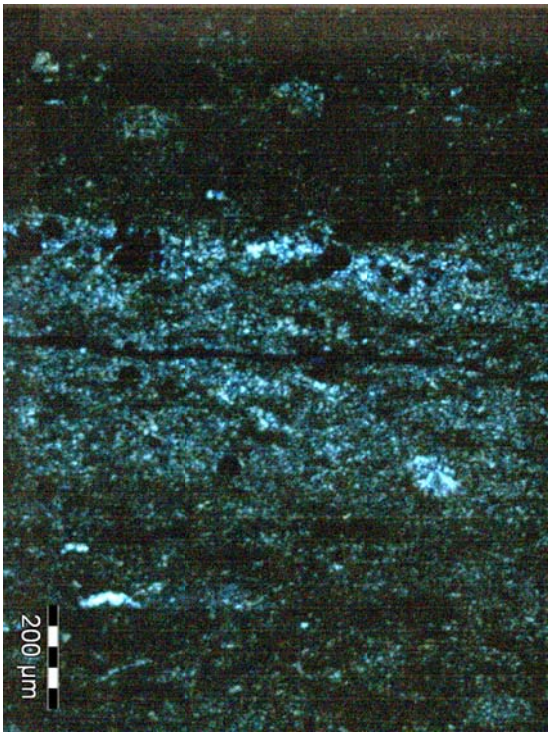

Siliceous shale sample with a phosphate nodule that was collected from the Upper Woodford shale.

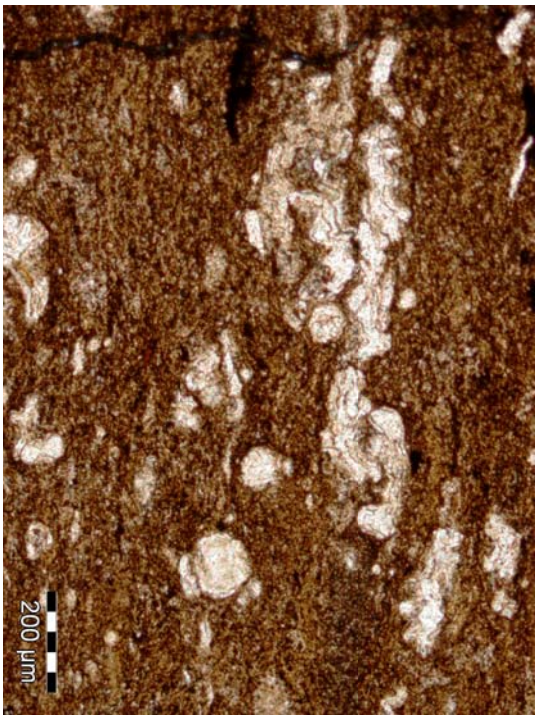

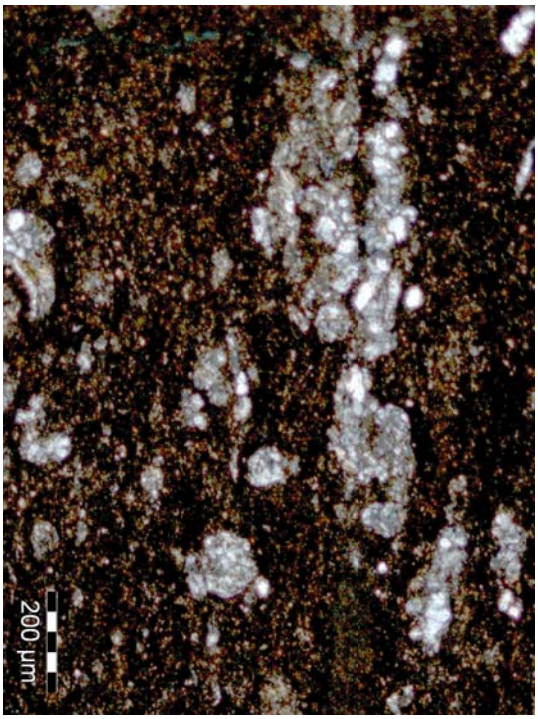

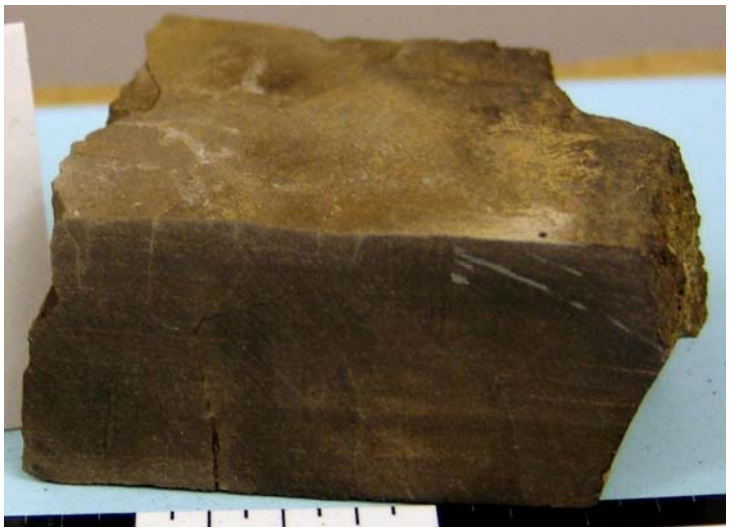

Siliceous shale sample collected from the Upper Woodford Shale.

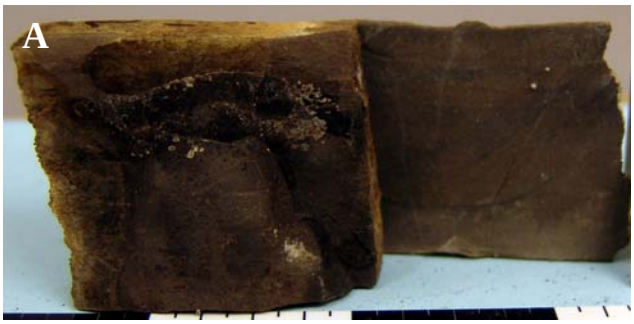

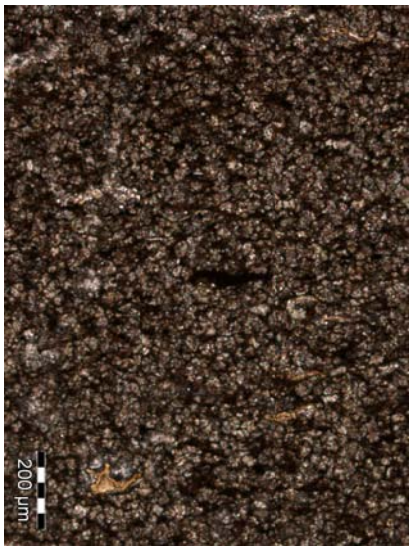

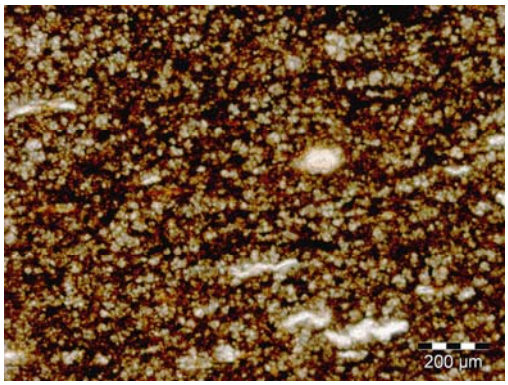

(A) Siliceous shale sample with dolomite located in the upper Woodford Shale.
(B) Fissile shale sample with dolomite located in the upper Woodford Shale.

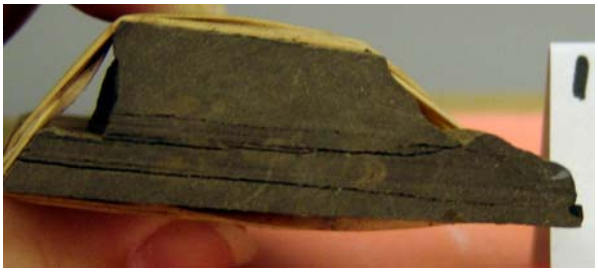

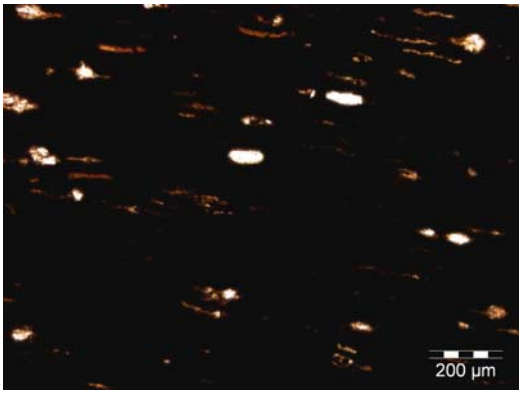

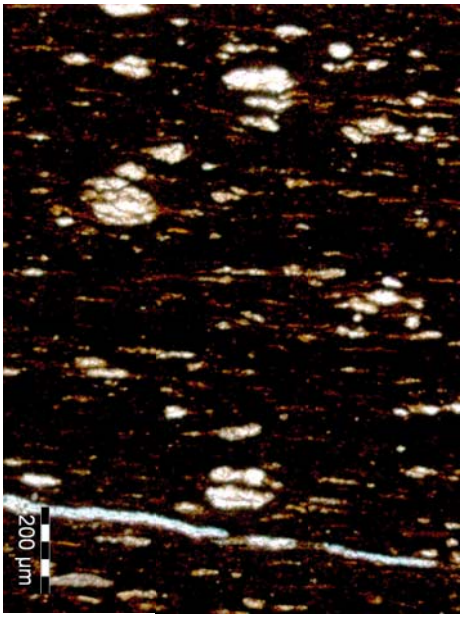

Fissile shale samples collected from the middle Woodford Shale.

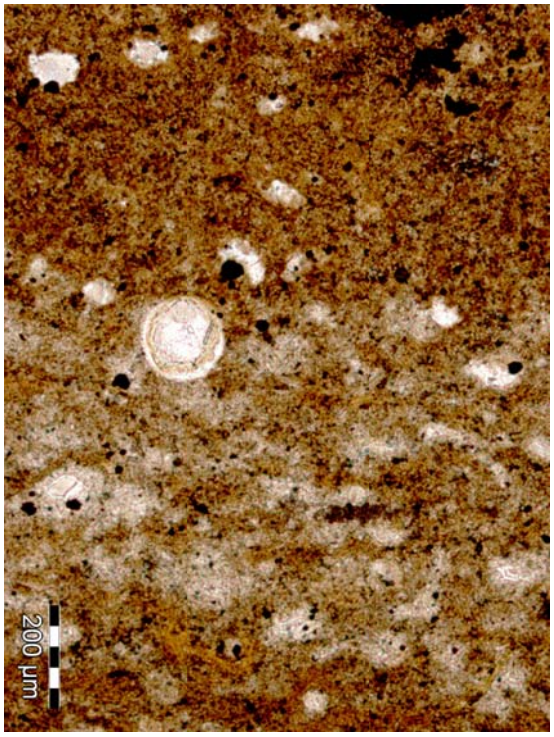

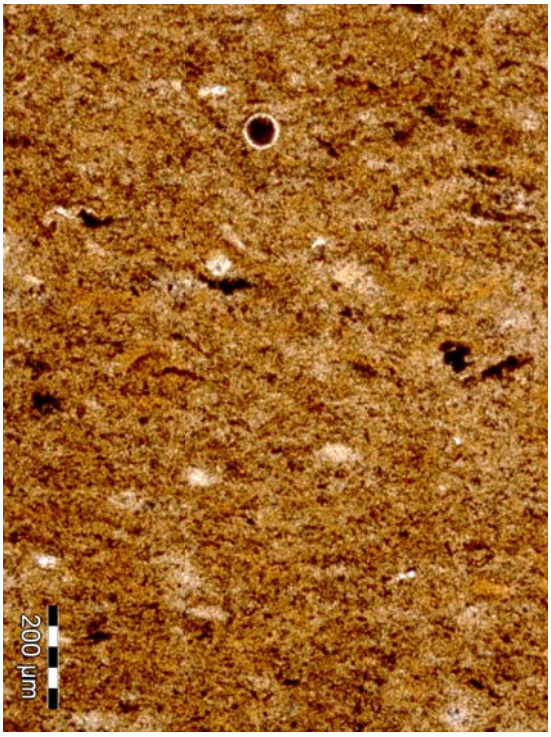

Siliceous shale sample collected from the middle Woodford Shale.

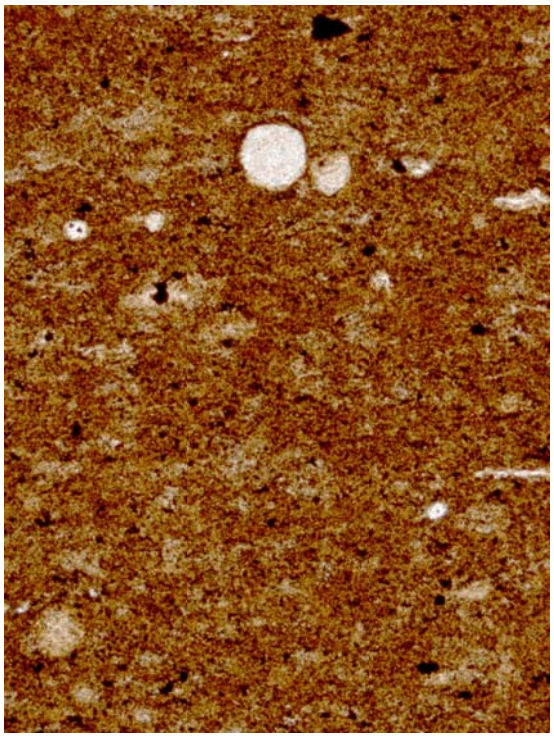

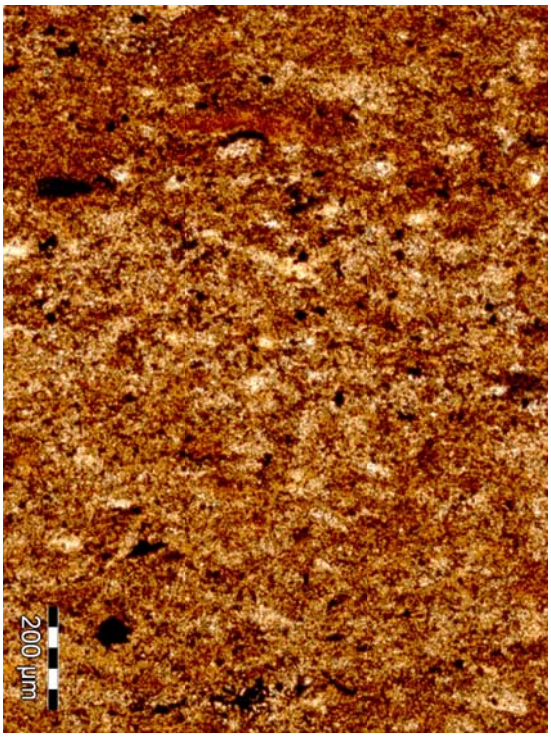

Siliceous shale sample collected from the middle of the Woodford Shale.

APPENDIX C

MCALESTER CEMETERY SHALE PIT ROCK SAMPLES AND THIN SECTION PHOTOGRAPHS LOCATED WITHIN DOCUMENTED AREAS OF THE OUTCROP

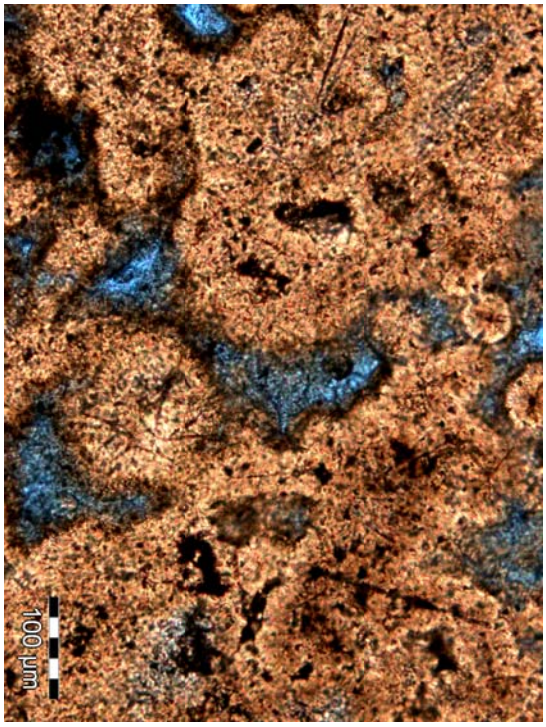

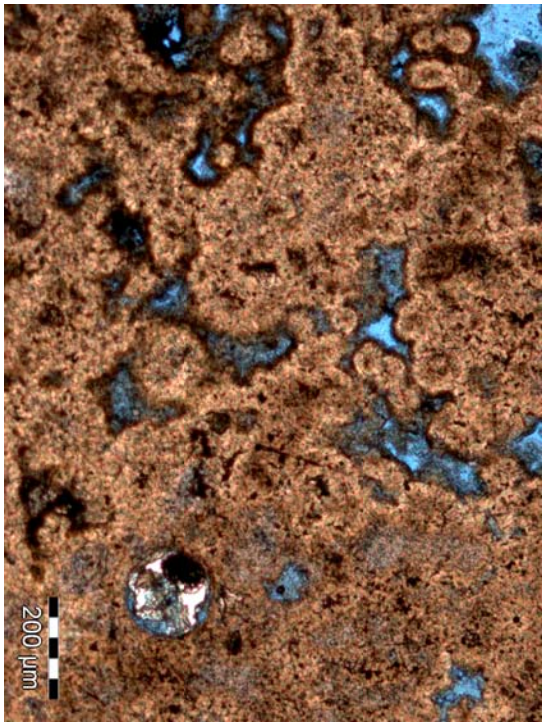

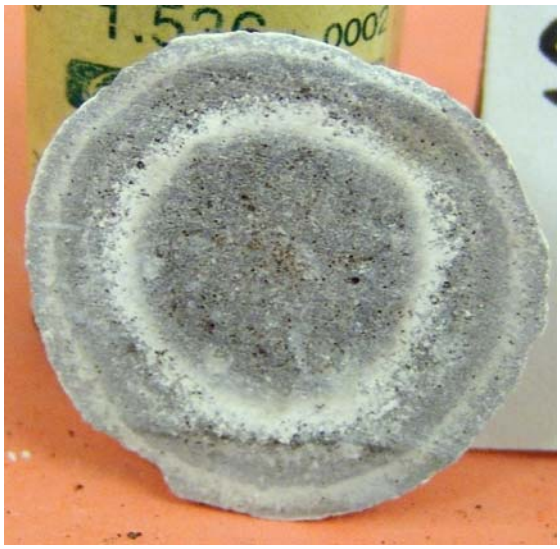

Phosphate nodule collected from the upper Woodford Shale.

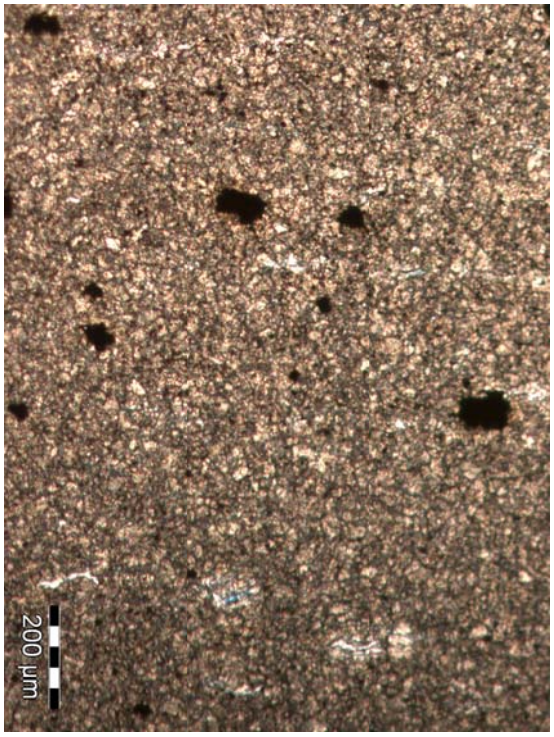

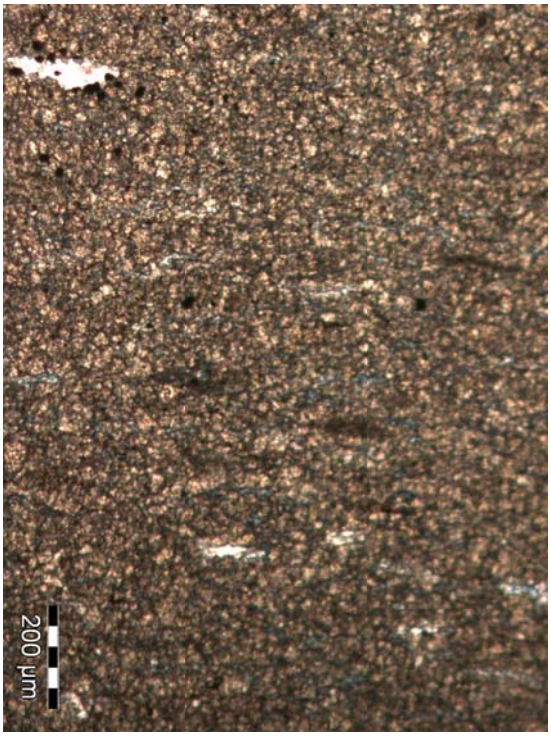

Sample of a dolomite bed that was collected from the upper Woodford Shale.

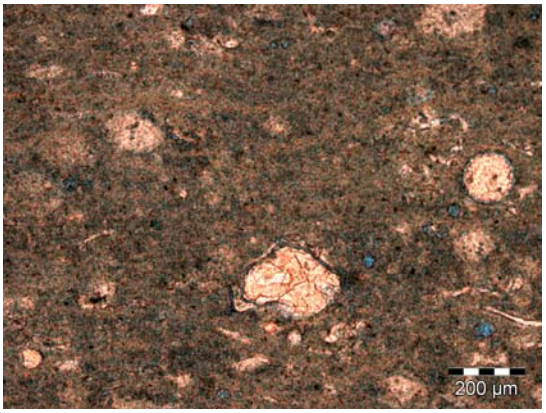

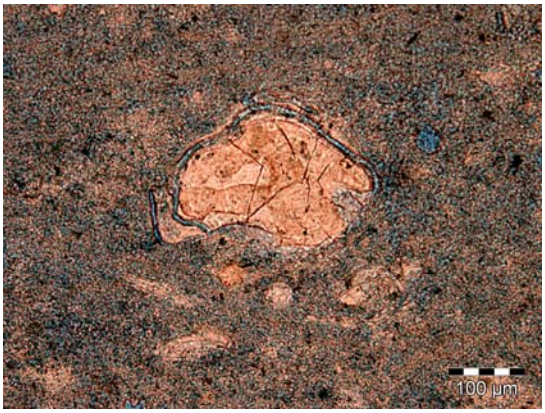

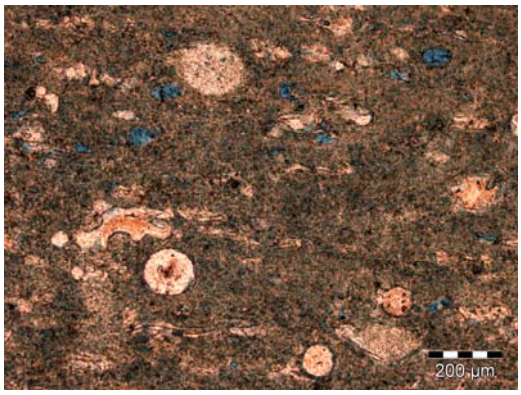

Chalk-like shale that was collected from the upper Woodford Shale.

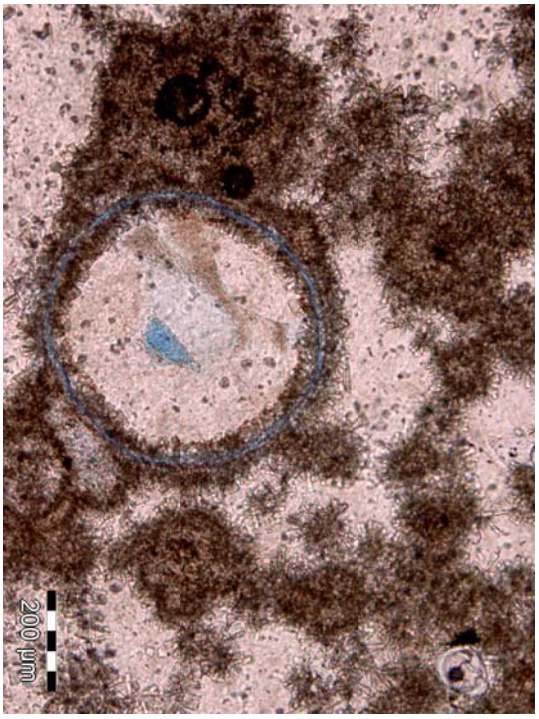

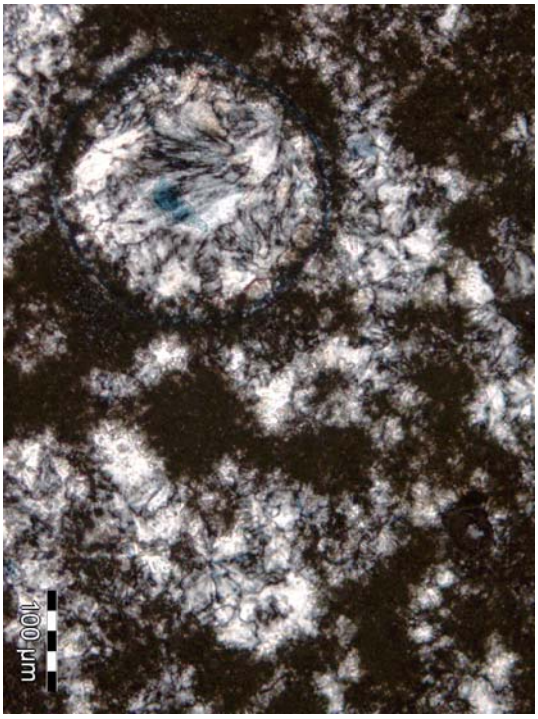

Chert sample that was collected from the upper Woodford Shale.

APPENDIX D

X-RAY DIFFRACTION DATA COLLECTED FROM THE I-35 OUTCROP

XRD Data

Sample #	Depth (in)	TOC	Quartz %	Na-Plag %	K-Spar%	Calcite %	Dolomite %	Pyrite %	Jarosite %	Kaolinite %	Chlorite %	Montomorillonite %	Ilite %	Mixed layer illite/smectite %
1	0" base	12.73	43	1	1	trc	trc	1	3	2			29	15
2	27	11.37	41	trc	2				3	2		11	25	6
3	45	9.01	44		2	trc	trc		4	1	trc	12	24	5
4	137	11.28	46	trc	1	trc			4	1			24	14
5	160	8.91	49	trc	1			1	4	trc			26	10
6	169	14.95	42	trc	2		trc		6	1	trc	20	13	7
7	180	12.34	53	trc	2				2	trc	trc	17	13	7
8	200	12.43	50	trc	1				4	1	1		22	12
9	209	15.43	52	trc	1				2	trc		2	24	10
10	216	0.83	75		trc			trc	5	1			8	7
11	221	14.48	37		1				2	trc			28	16
12	229	3.50	71		trc			trc	3	1		6	8	7
13	241	11.22	41		1				3	trc	trc		19	15
14	258	11.65	46		1				1	trc	1		21	15
15	264	0.86	76	trc	1				2	1	trc		6	8
16	280	12.42	41	trc	2	2		3	4	2			21	14
17	296	2.95	67						1	1			13	12
18	308	12.40	44	trc	1				2	2			24	11
19	325	10.23	47	trc	1	1			3	1	trc		24	13
20	350	12.32	43	trc	1	trc		trc	3	1			25	12
21	363		41	trc	1	trc			trc	1			26	13
22	379	14.31	70	trc	trc			trc	tc	trc			8	14
23	429	0.62	71		trc			trc	3	1			13	10
24	444	5.49	46	trc	1	trc			3	1			21	11
25	457	12.69	44		1			trc	4	2	trc		23	13
26	477	7.68	39	trc	1				4	1			23	16
27	484	10.65	43	trc	1			4	4	1	trc		24	11
28	500	10.78	40		1				1	1	trc		22	15
29	516	11.87	50		1	trc			3	1			21	13
30	529	14.72	39	trc	1	1			4	1			22	18
31	540	14.24	40	trc	1				5	1			23	18
32	558	14.36	41		1				2	1	trc		20	17
33	566	13.33	43		1	trc			3	2			21	19
34	571	17.01	42	trc	1				trc	trc			19	19
35	589	3.43	78						2	1			6	11
36	606	14.23	50	trc	trc				2	2	trc		20	17
37	620	10.08	54	trc	trc				4	1			19	13
38	628	14.49	46								1		19	14

APPENDIX E

TOC VALUES FROM SAMPLES COLLECTED AT THE I-35 OUTCROP

Sample ID	Depth (Inches)	TOC
1	0	12.73
2	27	11.37
3	45	9.01
4	137	11.28
5	160	8.91
6	169	14.95
7	180	12.34
8	200	12.43
9	209	15.43
10	216	0.83
11	221	14.48
12	229	3.50
13	241	11.22
14	258	11.65
15	264	0.86
16	280	12.42
17	296	2.95
18	308	12.40
19	325	10.23
20	350	12.32
22	379	14.31
23	429	0.62
24	444	5.49
25	457	12.69
26	477	7.68
27	484	10.65
28	500	10.78
29	516	11.87
30	529	14.72
31	540	14.24
32	558	14.36
33	566	13.33
34	571	17.01
35	589	3.43
36	606	14.23
37	620	10.08
38	628	14.49

APPENDIX F

VITRINITE REFLECTANCE DATA

Table 1
Dispersed Organic Matter Thermal Alteration, Kerogen Type and Total Compositional Analysis

Devon Energy

Sample Type: Outcrops

	Source Quality							% Source Material							Preservation				Recovery			% Kerogen Comp.							Vitrinite				
HGS ID	Sample Id.	TOC	S2	Hydrogen Index (HI)	Tmax (°C)	Color	TAI	Amorphous Debris	Finely Dissem. OM	Herb. Plant Debris (Vit.)	Woody Plant Debris	Coaly Fragments	Algal Debris	Palynomorphs	Good	Fair	Poor	Very poor	Good	Very Poor	Barren	Indigenous Vitrinite	Caved Vitrinite	Recycled/Oxidized Vitrinite	Inerinite	Solid Bitumen	Drilling Additive/Contamination	Amorphous Kerogen	# of Readings	Total Sample Ro (%)	# of Indigeonus Readings	Indigenous Ro (%)	*Comments*
05-2786-109747	1	12.73	-1	-1	-1	O, OB	2.3, 2.7	99	tr	tr				1	X				X			tr		tr	tr	tr		100	16	0.64	3	0.72	Tasmanites? sp.
05-2786-109757	10	0.83	-1	-1	-1	O, OB	2.3, 2.7	97	2	1				1	X				X			1		tr	2			97	40	0.67	22	0.70	spherical palynomorphs
05-2786-109770	24	5.49	-1	-1	-1	O, OB	2.3, 2.7	83	10	3				4	X				X			2		1	2			95	40	0.74	31	0.71	Tasmanites? sp.
05-2786-109784	38	14.49	-1	-1	-1	O, OB	2.3, 2.7	98	2	tr				tr	X				X			tr		tr	1			99	28	0.73	19	0.70	

" -1 = sample analysis not requested'

tr = trace

Color Abbreviations: GLY Green-Light Yellow; Y Yellow; YO Yellow-Orange; OB Orange-Brown; LB Light Brown; B Brown; DBDG Dark Brown-Dark Gray; DGBL Dark Gray-Black; BLK Black

TAI Scale: 1=Unaltered; 1+ or 1.5; 2=Slight alteration; 2+ or 2.5; 3=Moderate alteration; 3+ or 3.5; 4=Strong alteration; 4+ or 4.5; 5=Severe alteration

Immature:	0.02% to 0.60%
Oil window Maturity:	0.60% to 1.10%
Condensate and/or wet-gas window:	1.10% to 1.40%
Dry gas window:	1.40% to 3.0 or 4.0%

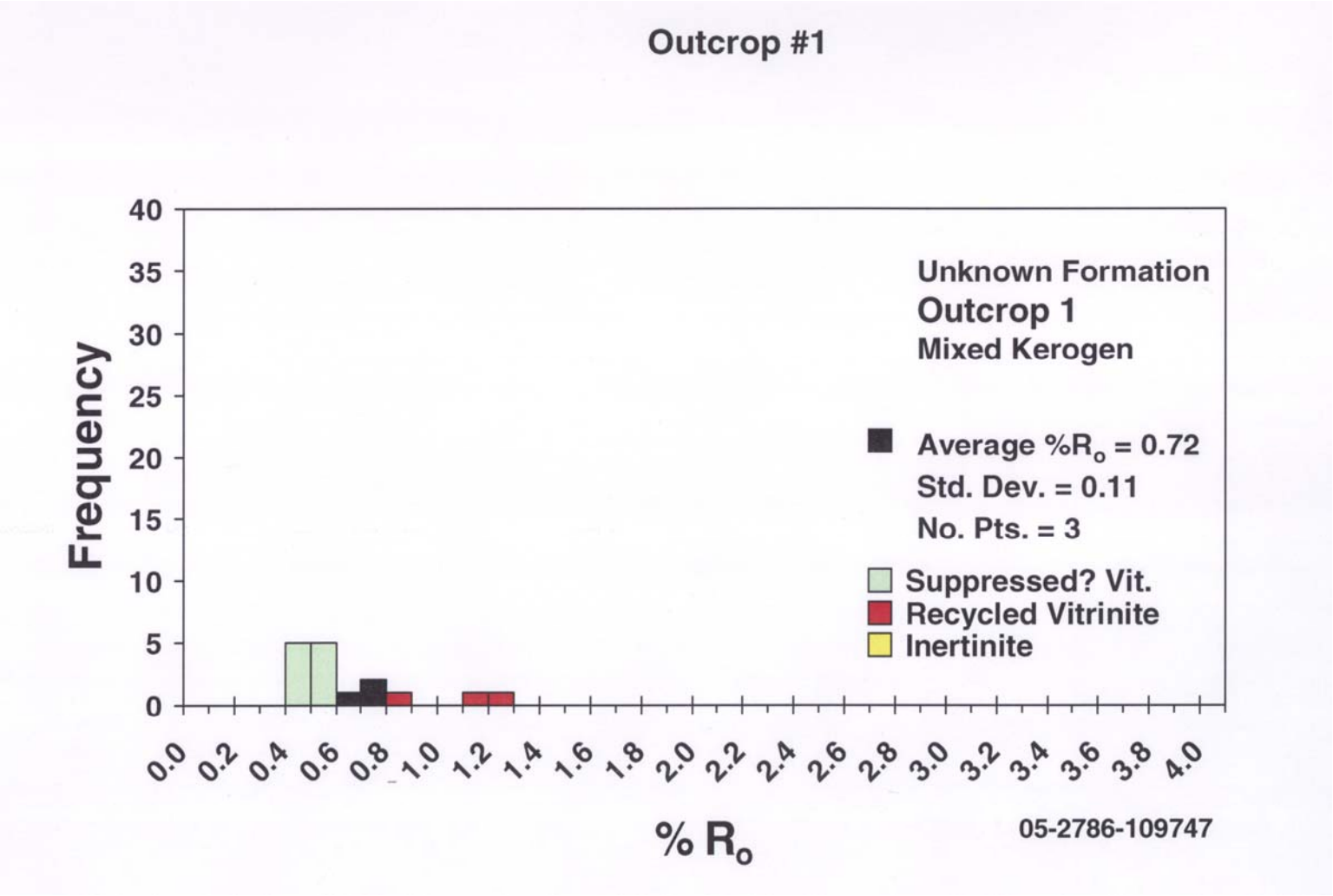
Outcrop #1
Frequency
40
35
30
25
20
15
10
5
0
Unknown Formation
Outcrop 1
Mixed Kerogen
Average %R$_o$ = 0.72
Std. Dev. = 0.11
No. Pts. = 3
Suppressed? Vit.
Recycled Vitrinite
Inertinite
0.0 0.2 0.4 0.6 0.8 1.0 1.2 1.4 1.6 1.8 2.0 2.2 2.4 2.6 2.8 3.0 3.2 3.4 3.6 3.8 4.0
% R$_o$
05-2786-109747

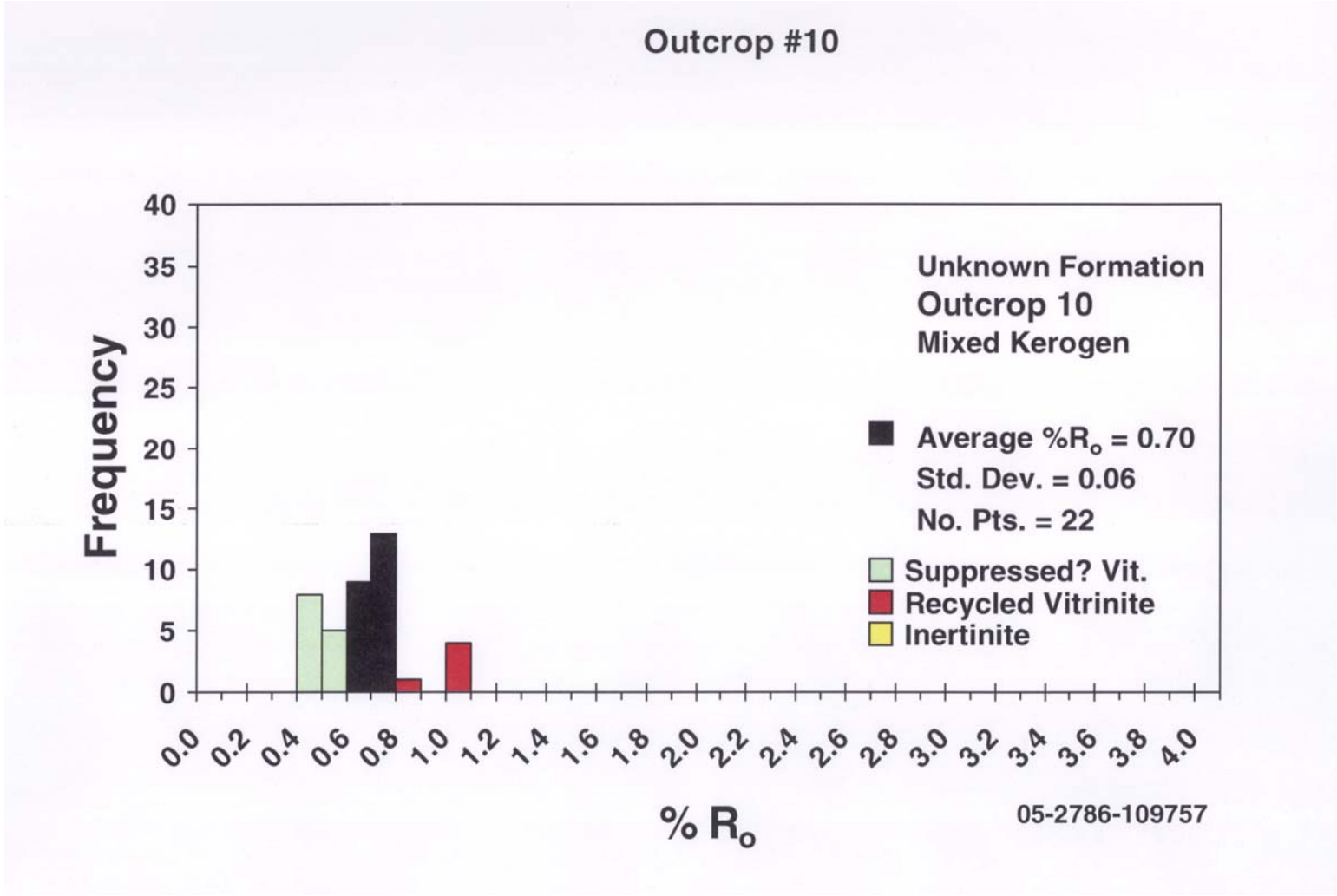
Outcrop #10
Frequency
40
35
30
25
20
15
10
5
0
Unknown Formation
Outcrop 10
Mixed Kerogen
Average %R$_o$ = 0.70
Std. Dev. = 0.06
No. Pts. = 22
Suppressed? Vit.
Recycled Vitrinite
Inertinite
0.0 0.2 0.4 0.6 0.8 1.0 1.2 1.4 1.6 1.8 2.0 2.2 2.4 2.6 2.8 3.0 3.2 3.4 3.6 3.8 4.0
% R$_o$
05-2786-109757

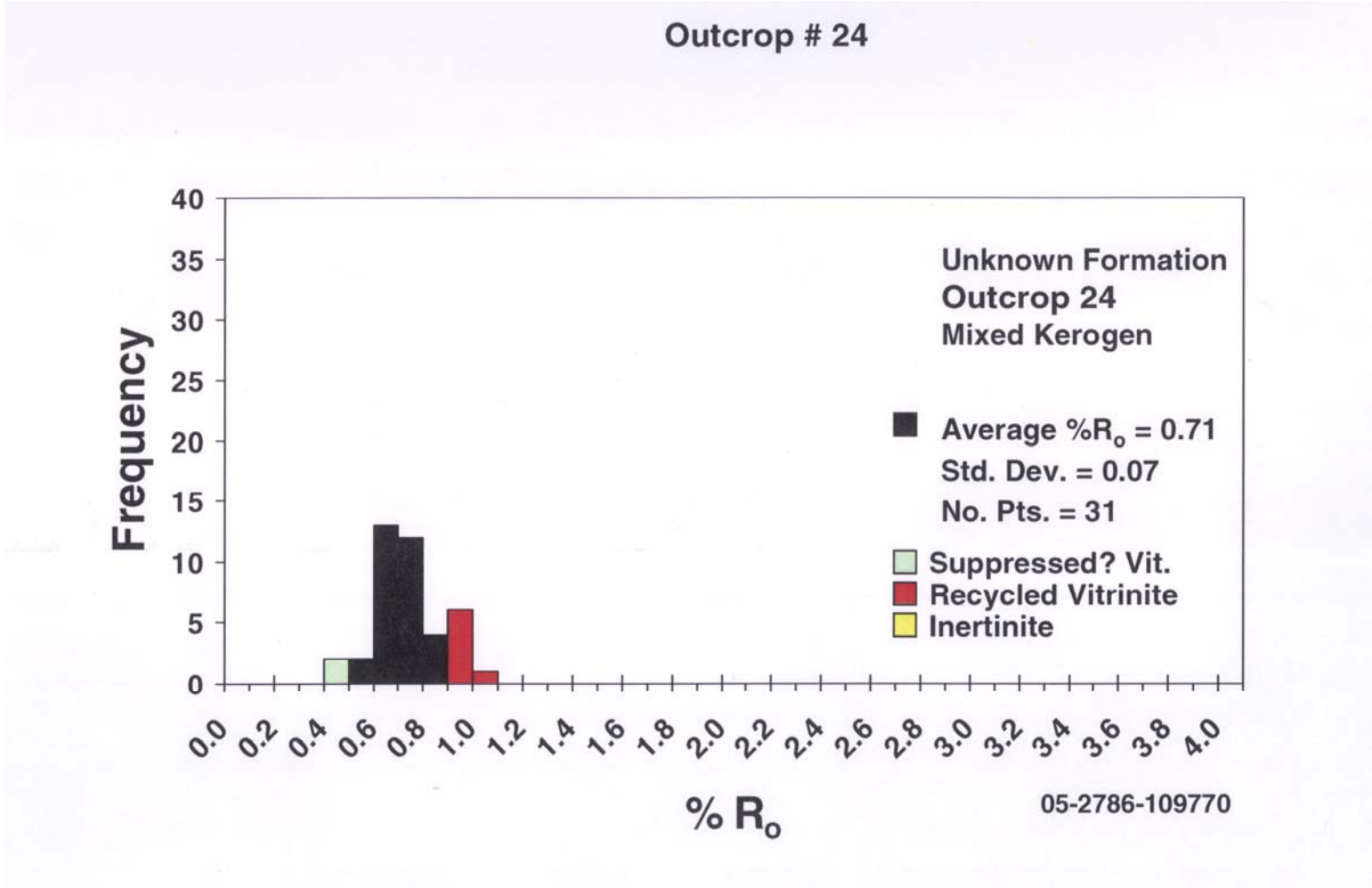
Outcrop # 24
Frequency
40
35
30
25
20
15
10
5
0
0.0
0.2
0.4
0.6
0.8
1.0
1.2
1.4
1.6
1.8
2.0
2.2
2.4
2.6
2.8
3.0
3.2
3.4
3.6
3.8
4.0
% Ro
Unknown Formation
Outcrop 24
Mixed Kerogen
Average %Ro = 0.71
Std. Dev. = 0.07
No. Pts. = 31
Suppressed? Vit.
Recycled Vitrinite
Inertinite
05-2786-109770

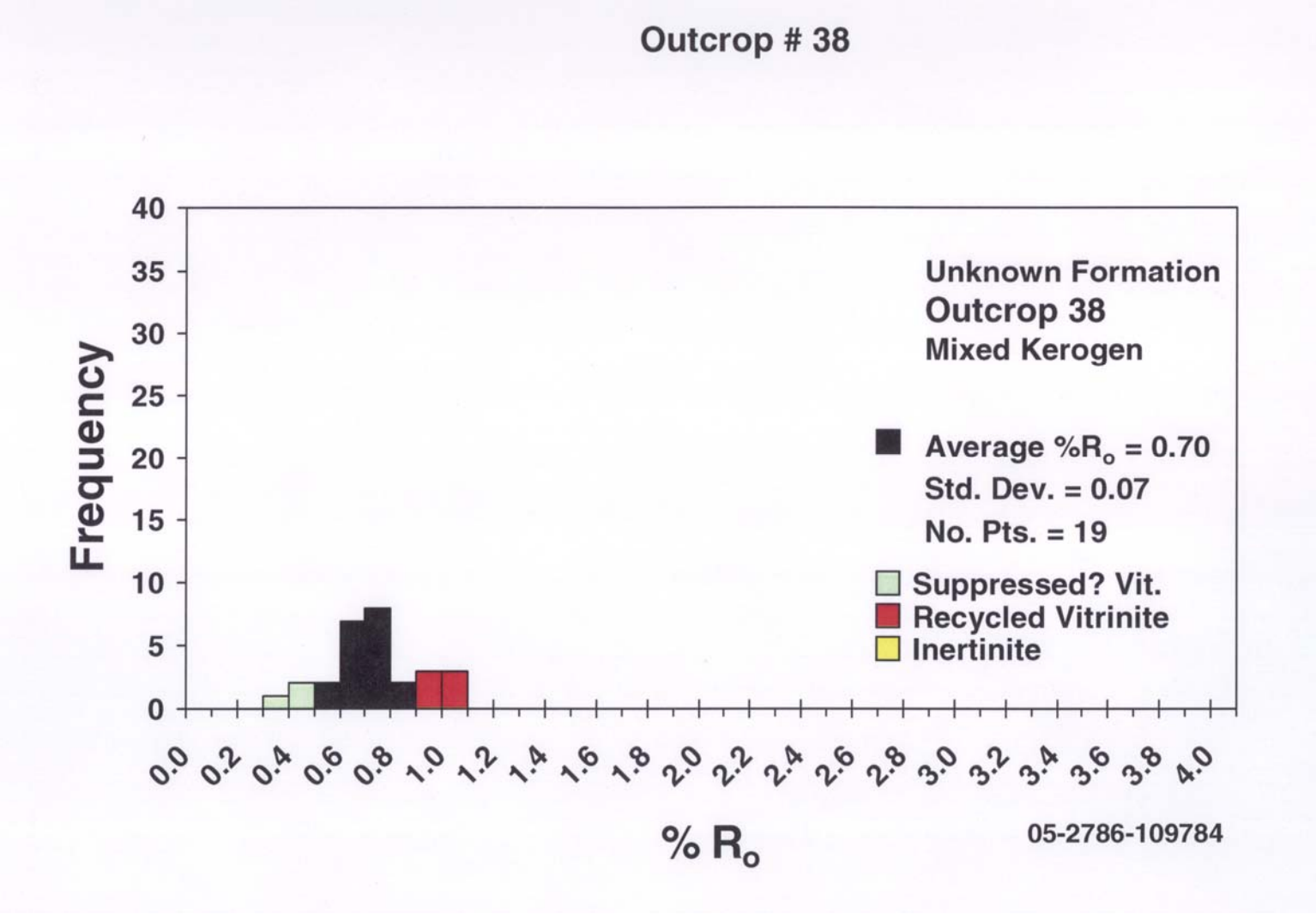
Outcrop # 38
Frequency
40
35
30
25
20
15
10
5
0
0.0
0.2
0.4
0.6
0.8
1.0
1.2
1.4
1.6
1.8
2.0
2.2
2.4
2.6
2.8
3.0
3.2
3.4
3.6
3.8
4.0
% Ro
Unknown Formation
Outcrop 38
Mixed Kerogen
Average %Ro = 0.70
Std. Dev. = 0.07
No. Pts. = 19
Suppressed? Vit.
Recycled Vitrinite
Inertinite
05-2786-109784

ARKOMA AREA DATA - Main data set for Arkoma Basin

CLEVELAND
POTTAWATOMIE
SEMINOLE
HUGHES
McCLAIN
I-177
HWY-3W
PONTOTOC
A'
GARVIN
COAL
Hunton Quarry Outcrop
Brimley Residence Outcrop
MURRAY
Amis 1-3
JOHNSTON
ATOKA
CARTER
I-35 Outcrop
Henryhouse Creek Outcrop
A
MARSHALL
LOVE
McAlester Cemetery Shale Pit Outcrop
BRYAN

30 0 30 60 Miles

0 17,993 FEET

PETRA 12/5/2005 3:22:56 PM

I-35 OUTCROP

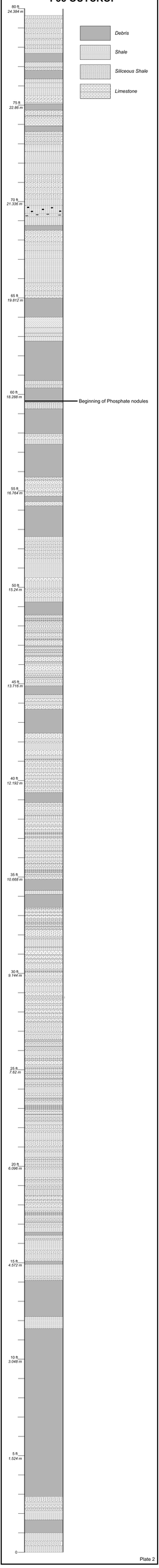

Plate 2

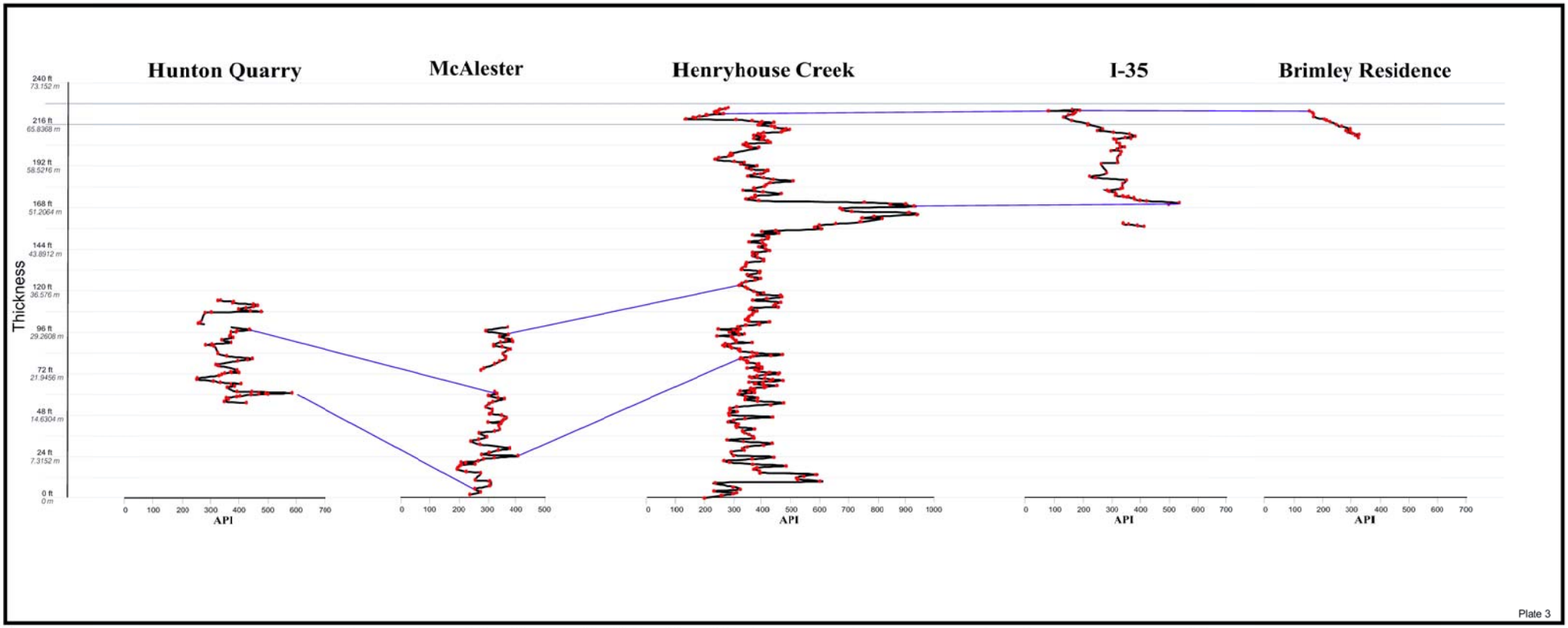

Plate 3

Correlation of the five studied Woodford Shale outcrops from outcrop-based gamma-ray profiles.

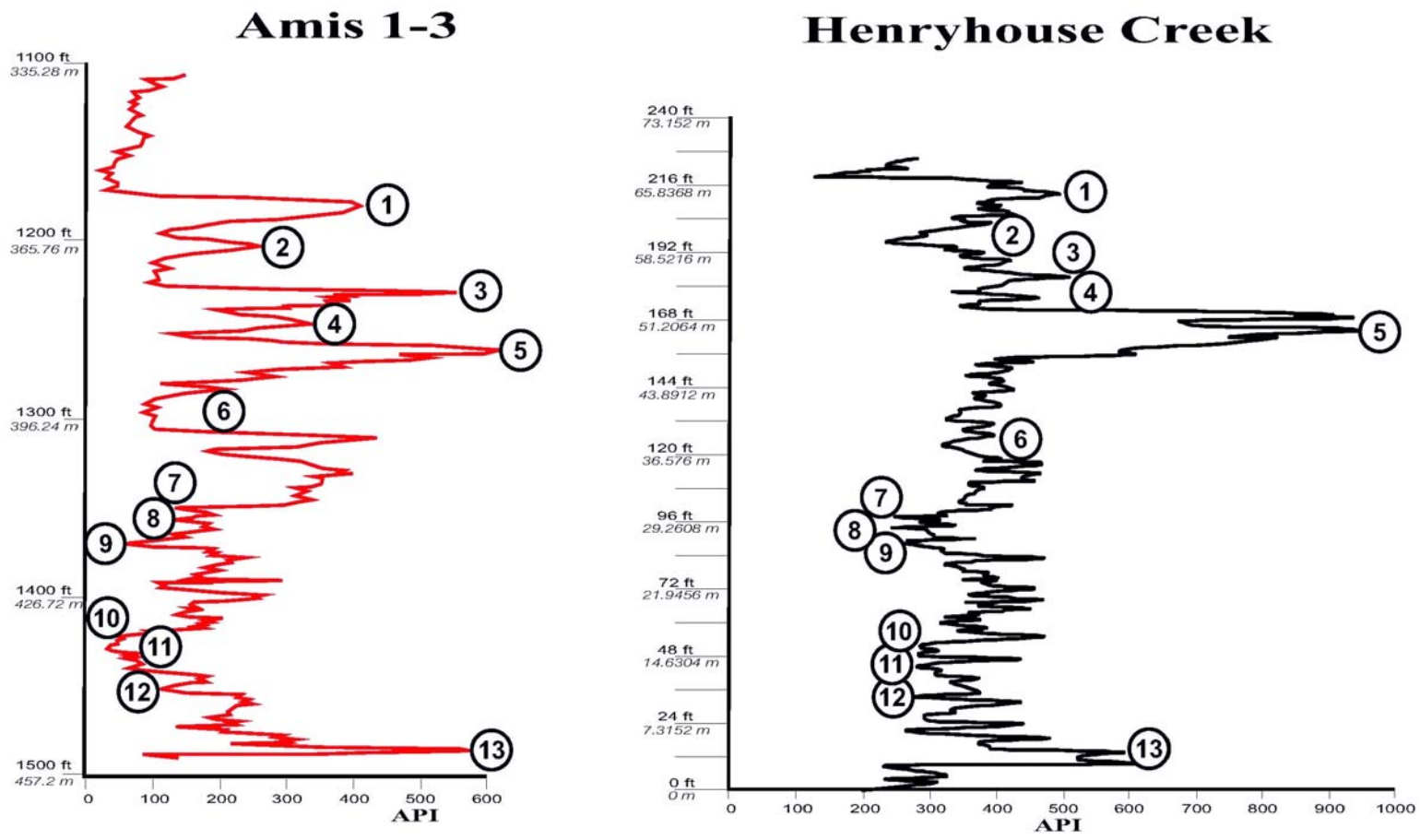

Plate 4

Correlation between subsurface gamma-ray log of the Woodford Shale (east of the studied locations) and outcrop-based gamma-ray profile.

Alischa M. Krystyniak

Candidate for the Degree of

Master of Science

Thesis: OUTCROP BASED GAMMA-RAY CHARACTERIZATION OF THE WOODFORD SHALE OF SOUTH-CENTRAL OKLAHOMA

Major Field: Geology

Biographical:

Personal Data: Born in Westbranch, Michigan on March 20, 1978, the daughter of Chester and Frances Krystyniak

Education: Graduated from Standish-Sterling High School, Standish, Michigan in June 1997; received Bachelor of Science degree in Geological Sciences from Lake Superior State University of Sault Sainte Marie, Michigan in May 2003. Completed the requirements for the Master of Science degree with a major in Geology at Oklahoma State University in December, 2005.

Experience: Conodont research with Dr. Lew Brown at Lake Superior State University from January 1998 to May 2003; Worked as a teaching assistant for the School of Geology at Oklahoma State University from August 2003 to May 2005; Worked as an Intern at Devon Energy Corporation in Oklahoma City from May 2005 to December 2005.

Professional Memberships: Geological Society of America
American Association of Petroleum Geologists

Name: Alischa M. Krystyniak Date of Degree: December, 2005

Institution: Oklahoma State University Location: Stillwater, Oklahoma

Title of Study: OUTCROP-BASED GAMMA-RAY CHARACTERIZATION OF THE WOODFORD SHALE OF SOUTH-CENTRAL OKLAHOMA

Pages in Study: 149 Candidate for the Degree of Master of Science

Major Field: Geology

Scope and Method of Study: The late Devonian (Frasnian, Fammenian) and basal Mississippian (Tournasian) in age Woodford Shale was studied in Murray, Carter, and Pontotoc Counties, Oklahoma. The purpose of this study was to determine if a relationship exists between outcrop lithofacies and gamma-ray response and if ultimately this relationship can be extended into the subsurface. Over 500 gamma-ray readings were collected from five studied outcrops to complete this work. Thin-section analysis, total organic carbon, x-ray diffraction and vitrinite reflectance data were also integrated in this study.

Findings and Conclusions: The Woodford Shale falls into the uraniferous shale category (>20 ppm) with uranium readings as high as 106 ppm. Uranium is the main constituent controlling gamma-ray character. The greatest occurrence of uranium occurs in the lower Woodford and in the top of the middle Woodford.

The bulk of the Woodford contains two main shale habits, fissile and non-fissile. Lithofacies found in or associated with the non-fissile category are phosphatic shale, siliceous shale, dolomite beds, phosphate nodules and rare occurrences of chert and limestone. The fissile shale habits are composed of laminations that are <1 cm thick and are the most organic-rich of the Woodford shales.

Thin-section analysis of the upper Woodford indicates that radiolarians are the main source for silica in the Woodford. Thin-sections cut from phosphate nodules and surrounding shales suggests that radiolarians provide the nuclei for phosphate development.

The Woodford outcrop-based gamma-ray profiles can be correlated into the subsurface. This correlation is based upon pattern recognition of the connected points that compose a gamma-ray profile in comparison with the gamma-ray logs which are continuous curves.

ADVISER'S APPROVAL: Stanley T. Paxton